UNIVERSITY OF CALGARY

Transitions in Boreal Wetland Macroinvertebrate Community Composition Across a Natural Salinity Gradient

by

Brenten Earl Vercruysse

A THESIS
SUBMITTED TO THE FACULTY OF GRADUATE STUDIES
IN PARTIAL FULFILMENT OF THE REQUIREMENTS FOR THE
DEGREE OF MASTER OF SCIENCE

GRADUATE PROGRAM IN BIOLOGICAL SCIENCES

CALGARY, ALBERTA

JUNE, 2022

Abstract

Nearly 65% of Alberta's northern boreal landscape is comprised of wetlands (primarily peatlands), which are lost in the process of open pit mining for oil sands. Demonstration wetlands recently created in reclaimed postmining watersheds are productive and support diverse biota. However, their water tends to be sodic due to the presence of salts in the soils used in their construction and residual sodium from the bitumen extraction process. Saline wetland systems occur in northern Alberta in areas where deep aquifer upwellings contribute significantly to a wetland's water budget. I sampled the water chemistry and aquatic invertebrates in a suite of 52 pools ranging in specific conductance from 3,757 to 20,170 μS/cm in a patterned fen southeast of Fort McMurray, Alberta, to identify patterns of community composition along the salinity gradient. Sodium, chloride, magnesium, and calcium were the dominant ions present in the saline fen. Pools with relatively low salinity supported abundant densities of gastropods and odonates whereas the most saline pools were dominated by Diptera larvae, especially genera of mosquitos. Threshold Indicator Taxon Analysis (TITAN) identified a set of 11 sensitive and 9 tolerant taxa diagnostic of specific conductivity. Community composition changed markedly at a threshold of 6,335-9,385 μS/cm, equivalent to chloride concentrations of 1,579- 2,535mg/L. These findings may provide a useful frame of reference for anticipating community composition in wetlands forming in sodic areas of the reclaimed postmining landscape of the AOS.

Preface

This thesis is original, unpublished, independent work by the author, Brenten Earl Vercruysse.

Acknowledgements

There are many people I am grateful to have in my life who have supported me and guided me throughout this process. First, I would like to thank my supervisor, Dr. Jan Ciborowski for his knowledge, guidance, patience, and generosity while completing my degree requirements. I would also like to thank my committee members, Dr. Leland Jackson, Dr. Mary Reid, and Carla Wytrykush, who all provided support, advice and feedback throughout this process. I'd also like to thank everyone that was a part of the BWRAP lab and helped me along the way in sample collection and analysis: Michael Wendlandt, Ashlee Mombourquette, Steven Blair, Emily Moore, Liam Mebesius, Elizabeth Gillis, and Abisola Allison.

A special thanks to Andrea Borkenhagen for taking our field team to the saline fen complex for the first time; Dr. Mindi Summers for guiding me and helping me nurture skills in teaching; Alyssa Frazao for hours of phone calls about macroinvertebrates; and of course, my family and friends for their unconditional love and support.

This project was funded by grants from the Natural Sciences and Engineering Research Council of Canada Industrial Research Chair program and Canada's Oil Sands Innovation Alliance provided to Dr. Jan Ciborowski. I gratefully acknowledge the receipt of an Alberta Graduate Student Achievement Award, an Alberta Graduate Student Excellence Scholarship, as well as graduate teaching and research assistantships from the University of Calgary.

Table of Contents

List of Tables

List of Figures and Illustration

Chapter 1: General Introduction

The Athabasca oil sands region (AOS) is a vital component of the Albertan and Canadian economies, supporting a multibillion-dollar industry, employing many Canadians, and providing energy in the form of crude oil to millions of individuals internationally (Foote 2012). This region's oil has also become the centre of discussions relating to environmental and social uncertainties, mostly regarding planning and implementation of reclamation and mine closure (Foote 2012; Giesy et al. 2010; GOA 2021; NRCAN 2016). The AOS oil reserves are the second largest globally, containing approximately 1.71 trillion barrels of bitumen (GOA 2009). Of this, about 10%, (173 billion barrels) are recoverable (GOA 2009). This oil reserve includes an area of 4600 km^2 of bitumen strata, resulting in a total degraded land area in 2017 of 895 km^2 (Foote 2012; GOA 2009; GOA 2017; Hawkes et al. 2020). In 2008, the AOS produced nearly 1.2 million barrels of bitumen daily (Giesy et al. 2010).

Bitumen extraction in the AOS is conducted using the Clark Hot Water method, in which a sodium hydroxide solution is mixed with the extracted oil sands, separating the bitumen from the silt, sand and clay present in the oil sands (Kannel & Gan 2012). The solution remaining after the removal of the bitumen is a slurry waste containing oil sands process affected water (OSPW), fine solids and sands (Kannel & Gan 2012; BGC 2010).

Extracting one barrel of bitumen requires two to four barrels of water and produces four cubic meters of slurry waste (Kannel & Gan 2012). Tailings contain trace metals and organic compounds, with the most notable constituents of concern being sodium, acid extractable organic compounds (AEOs) and polycyclic aromatic compounds (PACs) (Kannel & Gan 2012). Although recycling OSPW reduces the total volume of freshwater used, it also increases the concentration of constituents of concern in OSPW, which are stored in tailings ponds until properly treated, released into the surrounding environment and/or used for reclamation (Giesy et al. 2010; BGC 2010; GOA 2015). Coarse sand particles in the tailings quickly separate from the solution, leaving fluid fine tailings (FFT) to pool in the centre of tailings ponds (BGC 2010). Fluid fine tailings contain silt, clay, water, and residual bitumen, and will settle over a two-year period, to become mature fine tailings (BGC 2010; Quagrine et al. 2005). While mature fine tailings have a greater density than fluid fine tailings, mature fine tailings can take 100 years to settle enough to form a trafficable surface (BGC 2010). One of the methods used to accelerate tailing densification, tailings sand is often mixed with mature fine tailings and gypsum, creating composite tailings, which densifies and creates a trafficable surface in as little as one year (BGC 2010). Other methods include centrifugation to form terrestrial deposits or leaving them untreated under a water cap to form a pit lake, such as Syncrude's Base Mine Lake (BGC 2010; Risacher et al. 2018).

Under the Environmental Protection and Enhancement act of Alberta (GOA 2021; GOA 2015; AEP 2017), all land degraded by the mining processes must be reclaimed to "equivalent land capabilities." One interpretation of this is that the reclaimed land must support similar processes to those occurring on the land before degradation; but the processes do not need to be identical, and the land does not necessarily need to consist of the same habitat type that was present previously (GOA 2015, Rooney & Bayley 2011).

Wetlands

Almost two-thirds of Alberta's boreal region consists of wetlands, of which about 60% are peatlands (Rooney & Bayley 2011). To be classified as a peatland, the accumulated organic soil must be primarily undecomposed organic matter (AESRD 2015). Peatlands play a vital role as carbon sinks, storing carbon in the form of peat that has been accumulated over centuries (Vitt

2018). Mining approvals require a life-of-mine closure plan including entire plans for oil sands extraction, and land reclamation plans including wetland reclamation plans to be submitted to the government (BGC 2010; GOA 2021; GOA 2015).

Wetlands play an extremely important role in the environment, providing many far-reaching ecological services (Mitsch & Gosselink 2015). Wetlands support and protect their surrounding environment buffering the area from floods by forming natural flood plains, filtering and storing natural and anthropogenic contaminants entering wetlands from upland streams and reservoirs by removing nutrients via plant growth, and as aesthetic open spaces used for recreation such as hunting and fishing (Mitsch & Gosselink 2015; Foote & Krogman 2006). Wetlands also act as a vital source of biodiversity, and provide a unique form of habitat, hosting a variety of unique flora and fauna that can survive in their wetlands' hygric environment (Mitsch & Gosselink 2015; Foote & Krogman 2006; Gibbs 2000).

Peatlands are wetlands in which carbon accumulation exceeds the rate of decomposition, resulting in a minimum accumulation of 40 cm of peat (Vitt et al. 2009; Volik et al. 2018). Over time, organic litter transforms into peat that may be stored for centuries (Mitsch & Gosselink 2015). Peat persists under anoxic conditions, which are sustained in wetlands that have a positive water balance producing water-logged soils (Mitsch & Gosselink 2015). Peatlands accumulate and store about one third of the world's soil carbon of which Canada and the United States of America to account for 1.65 million km^2, nearly half, of the peatlands' area globally (Mitsch & Gosselink 2015; Harenda et al. 2018; Kovalenko et al. 2013). Peatlands in northern regions have become an important area of concern with respect to climate change, as melting permafrost potentially exposes previously frozen peat to microbial decomposition (Heffernan et al. 2020). Peat decomposition releases carbon in the form of carbon dioxide resulting in a positive feedback cycle in which the loss of permafrost storing peat may exacerbate the loss of permafrost through the release of greenhouse gases and the kinetic properties of peat degradation (Swindlers et al. 2015; Sjogersten et al. 2016).

Peatlands in northern Alberta formed between 10,000 and 13,000 years ago via terrestrialization and paludification in the mid-Holocene (Bauer & Vitt 2011; Hutton et al. 1994; Mitsch & Gosselink 2015; Halsey et al. 1998). Terrestrialization occurs when shallow lakes become filled in over time from the surface by a floating mat of *Sphagnum*, sedges and grasses, that grows from the edges to eventually cover the shallow lake. Paludification is the growth of peat outwards over previously mineral soils (Mitsch & Gosseling 2015). Having a consistent water table near the mat's surface creates anoxic conditions, under which, moss is not degraded resulting in peat accumulation (AEP 2017; Mitsch & Gosselink 2015; Vitt 2018). Peatland ecosystems include broad group classifications of bogs and fens, in which bogs obtain their water budget primarily through precipitation while fens receive groundwater influx (AESRD 2015; AEP 2017). Fens can be classified into poor fens, moderate rich fens, extreme rich fens and saline fens, depending on their acidity, alkalinity, and bioavailable ionic concentrations in porewater (AESRD 2015; Vitt et al. 2009).

Replicating the complex interactions that occur over centuries in the natural formation of fens in a constructed wetland is likely to be very difficult (Nwaishi et al. 2015; AEP 2017). During wetland formation, a key difference between fen/bog formation and marsh/swamp formation is the presence of a stable water table, as fluctuating water levels result in marsh vegetation instead of peatland vegetation (Vitt 2018; CEMA 2003). As a result, most of the wetland reclamation work done so far has been focused on reclaiming marshes, since marshes have formed opportunistically in degraded areas of the mining site (Daly 2011; Hawkes et al.

2020; Little-Devito et al. 2019). Additionally, many marsh plant species are more likely to survive the sodic conditions of OSPW than the moss species typical of a characteristic peatland (Daly 2011; Volik et al. 2018). Saline fens do exist in northern Alberta; their predominant vegetation consists of graminoid species (e.g. *Triglochin*, *Juncus*, and certain *Carex*) rather than mosses (Hartsock 2020; Daly 2011). Construction of a fen complex was previously thought to be somewhat unachievable given the geochemical and hydrological conditions required to form peatlands, which typically take place and develop over thousands of years (Daly 2011; CEMA 2003; AEP 2017). However, in the mid 2000s, both Syncrude ad Suncor began pilot programs to assess the feasibility of creating fen systems by constructing conditions to allow a fen system to form over time. Since then, Suncor's Nikanotee Fen (Daly 2011; Borkenhagen & Cooper 2016; Price et al. 2010), and Syncrude's Sandhill Fen Watershed (Wytrykush et al. 2012) have been constructed and monitored to assess the hydrology and water chemistry (Ketcheson et al. 2016; Hartsock et al. 2020; Simhayov et al. 2017; Clark et al. 2019), vegetation (Vitt et al. 2016; Vitt & House 2015; Borkenhagen & Cooper 2019; Borkenhagen & Cooper 2016), and invertebrate community (Menard 2017). Since construction, both Nikanotee Fen and Sandhill Fen watersheds have shown patterns of carbon sequestration (Popovic et al. 2022; Clark et al. 2019) and contain areas with vegetation similar to what is observed in natural fen systems in northern Alberta (Popovic et al. 2022; Hartsock et al. 2021a; Vitt et al. 2016).

Wetland Reclamation

Bitumen in the AOS is removed and extracted through open pit mining (BGC 2010; GOA 2015). This process entails removing vegetation, and up to 100 m of soil and overburden to expose the underlying oil sands (BGC 2010; GOA 2015). Surface materials are stored on site in overburden dumps, while the ore body is transported to a plant where bitumen is extracted (BGC

2010). Material remaining after bitumen extraction (tailings) is transported and stored on site in tailings ponds (BGC 2010; GOA 2015). After all bitumen has been extracted from a pit, the reclamation process can begin, following the landscape design submitted in the life-of-mine closure plan (AEP 2017; COSIA 2017). Two general approaches are used for landscape reclamation - wet reclamation, and dry reclamation (BGC 2010). Wet reclamation involves storing mature fine tailings in an end pit, and water-capping the end pit with at least 5 m of freshwater to create a stratified end-pit lake, such as Syncrude's Base Mine Lake (BGC 2010; Risacher et al. 2018). Dry reclamation methods are used to create upland areas that will become forests and wetlands (BGC 2010). Dry reclamation involves filling an end pit with a combination of mature fine tailings or composite tailings, and overburden, and capping the tailings with sand or petroleum coke (a coal-like by-product of bitumen extraction) (BGC 2010). This cap is then overlain with soil that is graded, contoured, fertilized and vegetated based on the end land design (Wytykush et al. 2012). Wetlands can be created using dry reclamation methods, or form opportunistically in areas designed as an upland forest (Wytrykush et al. 2012; Hawkes et al. 2020; Little-Devito et al. 2019).

Because of their marine origins, both the clay overburden and the tailings sands used to cap an end-pit are sodic (BGC 2010; Purdy et al. 2005; Volik et al. 2018). The overburden consists of Cretaceous marine sodic shale known as the Clearwater Formation, which accumulated above the oil sands ore layer (BGC 2010). Salinity in the tailings is derived from both the marine salts associated with the bitumen and sodium hydroxide used to facilitate separating the bitumen from its parent material (Biagi et al. 2019). As a result, salinization in reclaimed aquatic ecosystems in the AOS has been a concern and wetlands have been constructed to limit the potential salinization of the wetland systems (Biagi et al. 2019; Vitt et al.

2016; Wytrykush et al. 2012). Elevated salinity in aquatic environments is associated with a reduced diversity of emergent vegetation (Trites & Bayley 2009), submerged aquatic vegetation (Rooney & Bayley 2011) and differences in composition among aquatic invertebrate communities (Kovalenko et al. 2013; Preston et al. 2018) when compared to natural, reference condition wetlands from the surrounding area.

Effects of Salinity on Aquatic Invertebrates

Invertebrates are a key component of aquatic food webs, converting a wide range of organic materials' carbon into a form that supports higher trophic levels, including species of other invertebrates, mammals, amphibians, reptiles, and birds (Gullan & Cranston 2010). Emerging adult aquatic insects also facilitate nutrient cycling and plant pollination, providing many ecological services to the ecosystem and landscape (Gullan & Cranston 2010). Invertebrates are a diverse group, with morphological and functional features that adapt them to environmental conditions varying in habitat, water quality and food availability (Gullan & Cranston 2010). As a result, the diversity of invertebrates present in a wetland or a specific site, can inform us about the quality of an area (Mitsch & Gosselink 2015). Invertebrates are therefore often used in indices of biological integrity (IBIs), and as biological indicators (Mitsch & Gosselink 2015; Merritt et al. 2019; Hilsenhoff 1982).

In the AOS, salinity is a key component driving biological and ecological outcomes of reclaimed wetlands, and thus will be the focus of this project. Many wetlands in the Alberta oil sands region have fresh water. Natural saline marshes and fens do occur where saline aquifers transport salty water to the surface through permeable substrates (Trites & Bayley 2009; Purdy et al. 2005; Wells & Price 2015). The Alberta Environment and Sustainable Resource Development wetland classification system identifies classes of wetlands based on the wetlands conductivity values (Table 1.1; AESRD 2015) Salinity is one of many environmental factors that can influence aquatic invertebrate community composition in both natural and reclaimed wetlands.

Table 1.1: Alberta Environment and Sustainable Resource Development Salinity Wetland Classification System

Wetland Classification	Conductivity (µS/cm)
Freshwater	<500
Slightly Brackish	500 – 2,000
Moderately Brackish	2,000 – 5,000
Brackish	5,000 – 15,000
Subsaline	15,000 – 45,000
Saline	>45,000

Salinity is a measure of the sum concentration of ions dissolved in water, typically expressed in units of mg/L (Wetzel, 2001). The procedure for determining the total dissolved solids in a water sample involves evaporating a known volume of water and weighing the residue. Alternatively, salinity is often inferred by measuring specific conductance, which is a measure of electrical conductance of the water adjusted to 25˚C. Specific conductance can be measured in situ with a portable meter (Wetzel, 2001a). As a result, much of the scientific literature dealing with salinity levels in water report specific conductance (Wells & Price, 2015).

Elevated salt concentrations in aquatic habitats cause physiological stress in fauna and flora, resulting in compositional differences at the community level (Herbert et al. 2015). Salinization affects aquatic invertebrates' ability to regulate water balance due to a hypertonic environment, resulting in dehydration, which increases ionic concentrations in tissues and causes death if the organism is not adapted to these higher ion concentrations (Herbert et al. 2015; Palleres et al. 2015). Insects have Malpighian tubules – organs that control the volume and the nutrients within the haemolymph (Chapman 1975; Grueber & Bradley 1994). Malpighian lie in the body cavity, originating near the connection of the mid-gut to the hind-gut, and terminating near the rectum (Chapman 1975; Jonusaite et al. 2017; Pallares et al. 2015). Malpighian tubules regulate osmotic balance by absorbing excess nutrients or water from the haemolymph and excreting the materials into the posterior portion of the gut in arthropods, myriapods and arachnids (Chapman 1975). Aquatic insects inhabiting a saline environment maintain osmotic balance via controlled reuptake of water, but not of salts, in the midgut and in the rectum, via Malpighian tubules, thus releasing feces and urine that is hypertonic to their haemolymph (Chapman 1975; Jonusaite et al. 2017; Pallares 2015). In contrast, aquatic insects inhabiting waters with very low ionic concentrations selectively take up salts from the environment in their midgut and rectum, and release excess water in their feces, which is hypotonic to their haemolymph (Chapman 1975; Jonusaite et al. 2017; Pallares 2015). Euryhalic species, which can survive in a wide range of salinity, are able to do both (Pallares et al. 2015).

Due to differences in abilities of salt regulation, different communities tend to arise across a salinity gradient in which a freshwater community is composed of stenohalic halophobes and tolerant euryhalic species, while a saline community is composed of stenohalic halophiles and tolerant euryhalic species (Chapman 1975; Lancaster & Scudder 1986). Lancaster and Scudder (1986) observed a loss of invertebrate biodiversity across a suite of saline lakes in interior British Columbia. Richness declined from 22 species of Coleoptera and Hemiptera present in a lake with specific conductance of 56 μS/cm, to 11 species of Coleoptera and Hemiptera present in a much more saline lake (13,115 μS/cm). They identified several characteristic species of water boatmen and beetles that only occurred in the most saline areas, as well as species that only occurred in the least saline areas, while other species were present in lakes that spanned the entire salinity gradient (Lancaster & Scudder 1986). Thus, community composition as well as biodiversity clearly varies across a salinity gradient. Bendell-Young et al. (2000), compared the biota of reference wetlands to those of constructed-post mining wetlands in which specific conductivity±SD ranged from 1,860±250 to 56.6±58 μS/cm. Biodiversity was reduced in more saline wetlands, but biomass was unaffected (Bendell-Young et al. 2000). However, in both studies it is unclear whether increasing salinity produces a gradual loss of species and shift in community composition or whether salinity thresholds exist that may regulate community structure.

Thresholds may occur within ecological communities for several reasons. One rationale for the occurrence of thresholds is due to predator avoidance in tolerant taxa. This may occur when salt-tolerant taxa seek refuge from predators that primarily exist in freshwater. For example, Storm et al. (2012) evaluated the salinity tolerance of a harmful raphidophyte alga (*Heterosigma akashiwo*) that can survive across a broad range of salinity in estuarine environments. *Heterosigma akashiwo*'s main predators are protists, most of which can only survive in water with little salinity. As a result, more saline areas provide *H. akashiwo* with a refuge from predators. In such areas, their uncontrolled growth results in their forming of large blooms. In lower salinity area, the presence of its main predators limits the presence of *H. akashiwo*, creating the observation of a threshold due to this predator/prey interaction.

Silberbush and Blaustein (2011) provided another example, in which oviposition rates of mosquitos (*Culiseta*) were compared across experimental mesocosms with varying densities of predators. They found that mosquitoes consistently oviposited in mesocosms with fewer predacious individuals (Silberbush & Blaustein 2011). Taxa able to survive across a wide range of salinity, such as the mosquito genus *Aedes*, oviposited in areas with few predators. This may result in oviposition occurring primarily in areas with greater levels of salinity where predators are rare, creating a threshold formed from seeking refuge from predators.

Study Site

I assessed the biodiversity and composition of aquatic invertebrate communities and associated water quality parameters in pools and flarks spanning a naturally occurring salinity gradient in a 27-ha boreal fen complex located 10 km southeast of Fort McMurray, Alberta, Canada (Figure 1.1; Figure 1.2; Wells & Price 2015). Flarks are common features of patterned fens, in which a flark is a shallow depression filled with water and occur between areas of raised sediment called strings (AEP 2017).

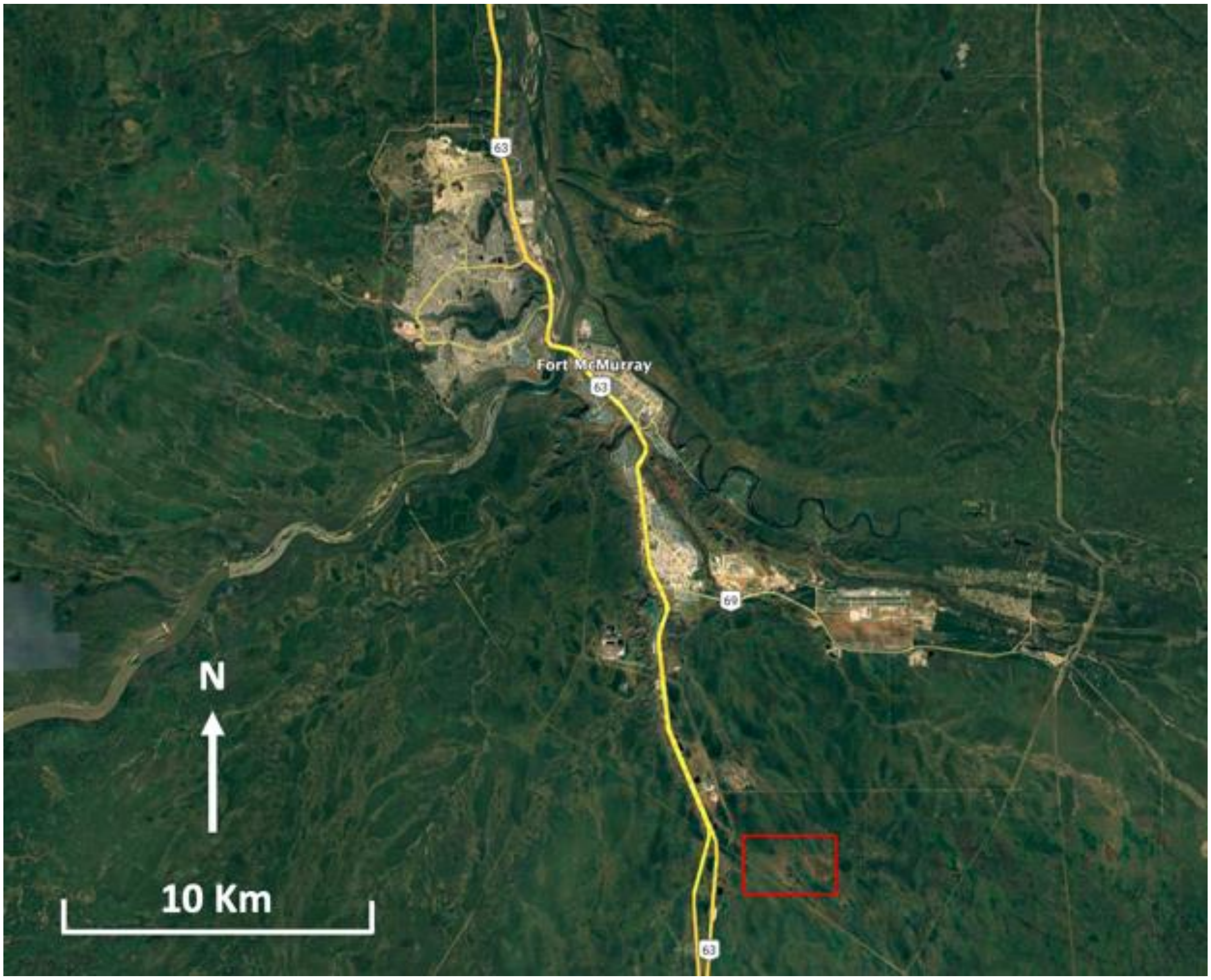

Figure 1.1: Map showing the location of the saline Fen Complex. Area shown in Figure 1.2 outlined in red. Satellite image taken from Google Earth.

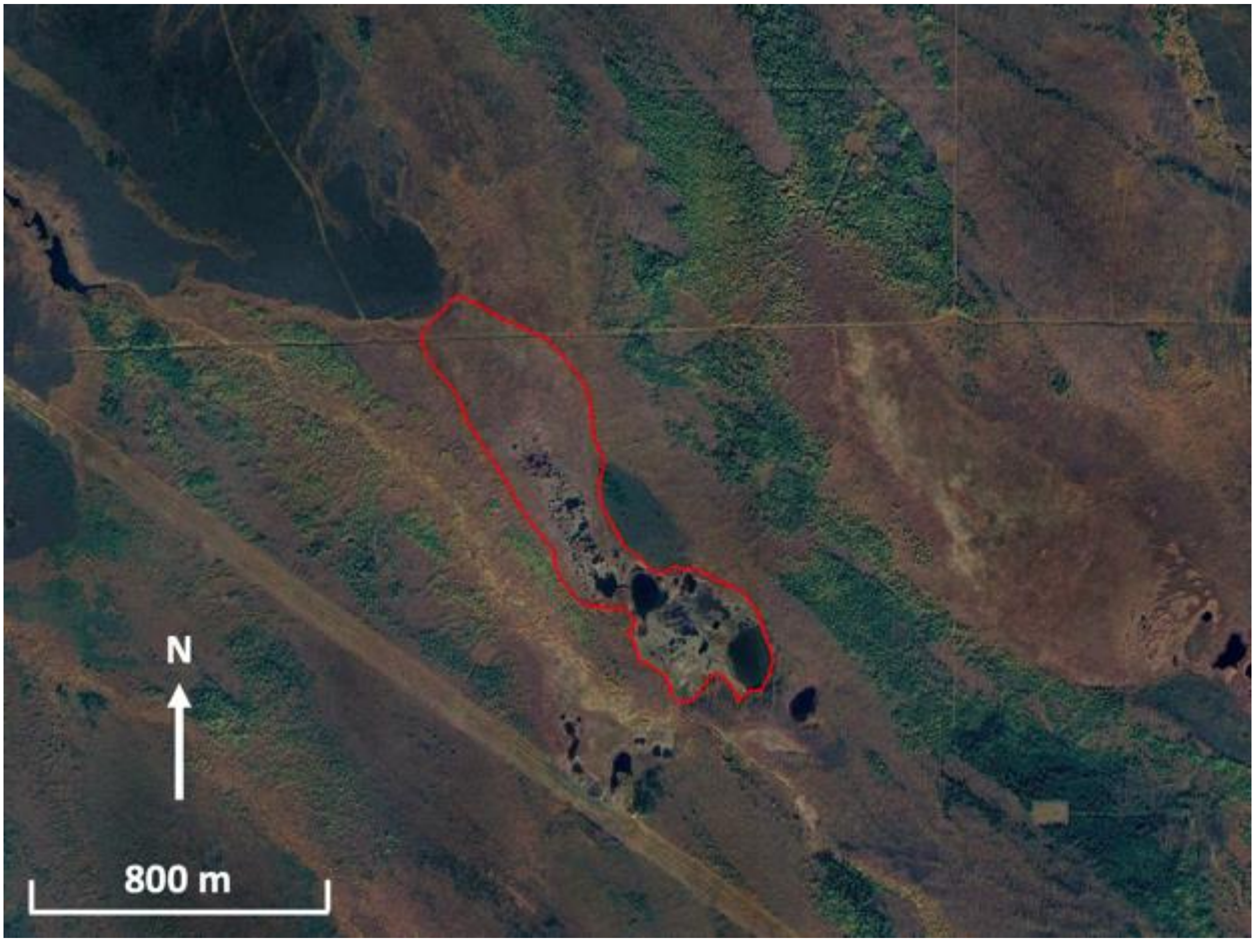

Figure 1.2: Satellite image of the saline fen complex (outlined in red) and surrounding area. Metrics of outlined area: Area = 27.2 ha, Length = 1.23 km. (Satellite image and metrics from Google Earth).

The fen complex contains pools, ranging from hypersaline (up to 120,000 μS/cm) in the south fen to moderately brackish (as low as about 3,000 μS/cm) in the northern region of the 1,200 m long fen complex (Wells & Price 2015). The pools differ in elevation by only 10 m (Wells & Price 2015). Saline groundwater flows northward from the south end of the fen complex and contains mainly sodium (195 – 25,680 mg/L) and chloride ions (1,785 – 56,249 mg/L; Wells & Price 2015). The gradient of salinity is created and maintained via geological structures of mineral ridges, keeping saline water inside the fen complex, and an impermeable clay layer in the north, preventing salt-rich upwelling from occurring in the fen's northern portion (Wells & Price 2015).

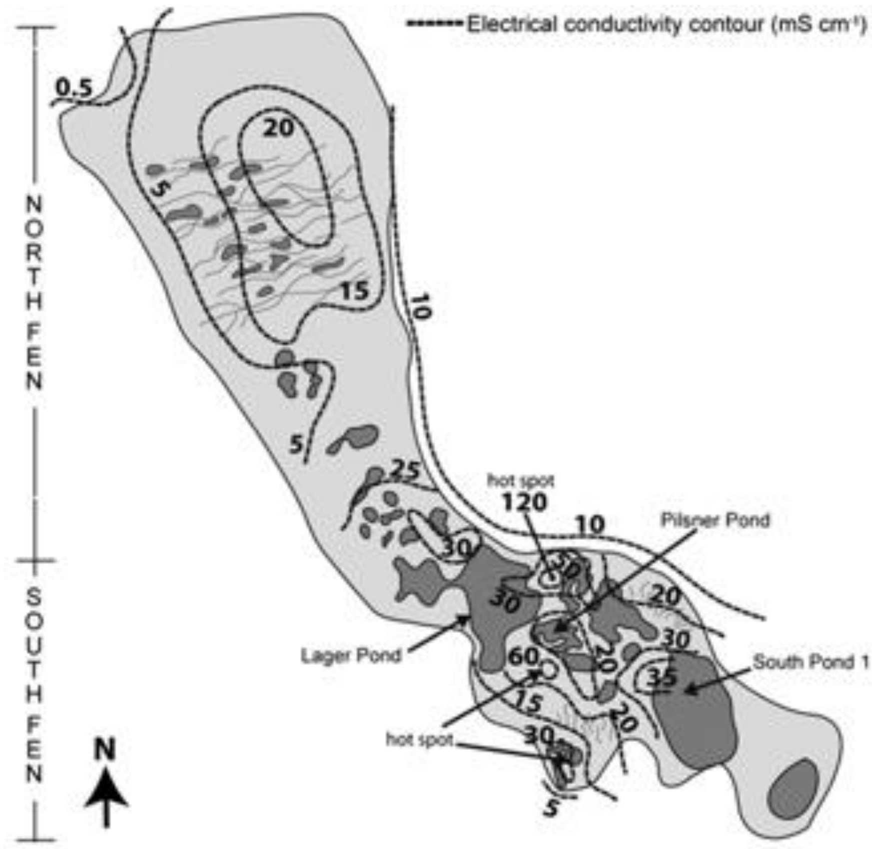

Figure 1.3: Electrical conductivity contour map of saline fen complex measured in mS/cm (from Wells & Price, 2015)

Thesis Objectives

The objective of my research was to answer the following questions:

1. What is the macroinvertebrate biodiversity at different levels of conductivity in a naturally saline boreal fen complex in the AOS?
2. How does macroinvertebrate community composition vary across the salinity gradient of the complex?

This thesis documents the aquatic invertebrate community composition and biodiversity in a suite of wetland pools comprising a naturally occurring salinity gradient ranging from hypersaline to freshwater (Wells & Price 2015). The pools are located in a northern Alberta fen complex that receives upwellings of saline groundwater (Wells & Price 2015). This information will complement the existing information on the fen complex's water chemistry (Volik et al. 2017), plant biodiversity (Hartsock 2020) and carbon dynamics (Volik et al. 2019).

The current chapter is an overview of relevant information regarding the purpose and significance of this study. I discuss the importance of wetland ecosystems and their significance in the Wood Buffalo region of Alberta, provide an overview of wetland reclamation practices in oil sands mining regions of Alberta, summarize information regarding how salinity influences macroinvertebrate community composition, and describe the study site.

The second chapter describes the environmental features, principally water chemistry, of a suite of flarks at the time of sampling in September 2020.

The third chapter examines variation in benthic invertebrate community composition across the salinity gradient. It also identifies conductivity level change points in macroinvertebrate community composition and determines a set of saline-tolerant and saline-sensitive taxa.

The fourth chapter provides a conclusion and synopsis of findings, outlines the limitations and significance, and recommends future research to further understanding of the effects of salinity on the invertebrate community and its relevance to reclaimed wetlands in the AOS.

A set of Appendices provides information on the influence of morphometric variation on the aquatic macroinvertebrate community and water chemistry parameters in the saline fen complex (Appendix A1), summary tables for analyses performed in Chapter 2 (Appendix A2), and summary tables for analysis in Chapter 3 (Appendix A3).

Documenting how aquatic macroinvertebrate communities vary with respect to levels of salinity in naturally occurring (reference condition) wetlands provides an important frame of reference against which to compare the fauna in reclaimed wetlands in the mining lease areas of northern Alberta. In addition to describing the biodiversity of a little-studied boreal habitat, this thesis will document the limits of salinity that control attributes of aquatic invertebrate communities. This information can provide important guidelines useful to regulators and reclamation ecologists constructing wetlands in the AOS.

Chapter 2: Environmental Variables of Alberta Oil Sands Region Wetlands Along a Gradient of Salinity in a Boreal Fen Complex

Introduction

Much of the northern Alberta landscape is comprised of wetlands, the majority of which are classified as peat-forming wetlands or peatlands (Rooney & Bayley 2011; Vitt et al. 2016). Peatland characteristics are largely determined by their water source and the nutrients contained therein (Hartsock 2020). Bogs are peat-forming wetlands that obtain their water through precipitation, and fens are peatlands that receive groundwater influx (AEP; 2017; Hartsock 2020). Fens can be further distinguished as poor, moderate, rich, and saline, wherein the terms poor, moderate and rich refer to the system's species richness of plants and are characteristic of peatlands whose water is acidic, circumneutral or alkaline, respectively (AEP; 2017; Hartsock 2020).

Reclaimed wetlands in the AOS were expected to be more saline than the freshwater wetlands that comprise the majority of the surrounding ecosystem due to salts diffusing to the surface from the underlying overburden and tailings sand (Wells & Price 2015; Purdy et al. 2005); however, many of the reclaimed wetlands contain water ranging from fresh to moderately brackish (AEP 2017; Hawkes et al. 2020; Little-Devito et al. 2019; Biagi et al. 2019; Hartsock et al. 2021b). Most fens of the northern Alberta boreal region contain freshwater. However, saline fens occur when deep aquifer upwellings contribute a significant proportion of a wetland's water budget (Purdy et al. 2005). Such wetlands' hydrology, ecological communities, and chemistry can provide a potentially useful frame of reference against which to compare wetlands in sodic areas within oil sands mine leases (Wells & Price 2015; Hartsock et al. 2021a; Purdy et al. 2005). The objective of this chapter is to summarize variation in the water chemistry of a series of wetland pools (flarks) arranged along the salinity gradient of a boreal saline fen complex in northeastern Alberta. I conducted analyses to elucidate spatial trends and interrelationships among various environmental variables to further understand the chemical composition of wetted areas within the saline fen complex.

The saline fen complex contains pools ranging from moderately brackish (as low as 3000 μS/cm) in the northern portion of the fen, to saline (up to 120,000 μS/cm) in hotspots located in the southern portion of the fen, spanning roughly 1,200 m (Figure 1.2; Wells & Price 2015). Elevation is roughly equal across the fen complex, and altitude varies by only 10 m (Wells & Price 2015). The salinity of the fen complex is derived from an underlying saline aquifer and is comprised primarily of sodium (195 – 25,680 mg/L) and chloride (1,785 – 56,249 mg/L) ions (Wells & Price 2015). ern regionA salinity gradient is formed, with conductivity values increasing among pools in a southeasterly direction along the fen complex due to the northerly flow of groundwater, and the presence of an impermeable clay layer in the north of the fen, which prevents the salt-rich upwellings that occur in the southern portion of the fen from occurring in the north (Wells & Price 2015).

Methods

Pilot Survey

A pilot survey of variation in water chemistry parameters (especially specific conductance) among pools was conducted at the saline fen complex between September 3 and 5 2020. Readings of water temperature, dissolved oxygen concentration, pH, Redox potential and specific conductance were taken with a YSI Proplus multiparameter meter at 122 pools (Figure 2.1). The specific conductance ranged from 3,717 to 21,100 μS/cm (Figure 2.2). Subsequently, 52 waterbodies were stratified-randomly selected for further study based on specific conductivity values, providing a suite of study locations whose conductivity was evenly distributed along a log-transformed conductivity gradient (Figure 2.2; Figure 2.3).

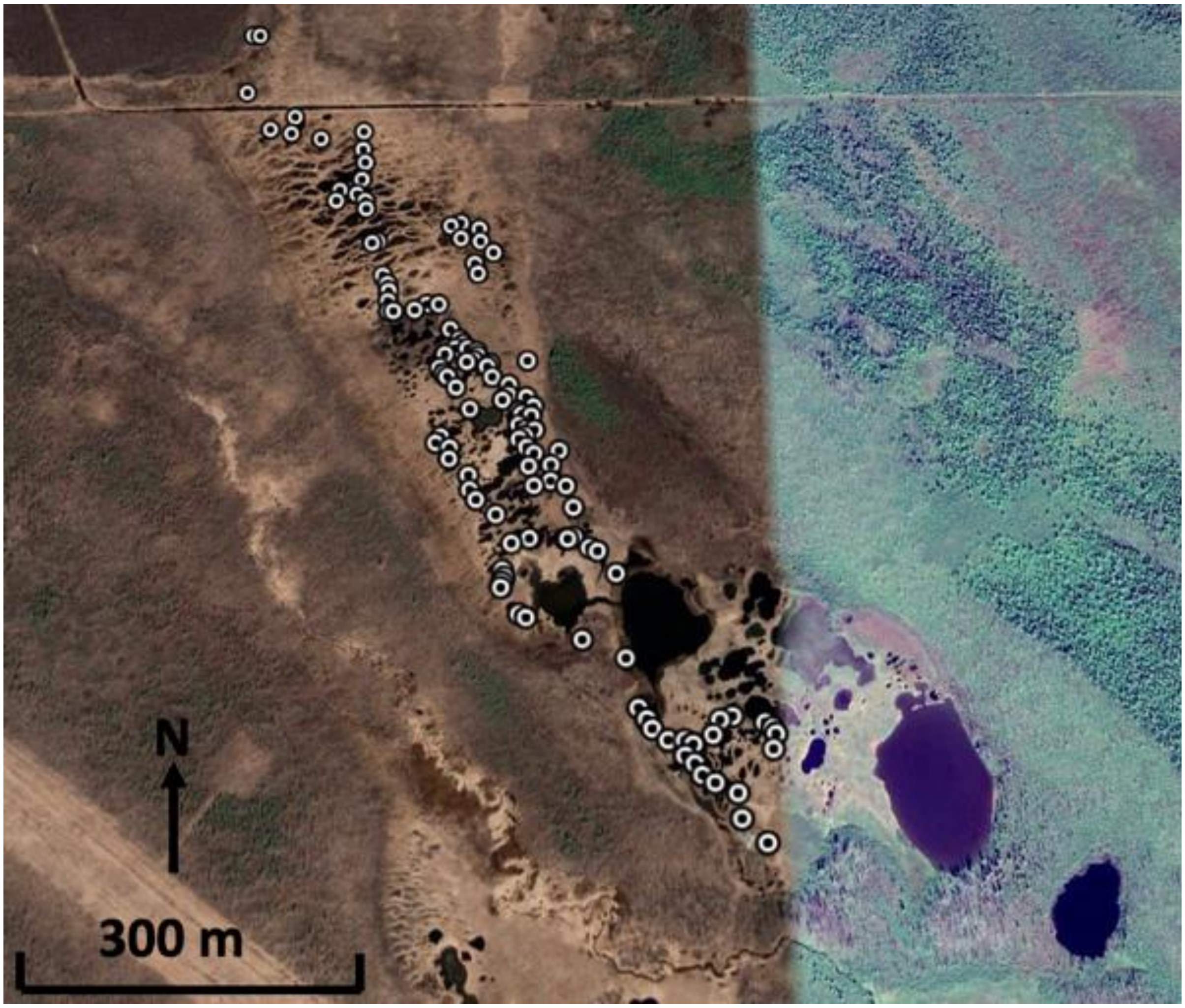

Figure 2.1: Map of locations for conductivity readings collected during the conductivity pilot survey (n=122). Image taken from Google Earth dated August 18 2020.

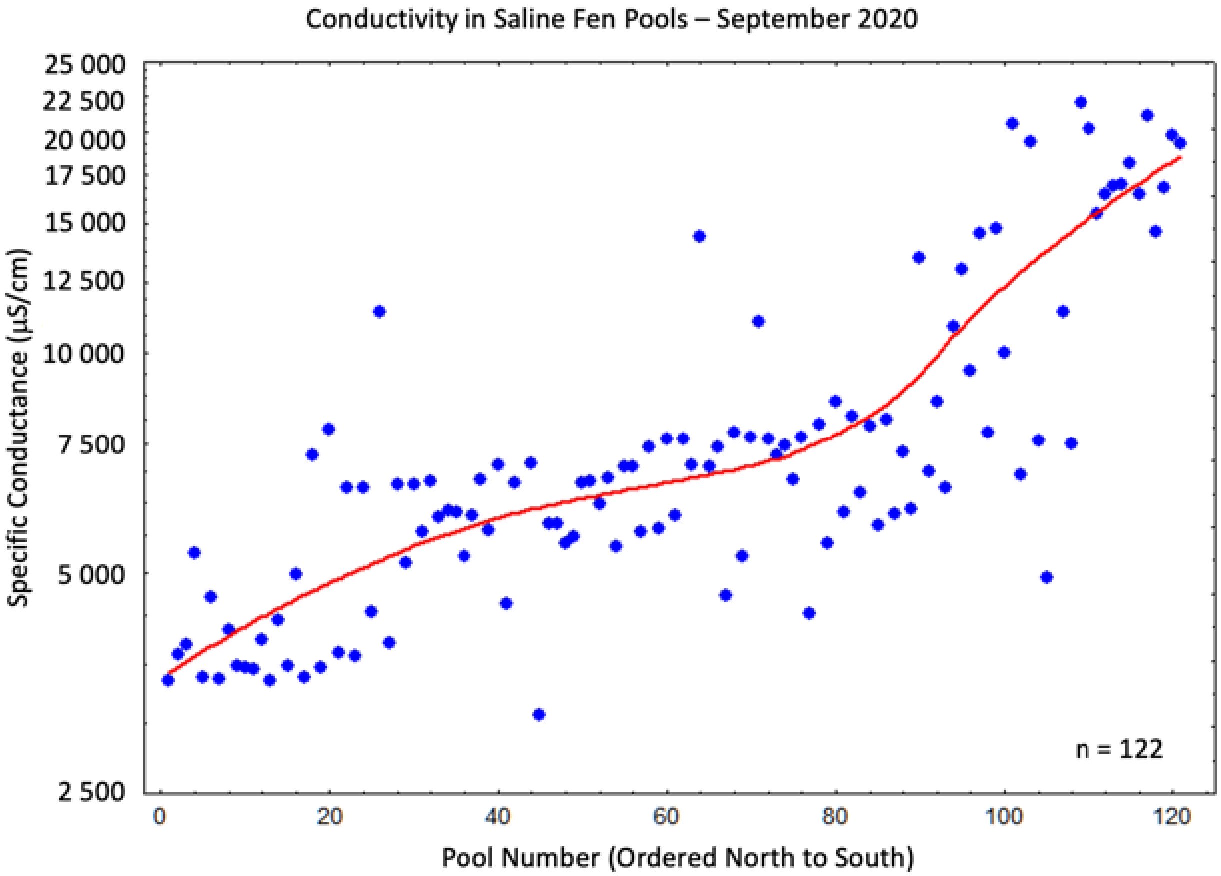

Figure 2.2: Scatterplot of conductivity readings collected from 122 pools. The line (red) is a loess regression of the data. Sites sampled were numbered according to their geographic position along a north-south alignment (northernmost location = 1).

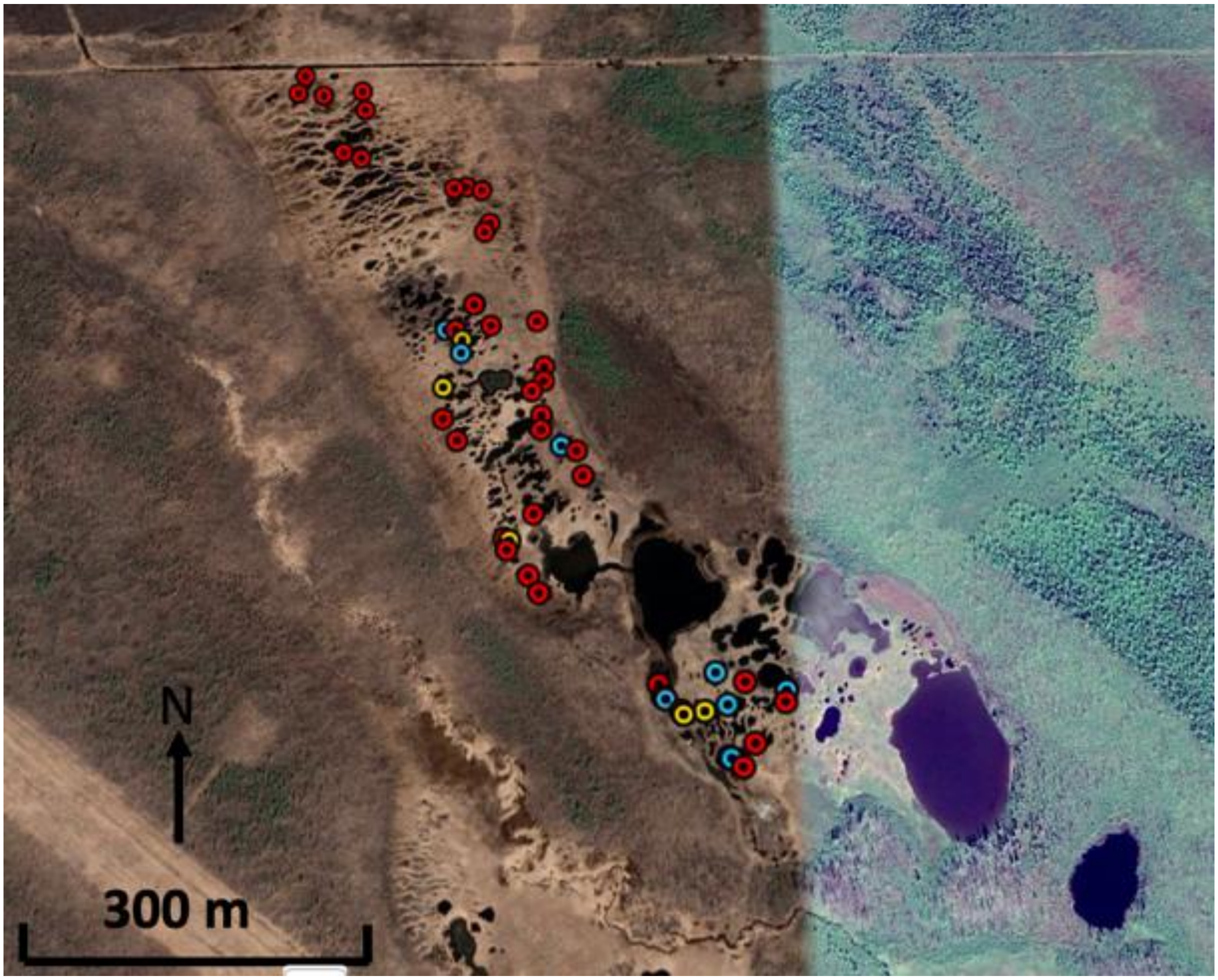

Figure 2.3: Location of 52 sites selected for detailed study, colour-coded by waterbody type - flarks (red; n=38), flark/ponds (blue; n=9), and ponds (yellow; n=5). Image taken from Google Earth dated August 18 2020.

Field Methods

The 52 unique wetted areas within the salinity gradient were classified as either a flark (n = 38), a pond (n=5), or a flark/pond (n=9) depending on their shape, amount of water and characteristics of the location. A flark is a shallow, water-filled depression whose longest axis runs perpendicular to the direction of groundwater flow (AEP 2017). At the time of sampling, flarks were typically 8 to 15 cm deep, and were dominated by emergent vegetation including *Juncus balticus* and *Triglochin maritima* (Hartsock 2020). Ponds were circular or irregularly-shaped waterbodies of variable depth, but in which emergent vegetation was limited to a band around the periphery where water was 15-30 cm deep at the time of sampling. They contained minimal submerged aquatic vegetation, or no vegetation at all. Flark/ponds combined elements of both flarks and ponds. Most of their wetted area contained emergent vegetation including *Juncus balticus* and *Triglochin maritima*. However, they also had a small central open water zone containing either minimal submerged aquatic vegetation (SAV) or no vegetation at all. Water was collected from the deepest part of flarks. In ponds and flark/ponds, samples were collected at the boundary between emergent vegetation and the open water zone, where depth was 15-30 cm deep

Upon arrival at each site, the dimensions (approximate length and width) of the wetted area were estimated, and 3 locations were chosen for sample collection semi-randomly based on previously stated criteria. At each location, a water sample was collected by submersing a 250-mL Nalgene bottle so that its neck was midway between the surface, and the bottom. The 3 samples were poured into a 1-L container, creating a composite for each site. Dissolved oxygen, pH, water temperature and specific conductance of the composite sample were measured using a YSI Proplus multiparameter meter. Two 20-mL aliquots of the sample were filtered through a

0.45-μm glass fibre filter into scintillation vials. The contents of one vial were preserved with 1.0 mL of 2.0 M nitric acid for analysis of major cations The other sample was saved for analysis of anions and nutrients. Samples were stored refrigerated until analysed.

Water samples were analysed for major cations, anions, and nutrients by the Natural Resources Analytical Laboratory (NRAL) facility at the University of Alberta (Edmonton, AB). Cation concentrations were analyzed using Thermo iCAP6300 Duo inductively coupled plasma-optical emission spectrometer (ICP-OES). Dissolved ionic concentrations were calculated for the following elements: *Ag*, Al, *As*, B, Ba, *Be*, Ca, *Cd*, *Co*, *Cr*, *Cu*, Fe, K, Li, Mg, Mn, *Mo*, Na, *Ni*, *P*, *Pb*, S, *Sb*, *Se*, Si, Sr, *Ti*, *Tl*, *V*, *Zn* (Italicized elemental symbols were excluded from the analyses due to concentration levels below the limit of detection).

Elements whose concentrations were below the instrument's limit of detection were dealt with in 2 potential ways as suggested by Antweiler (2015). Elements for which >40% of the readings fell below the limit of detection were removed from further analysis. For elements for which <40% of the measurements were below the limit of detection, surrogate values were substituted using the R2D method (Antweiler 2015), according to the formula: sqrt (2)/2*Limit of Detection. Antweiler (2015) compared data sets with known values to the same data set when portions of the dataset were replaced with surrogates. When fewer than 40% of values were replaced with surrogates, the R2D method was among the best methods used for determining replacement values (Antweiler 2015). When more than 40% of the readings were replaced using the R2D method, other replacement methods created data sets more similar to the original, and so the R2D method should not be used when more than 40% of the readings are below the limit of detection (Antweiler 2015).

Anion and nutrient concentrations were estimated by colorimetry using the ThermoFisher Gallery Beermaster Plus discrete analyser. Concentrations of chloride, sulfate, ammonium, nitrite, nitrate, total oxygenated nitrogen (TON), and phosphate were determined. Nitrite concentrations were below the limit of detection at 41 of the 52 sites, and so total oxygenated nitrogen was used instead of nitrite and nitrate concentrations in further analyses. The concentrations were determined using EPA method 325.2: Ferrithocyanate (chloride concentration), EPA method 375.4: barium chloride (sulfate concentration), salicylate hypochlorite method (ammonium concentration), EPA method 353.1: Hydrazine reduction (total oxygenated nitrogen and nitrate concentrations), EPA method 365.1: Molybdenum Blue (phosphate concentration), and nitrite concentration was calculated by subtracting nitrate concentration from total oxygenated nitrogen.

Statistical Analysis

The water in the fen's flarks and ponds is derived from two sources, each expected to have a distinct unique chemical signature - saline groundwater upwelling from the south, and precipitation-derived surface water from the north (plus substantial rainwater due to copious rainfall prior to and during sampling). Flarks were shallow and smaller in area than ponds and therefore were expected to show greater spatial heterogeneity in water chemistry. Consequently, only flark samples were included in the synoptic analyses. An analysis of the influence of the morphometric variation on the water chemistry and environmental data collected within the saline fen is provided in Appendix A1. All statistical analyses were conducted using R version 3.6.1 (R Core Team 2021).

Summary statistics were calculated for each variable using data collected from 38 flarks (Table 2.1). Variables were tested for the presence of outliers using Dixon's Q-test (Table A2.5), and statistical outliers were removed to avoid results biased to the outliers. Pearson's correlation coefficients and the associated p values were calculated to determine bivariate associations between pairs of variables (Table 2.2). Specific conductance values, and concentrations of nutrients, cations and anions were log transformed before the analysis. Probability values were then adjusted for multiple comparisons using Holm's correction method (Holm 1979; Aickin & Gensler 1996).

Principal component analysis was conducted to elucidate environmental variation among sites using values scaled to unit variance using the correlation matrix so that the data have zero mean and variance 1.0 (Borcard et al. 2018). Twenty-six variables were included in this analysis, specific conductance values, and concentrations of nutrients, cations and anions were log transformed before the analysis, and sites containing outliers were removed from the analysis (Table A2.5), resulting in 34 flarks of the original 38 included in the analysis. The principal component axes were Varimax rotated to more clearly portray correlations among environmental variables (Acal et al. 2020).

Results and Discussion

At the time of sampling (September 2020), surface water specific conductance values in the fen complex ranged from 4,160 μS/cm in the northernmost flark sampled, to 18,628 μS/cm in the southernmost sampled flark in the fen, resulting in salinity ranging from moderately brackish to subsaline (Table 2.1; AESRD 2015). However, previous studies of near surface groundwater in this fen complex have reported conductivity values greater than 50,000 μS/cm in certain groundwater influx "hotspots" that were not sampled for this study (Table 2.1; Wells & Price 2015, AESRD 2015). Ionic composition within the fen was heavily dominated by sodium and chloride ions (Table 2.1). The flarks sampled varied in depth from 6 cm to 27.5 cm. Surface water in these flarks remained close to neutral, with pH ranging from 6.27 to 7.24, while dissolved oxygen varied from 3.33 mg/L to 10.03 mg/L (31.5% to 97.1% of saturation) (Table 2.1). Oxidation reduction potential was positive at all sites measured in the fen complex ranging from 47.4 mV to 217.2 mV, yielding a slightly oxidative environment (Table 2.1). At these levels of redox, nitrogen and manganese are expected to be present primarily in their reduced form (ammonium and manganese (II) respectively), while iron, sulfur and carbon are likely to be present primarily in their oxidized form (iron (III), sulfate, and carbon dioxide respectively) (Mitsch & Gosselink 2015).

A suite of 26 environmental and water chemistry variables were used to characterize the saline fen complex (Table 2.1), as well as individual sites (Figure 2.4). As evidenced from the Pearson's correlation coefficient analysis (Table A2.4), specific conductance was strongly correlated with chloride, sodium, magnesium, calcium, strontium, potassium, sulfur, boron, lithium, and sulfate ion concentrations (+), as well as easting (+) and northing (-) ($r > |0.6|$) (Table A2.4). The strongest correlation with specific conductance was chloride concentration ($r = 0.967$; Table A2.4). Phosphate concentration was significantly correlated with iron concentration and easting (+) (Table A2.4). Other nutrients were weakly correlated or uncorrelated with all of the other variables. Oxidation reduction potential was positively correlated to pH (Pearson correlation coefficient = 0.595, Holm's adjusted p-value = 0.126) (Table A2.4)

Table 2.1: Summary statistics of environmental and water chemistry variables for flark sites. Values below limit of detection (Table A2.1) were accounted for using the R2D method (Antweiler 2015). Outliers were removed using Dixon's Q test (Table A.2.5; Table A.2.1; Table A2.2; Table A2.3).

Variable (units)	n	Minimum	First Quartile	Median	Third Quartile	Maximum	Mean	Sd
Water Temp (˚C)	38	8.5	11.975	13.55	14.175	17	13.20	1.89
Dissolved Oxygen (mg/L)	38	3.33	5.47	6.655	8.05	10.03	6.69	1.813
Dissolved Oxygen (%)	38	31.5	54.875	66.95	81.425	97.1	66.46	18.36
Spec. Cond. (µS/cm)	38	3757	5727.5	8664.5	10369	18628	8731	3678.2
pH	36	6.27	6.8125	7.085	7.23	7.64	7.029	0.284
Redox (mV)	38	47.4	107.425	151.7	194.7	217.2	149.23	49.01
Maximum Depth (cm)	38	6	9.375	13	17.75	27.5	14.19	5.76
Cl (mg/L)	38	787	1539.75	2117.5	2769.5	5395	2330.4	1109.9
SO4-S (mg/L)	38	0.283	0.283	0.7335	15.7225	54.44	8.8704	14.3216
NH4-N (µg/L)	36	19.84	34.7025	81.11	207.85	372.3	121.782	103.052
PO4-P (µg/L)	36	2.828	3.124	4.7535	5.6325	21.41	5.9901	4.2704
TON-N (µg/L)	36	8.83	15.6925	19.04	26.9	55.01	22.2761	11.0677

NO3-N (µg/L)	36	8.83	15.6425	18.28	26.9	55.01	21.8189	11.1906
Al (mg/L)	38	1.898	2.92625	3.2325	3.73025	7.186	3.4542	0.9172
B (mg/L)	38	1.867	2.0785	2.2315	2.44725	3.139	2.2996	0.3115
Ba (mg/L)	38	0.04	0.042	0.045	0.06025	0.096	0.0517	0.0142
Ca (mg/L)	38	34.959	45.69275	64.003	84.18925	147.692	68.7697	27.6698
Fe (mg/L)	38	0.197	0.2985	0.422	0.741	5.194	0.7678	0.9913
K (mg/L)	38	1.174	2.8865	4.346	6.29575	13.302	5.1006	3.1108
Li (mg/L)	38	0.151	0.23425	0.3495	0.43925	0.562	0.3479	0.1174
Mg (mg/L)	38	18.607	24.9385	35.55	47.10675	85.44	38.0352	17.2584
Mn (mg/L)	38	0.024	0.04475	0.0635	0.11525	0.251	0.0825	0.0512
Na (mg/L)	38	623.262	849.6175	1296.083	1720.4395	3195.04	1436.9903	718.5608
S (mg/L)	38	1.884	2.4955	5.375	17.05875	46.613	10.9133	11.9561
Si (mg/L)	38	1.653	2.204	2.6725	3.38075	6.602	2.9449	1.1065
Sr (mg/L)	38	1.413	2.271	3.6435	4.6905	8.931	3.855	1.9124

The principal component analysis identified 7 principal components with eigenvalues >1.0, and an eighth principal component with an eigenvalue of 0.95, together explaining roughly 86% of the variation among the original variables (Table A2.6). Varimax rotation of these 8 components clarified the key associations among the environmental variables. Specific conductance and the most abundant anions and cations were strongly associated with the first componen5 (Table 2.2). Northing and easting UTM coordinates were also associated with the first component reflecting the northwest to southeast orientation of the salinity gradient. The first principal component explained 36.3% of the variance.

Concentrations of a suite of nutrients - phosphate, nitrates, silica as well as iron were associated with the second component and explained 11.4% of the measured variance (Table 2.2). Phosphate and oxygenated nitrogen are both common nutrients, and areas with increased nutrients are likely to have high primary productivity during the day, and increased respiration at night (Wetzel 2001). Silica is an important nutrient, especially in lower trophic levels, for organisms such as diatoms (Wetzel 2001; Volik et al. 2017). An increase in phosphate and oxygenated nitrogen would likely increase the amount of phytoplankton present, as diatoms assimilate silicon to form their frustule, or outer shell (Wetzel 2001). Under oxidizing conditions, iron is present as iron (III), which is insoluble and binds phosphate. When iron is reduced, forming iron (II), the iron dissolves, releasing the previously bound phosphate (Golterman 1995). Redox potential loads negatively onto this component meaning that as oxidation reduction potential decreases, insoluble ferric iron becomes reduced to soluble ferrous iron, thereby increasing dissolved iron concentration, and increasing phosphate concentration as well, as bound oxygenated phosphorous is released from ferric iron as it is reduced.

The third rotated component describes a relationship between dissolved oxygen and ammonium-N concentrations were negatively and positively associated with the third component respectively, accounting for 6.7% of the overall variance (Table 2.2). Thus, sites with high values on component 3 tended to be hypoxic and enriched in ammonium. Various redox potentials are reported for the approximate range in which nitrification/denitrification occurs, with values ranging from -100mV to +250mV (Mitsch & Gosselink 2015). When less oxygen is available, nitrification is less likely to occur resulting in ammonium concentration increases.

Concentrations of manganese and barium were associated with values of the fourth component accounting for 8.2% of the variance (Table 2.2). Both elements are minor cations in the fen complex, with concentrations of barium ranging from 0.04 mg/L to 0.096 mg/L and concentrations of manganese ranging from 0.024 mg/L to 0.251 mg/L (Table 2.1). Using Pearson's correlation coefficient, these cations are two of the five cations whose concentrations are independent of specific conductance, and they are also uncorrelated to northing (Table 2.2), suggesting that their presence in the surface waters is not derived from groundwater influx.

pH and redox values were both positively associated with scores of the fifth component accounting for 7.4% of the variance (Table 2.2). In the saline fen complex, pH values ranged from 6.27 to 7.64, while oxidation reduction potential ranged from 47.4 to 217.2 (Table A2.1; Table 2.1). This suggests that both pH and redox potential remain rather stable throughout the saline fen complex.

Aluminum concentration, water temperature, and maximum depth were independent of one another and of all other variables as indicated by their strong and unique associations with components 6,7, and 8, and accounted for 5.1%, 6.3% and 4.9% of the variance respectively (Table 2.2).

Table 2.2: Varimax rotated component loadings of environmental data along with factors' variance sums of squares after extraction, and proportions of variance explained by 8 rotated components. Bold-faced values indicate the strongest association of each variable with a component. Variables are sorted in decreasing order of their strength of association with their most highly-associated component.

Variable (Units)	PC1	PC2	PC3	PC4	PC5	PC6	PC7	PC8
Sr (mg/L)	**0.939**	<0.001	<0.001	0.254	<0.001	<0.001	<0.001	<0.001
Mg (mg/L)	**0.935**	<0.001	<0.001	0.262	<0.001	<0.001	-0.128	<0.001
Na (mg/L)	**0.925**	0.162	<0.001	0.187	<0.001	-0.126	<0.001	<0.001
Cl (mg/L)	**0.919**	0.173	<0.001	<0.001	<0.001	<0.001	-0.101	<0.001
Spec Cond (μS/cm)	**0.914**	0.125	<0.001	<0.001	0.123	<0.001	<0.001	<0.001
Ca (mg/L)	**0.895**	<0.001	-0.123	0.359	<0.001	<0.001	-0.111	<0.001
S (mg/L)	**0.856**	<0.001	-0.117	-0.170	<0.001	0.107	-0.361	<0.001
K (mg/L)	**0.816**	<0.001	<0.001	0.167	0.302	-0.138	0.212	<0.001
SO4-S (mg/L)	**0.767**	<0.001	<0.001	-0.283	<0.001	0.222	-0.312	<0.001
B (mg/L)	**0.761**	<0.001	0.175	<0.001	0.169	<0.001	<0.001	<0.001
Li (mg/L)	**0.733**	<0.001	0.144	0.288	<0.001	-0.227	0.282	<0.001
Easting	**0.648**	0.612	-0.241	<0.001	<0.001	-0.102	0.116	0.105
Northing	**-0.694**	-0.440	0.357	0.186	<0.001	<0.001	-0.102	-0.110
Fe (mg/L)	<0.001	**0.849**	0.110	0.209	-0.222	-0.111	-0.248	<0.001
PO4 (μg/L)	0.331	**0.846**	-0.117	0.101	<0.001	-0.115	-0.102	<0.001
TON (μg/L)	<0.001	**0.557**	0.522	<0.001	-0.153	0.245	<0.001	0.178
Si (mg/L)	<0.001	**0.573**	<0.001	<0.001	-0.290	0.406	<0.001	0.439
DO (mg/L)	-0.212	-0.129	**-0.529**	-0.223	0.284	0.132	0.436	0.290
NH4 (μg/L)	<0.001	<0.001	**0.832**	<0.001	<0.001	0.102	0.262	<0.001
Mn (mg/L)	0.138	0.213	0.226	**0.854**	0.133	<0.001	<0.001	<0.001
Ba (mg/L)	0.303	<0.001	-0.244	**0.832**	-0.140	0.147	-0.109	0.160
pH	0.119	<0.001	-0.114	<0.001	**0.913**	-0.115	-0.134	<0.001
Redox	<0.001	-0.268	0.104	<0.001	**0.793**	0.144	0.243	<0.001
Al (mg/L)	-0.174	<0.001	0.121	<0.001	<0.001	**0.877**	<0.001	-0.162
Water Temp.(˚C)	-0.127	-0.244	0.179	<0.001	<0.001	<0.001	**0.879**	<0.001

Maximum Depth (cm)	<0.001	<0.001	<0.001	<0.001	0.121	-0.160	<0.001	**0.919**
Factor Var.	9.442	2.951	1.74	2.124	1.931	1.338	1.64	1.265
Prop. Var. Expl.	0.363	0.114	0.067	0.082	0.074	0.051	0.063	0.049
Cum. Var. Expl.	0.363	0.477	0.544	0.626	0.7	0.751	0.814	0.863

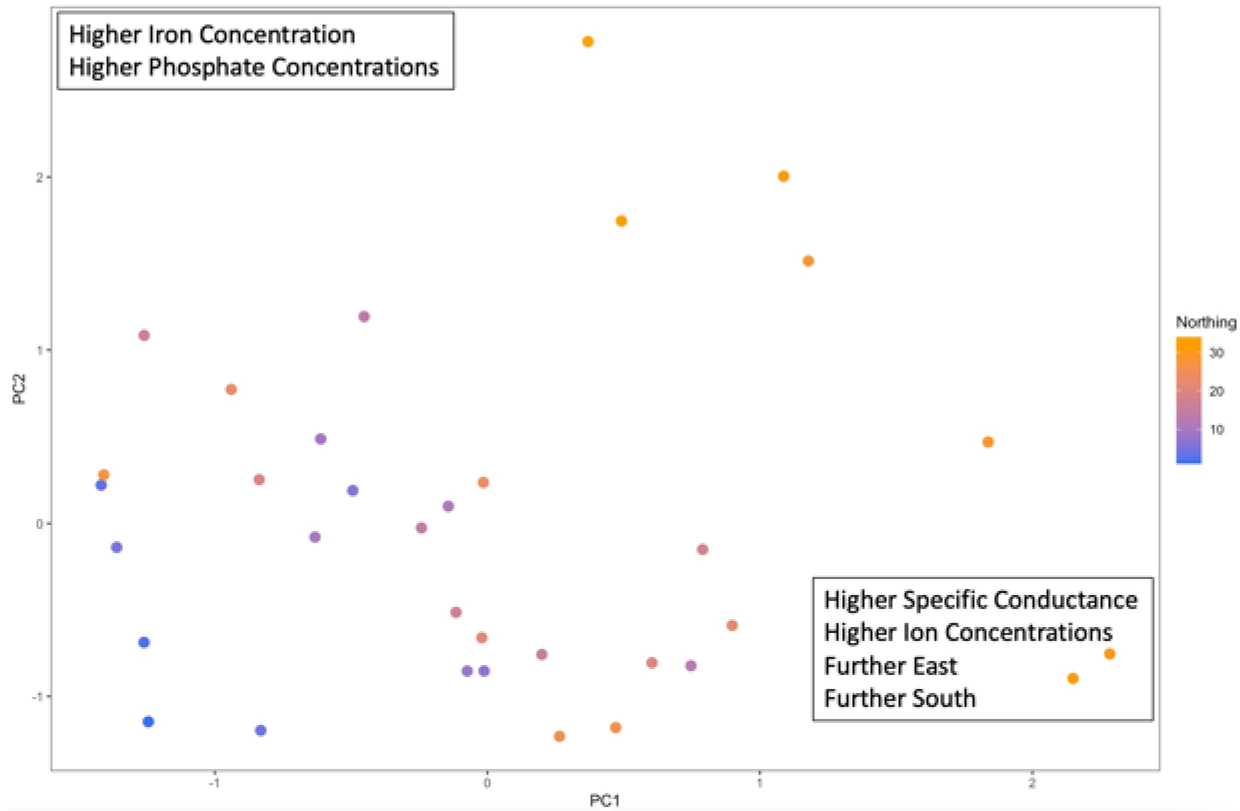

Figure 2.4: Distribution of 34 sample sites relative to scores of rotated principal components 1 (summarizing salinity) and 2 (summarizing nutrient concentrations). The colour gradient depicts the location of the site within the saline fen complex, where the northernmost site was given a northing score of 1, and northern sites are depicted in blue, while southern sites are depicted in orange.

The conductivity gradient located at the saline fen complex is correlated to only various ion concentrations and location within the fen (Table 2.2), which can allow for in depth analysis of how conductivity influences biotic and abiotic processes in a natural fen complex.

Sandhill fen watershed was constructed in 2012 as a proof-of-concept investigation to create initial conditions allowing for the eventual formation of a self-sustaining fen complex (Wytrykush et al. 2012; Syncrude Canada Ltd. 2020; Hartsock et al. 2021a; Vitt et al. 2016; Clark et al. 2019). Sandhill fen was constructed on top of consolidated tailings and tailings sand, with a 10-m tailings sand cap (Vitt et al. 2016; Syncrude Canada Ltd. 2020). A layer of clay till and a layer of peat were placed on top of this cap (Vitt et al. 2016; Syncrude Canada Ltd. 2020). Over the 6 years since its creation in 2013 the specific conductance!SD of its surface waters increased gradually from 1,143!275 μS/cm (n=10) in 2015, to 2,560!305 μS/cm (n=5) in 2019 (Hartsock et al. 2021b). Surface water conductivity in the reclaimed landscape has a reported maximum near 3,000 μS/cm occurring in 2015 (Biagi et al. 2019) and in 2019 (Hartsock et al. 2021), with opportunistic wetlands predominantly containing freshwater, conductivity ranges from fresh to moderately brackish (Hawkes et al. 2020). While these conductivity values continue to be lower than observed in naturally saline systems in Alberta’s boreal region (Table A2.1) final results of reclamation projects may potentially result in slightly brackish to saline systems (Purdy et al. 2005; Hartsock et al. 2021b). Therefore, it is important to understand the influence of elevated conductivity on biotic and abiotic factors associated with the ecosystem to provide a frame of reference for assessing the health of reclaimed ecosystems.

Part of the difficulty in assessing reclaimed landscapes within oil sands mine lease areas is that guidelines of success have only recently been identified (e.g., Rooney & Bayley 2011 for marshes; AEP 2015 for reclaimed well pads), and surface waters in reclaimed landscapes have not yet reached equilibrium (Hartsock et al. 2021b). Additionally, water quality guidelines are exceeded in many undisturbed systems including the saline fen complex, and acid fens (Hartsock et al. 2021b). Naturally saline and acidic aquatic ecosystems occur in undisturbed environments in northern Alberta due to the groundwater that sustains them (Wells & Price 2015, Purdy et al. 2005; Trites & Bayley 2009), and reclaimed systems with abiotic and biotic features similar to these systems should meet the criteria of successful reclamation. Local water quality guidelines reflecting the natural surrounding habitat are essential in developing proper assessment tools to use in the AOS.

Summary

The objective of this chapter was to summarize the chemical conditions present along the salinity gradient at the saline fen complex and elucidate patterns among chemical conditions along various chemical gradients. The salinity gradient within the saline fen complex increases in a northwesterly to southeasterly direction, as described by Wells and Price (2015). The conductivity values within the fen system are greater than what is typically seen in the reclaimed landscape (Hartsock et al. 2021b; Biagi et al. 2019; Hawkes et al. 2020), but the wetlands forming in reclaimed portions in the Athabasca oil sands region may be more likely to represent naturally saline systems (Hartsock et al. 2021b; Purdy et al. 2005) than freshwater systems. Thus, biological and physicochemical information describing naturally saline systems is essential to allow one to compare reclaimed systems with natural systems containing similar water quality.

Chapter 3: Variation in Macroinvertebrate Community Composition Along a Gradient of Salinity in a Boreal Saline Fen Complex

Introduction

Wetlands are important ecosystems that provide many important ecological services to the surrounding landscape. Wetlands protect the surrounding area from floods by acting as natural flood plains, which store water, and filter water by sequestering natural and anthropogenic contaminants in sediments and plant tissues (Mitsch & Gosselink 2015; Foote & Krogman 2006). Additionally, wetlands are a source of biodiversity supporting flora and fauna uniquely adapted to these ecosystems (Wissinger 1991; Gibbs 2000; Foote & Krogman 2006; Mitsch & Gosselink 2015). Wetlands account for nearly two thirds of the landscape in northern Alberta's boreal region (Rooney & Bayley 2011). Open pit mining for bitumen extraction has changed the landscape drastically in certain areas in which lease areas are excavated to create open pit mines. Activity to 2017 had created a mining footprint with an area of roughly 900 km^2 (GOA 2017). However, mining companies must conduct research to determine best reclamation practices as part of the terms of reference of their mining licenses (Wytrykush et al. 2012; Vitt et al. 2016; Rooney & Bayley 2011; Kovalenko et al. 2013; Hartsock et al. 2021b). Although reclaimed areas need not be identical to the ecosystems lost, they must have equivalent land capabilities, meaning that they must support the ecological processes that occurred prior to mining (GOA 2021; GOA 2015; Rooney & Bayley 2011). Due to their abundance on the landscape, wetlands are a major focus of research into the reclamation process. A significant consideration in reclaiming wetlands relates to the materials used to rebuild the postmining landscape (BGC 2010). The use of saline sodic shale and tailings sand material (which contains residual tailings water enriched with NaOH used in the bitumen refining process) to create the subsoil results in reclaimed and opportunistic wetlands that tend to have conductivity levels and salt concentrations that are slightly higher than most natural freshwater ecosystems in the area (Hartsock 2021b; Purdy et al. 2005; Kovalenko et al. 2013; Wells & Price 2015). Synoptic studies of the aquatic invertebrates and submerged aquatic vegetation communities of opportunistic and constructed wetlands in mine lease areas suggest that many taxa are intolerant to waters where conductivity exceeds 1,500 uS/cm (Rooney and Bayley 2011; Moore 2021).

Ecosystem function is sustained by the transfer of energy from the detrital pool and photosynthetic producers at the base of the food web, through multiple levels of consumers to apex predators, with each trophic level playing an important role in maintaining the system through both top-down and bottom-up control (Pimm and Lawton 1977; Moore et al. 2004). Invertebrates play a key role in this energy transfer, supporting higher trophic levels by converting carbon stored in lower trophic levels, into a form that becomes available through predation to organisms at higher trophic levels (Gullan & Cranston 2010). Additionally, invertebrates often have well-defined environmental requirements and tolerances, reflecting on adaptations that have occurred through their evolution (U.S. EPA 2002). Consequently, the local invertebrate community can often yield insight into the condition of the ecosystem at that location (U.S. EPA 2002), and invertebrates are therefore often used as biological indicators (Mitsch & Gosselink 2015; Merritt et al. 2019). Indices of ecological condition using the aquatic macroinvertebrate community include the Hilsenhoff Biotic Index (HBI) (Hilsenhoff 1988), and Indices of Biotic Integrity (IBI) which were initially created to be used with fish taxa (Karr 1981), were later adapted to include benthic invertebrate taxa of streams (Kerans & Karr 1994), and then to include wetland invertebrate taxa (U.S. EPA 2002). Analyzing macroinvertebrate community composition in wetlands along a conductivity gradient is likely to yield insight in identifying taxa and community assemblages associated with (and ultimately diagnostic of) specific ranges of conductivity.

A species' presence at a given level of salinity can reflect, in part, their osmotic regulation capacity (Chapman 1975; Palleres et al. 2015; Silberbush & Blaustein 2011; Patrick & Bradley 2000). Species surviving in freshwater environments can hyperregulate and selectively absorb ions from their environments and release excess water in their feces and urine (Patrick & Bradley 2000). Species surviving in saline environments are either osmoregulators, which are able to concentrate salts in their urine and feces to regulate salt concentrations in their haemolymph, or osmoconformers, which concentrate non-toxic solutes (typically proline) in their tissues in order to maintain osmotic balance between the tissues and their environment (Pallares et al. 2015; Patrick & Bradley 2000). Euryhalic species able to survive in both environments can hyperregulate in freshwater environments, and either hyporegulate or osmoconform in more saline environments (Chapman 1975; Pallares et al. 2015). This is the case for members of the mosquito family Culicidae, specifically of the genera *Aedes* and *Culex*, which includes species able to survive to pupation in ecosystems containing freshwater, and in ecosystems containing water as saline as seawater (Chapman 1975; Grueber & Bradley 1994; Patrick & Bradley 2000). Stenohalic species (such as pond snails: Lymnaeidae; Mushet et al. 2015) can only perform one of these processes and therefore are limited to relatively narrow ranges of specific conductance. *Lymnaea stagnalis*, is a dominant gastropod species in aquatic systems with specific conductance values below 5,000 µS/cm, but is then replaced by *Stagnicola* species, which are unable to survive in specific conductance values greater than 10,000 µS/cm (Mushet et al. 2015). This results in a freshwater community that is comprised of euryhalic and stenohalophobic species, while saline communities are comprised of euryhalic and stenohalophilic species. Due to the energetic expense of osmotic regulation at higher levels of conductivity, body size of individuals is negatively related to conductivity (Lancaster & Scudder 1986) and will affect various organisms differently (Van Meter et al. 2011). However, the energetic costs of osmotic regulation by tolerant individuals able to survive in saline conditions (Chapman 1975; Lancaster & Scudder 1986; Mushet et al. 2015) may be reflected in small size rather than a reduced ability to survive and reproduce (Van Meter et al. 2011).

Community composition of aquatic macroinvertebrates varies along a gradient of conductivity (Kovalenko et al. 2013; Mushet et al. 2015; Lancaster & Scudder 1986). Lancaster and Scudder (1986) observed declining Coleoptera and Hemiptera diversity when studying a suite of lakes in British Columbia, Canada. Richness declined from 22 species in a lake with specific conductivity of 56 μS/cm, to 11 species in a lake with specific conductivity of 13,115 μS/cm. In the analysis, water boatmen (Corixidae) and beetle (Coleoptera) taxa were either present along the entirety of the gradient, present only in lakes with the highest levels of salinity identified in the analysis, or present only in lakes with the lowest levels of salinity present in the analysis (Lancaster & Scudder 1986). Thus, community composition as well as biodiversity clearly varies across a salinity gradient, as there was evidence of taxa turnover, yielding communities comprised of different subsets of taxa at lower levels of salinity when compared to communities present in lakes with higher levels of salinity (Lancaster & Scudder 1986). Bendell-Young et al. (2000) compared the macroinvertebrate community of reference wetlands to the community of constructed wetlands in the AOS, in which specific conductivity±SD ranged from 56.6±58 μS/cm in a reference wetland to 1,860±250 μS/cm in a wetland forming in post-mining lease areas. In wetlands with greater values of specific conductance, biodiversity was reduced, but biomass was unaffected (Bendell-Young et al. 2000). In both of these studies it remains unclear whether increases in salinity are associated with a gradual loss of species and shift in community composition or whether community change points (thresholds) exist along a salinity gradient yielding abrupt changes in community composition, and unique communities on either side of the change point. I postulate that invertebrate biodiversity (richness), biomass and abundance are independent of salinity (measured using specific conductivity (µS/cm)) until a threshold is reached, beyond which, richness, but not biomass, becomes reduced as invertebrates tolerant of high salinity levels seek refuge from predators at higher levels of salinity, thus minimizing competition and predation risk, allowing for an increased ability to survive and reproduce.

In this study of the influence of specific conductance, I minimized the influence of potentially confounding environmental variables by studying the fauna of a suite of morphometrically similar pools (flarks) in a boreal saline fen (Wells & Price 2015). The pools studied, constitute a naturally occurring gradient of salinity, with specific conductance values of pools sampled ranging from moderately brackish to subsaline at the time of sampling, all within a 1.2-km length of the complex and an elevation change of less than 10 m (Wells & Price 2015; Table 1.1; Figure 1.2; Table 2.1).

Postulates

1) Total abundance will be positively associated with greater specific conductance.
2) Family richness will be negatively associated with greater specific conductance.
3) A threshold of specific conductivity will be observed at which a subset of salt-intolerant species, will be replaced by a subset of salt-tolerant species.

Methods

Field Methods

52 locations within the saline fen complex were chosen from the 122 sites at which specific conductance values had previously been measured (September 5, 2020; Figure 2.1; Figure 2.2; Figure 2.3). Sites were stratified-randomly selected to be dispersed evenly across a log-transformed specific conductance gradient. The locations selected ranged from 3,757 μS/cm to 20,170 μS/cm (Figure 2.1; Figure 2.2). Each site was then classified as a flark (n=38), a pond (n=6) or a flark/pond (n=9) based on its shape, water volume and ecological characteristics (Figure 2.3). To minimize heterogeneity across the gradient, only flarks were used for this analysis (Figure 2.2; Figure 2.3; Table 2.1; Table A2.1). A flark was characterized as a shallow depression filled with water and covered in emergent vegetation.

Upon arrival at each site, the approximate length and width of the wetted area were estimated, and 3 locations were chosen for aquatic invertebrate sampling based on previously stated criteria (Chapter 2). Fauna were collected using a 32-cm wide D-frame sweep net with 250-μm mesh, following CABIN's jab and sweep method, in which the sweep net is used to collect invertebrates by jabbing the emergent vegetation and sediment to dislodge invertebrates that are then swept into the net by moving the net through the emergent vegetation (ECCC 2018). To standardize sampling effort, each sample consisted of 20 jabs. The net contents were emptied into a 250-μm mesh sieve bag, which was rinsed in the wetland to remove silt and fine organic material, before being emptied into a polyethylene soil bag and preserved with 70% ethanol. All samples were collected between September 6 and 8, 2020.

Laboratory Methods

In the laboratory, a sample was emptied onto a stacked set of standard soil test sieves (4.00, 1.00, 0.50, and 0.25 mm aperture) and rinsed with running tap water to separate the sample into its component size fractions (Ciborowski 1991). The invertebrates in each size fraction were sorted from aliquots of the sample beneath a dissecting microscope, identified to the lowest practical taxonomic level and enumerated. Invertebrates were identified using the keys of Merritt et al. (2019) and Clifford (1990). The invertebrates from 20 samples were sorted and identified in their entirety. Thereafter, rarefaction species abundance curves were created to estimate asymptotic species richness and to derive subsampling criteria that would provide acceptable precision of counts for the remaining samples. For the remaining samples, the first 100 individuals sorted from the 4.00 and 0.25-mm size fractions were identified and enumerated. The first 200 individuals sorted from the 1.00 and 0.50 mm size fractions were identified and enumerated. After sorting, the remaining sorted portion of the sample, and any unsorted sample fractions were air-dried separately at room temperature and weighed to the nearest 0.01 g. The remaining masses of sorted and unsorted fractions were used to estimate the total number of individuals within each size fraction. The sample total was determined by summing the estimated abundance of each taxon in each size fraction. For each site, two samples were sieved and sorted, and one sample was archived. Samples were sorted and their contents were identified in stratified-random order based on the specific conductivity values of their respective sites.

Statistical Analysis

The total abundance and family richness of each site were calculated by summing the number of individual invertebrates and the number of unique taxonomic families, respectively, found in the two replicates analyzed. All statistical analyses were conducted using R version 3.6.1 (R Core Team 2021).

Community composition – Similarities among sites

Variation in community composition was interpreted at the genus level of taxonomic resolution where possible. If genera were present in fewer than 5 sites, the genera of those families were combined to form family abundance, and if a family was present in fewer than 5 sites, those families were excluded from the community composition calculations.

Community composition was assessed in terms of the relative abundances of each taxon at each site. All data were Hellinger transformed (taking the square root of the relative abundance of each taxon), which minimizes the effect of zero values and of differences in total abundance among sample units (Legendre & Gallagher 2001).

Non-metric multidimensional scaling (NMDS) analysis was conducted using the Hellinger transformed values to evaluate similarity of community composition among sites (Table A3.4) and to identify the taxa (Table A3.5) most strongly associated with particular sites. The NMDS used 3 axes to fit the data to minimize the stress value associated with the analysis (Stress (3 axes) = 0.081; Stress (2 axes) =0.121).

Community Composition – Association with Environmental Variables

A transformation-based redundancy analysis (tb-RDA) was conducted to determine the influence of water chemistry and ecological variability on the community composition of macroinvertebrates (Borcard et al. 2018). Relative abundance (Hellinger transformed) data were used as dependent variables. To avoid collinearity among the independent variables used as explanatory variables in the redundancy analysis, only one representative variable loading onto each of the 8 Principal Components identified as characterizing environmental variation in

Chapter 2 was included in the redundancy analysis model (Table 2.2). The independent variables used in the analysis included specific conductance, pH, and concentrations of phosphate, ammonium, manganese, aluminum, water temperature, and maximum depth (Table 2.1). To verify that collinearity among included variables was acceptably low, the variance inflation factor (VIF) was evaluated for each independent variable in the model (Borcard et al. 2018). All VIFs were <2.0, corroborating that the explanatory variables were independent of one another (Borcard et al. 2018). The proportion of variation explained by the independent variables was then adjusted using Ezekiels' formula (equation 3.2) to remove biases associated with the number of explanatory variables used and random correlations (Borcard et al. 2018; Legendre & Legendre 2012).

Ezekiel's equation (Borcard et al. 2018):

$R^2_{adj} = 1 – ((n-1)/(n-m-1))*(1-R^2)$

n = number of objects in the model

m = number of degrees of freedom of the model.

Permutation tests were then conducted to determine the statistical significance of the model (Table 3.3), axes (Table 3.5), and independent variables (Table 3.4) (Borcard et al. 2018). A statistically significant model suggests that the community matrix and the explanatory variables used are linearly related to one another.

Threshold Indicator Taxon Analysis (TITAN) (Baker & King 2010)

Threshold Indicator Taxon Analysis (TITAN) evaluates individual taxon responses along an environmental gradient by calculating an indicator value (IndVal; Dufrêne & Legendre 1997) for either side of a partition dividing the environmental gradient into sections. The IndVal for a given species is a function of the species' relative abundances and occurrences at sample locations along the gradient. Although IndVal is a useful index when a taxon is abundant and occurs frequently, scores for rare, uncommon, or any non-dominant species are biased and underrepresent the taxon's true diagnostic value (Baker & King 2010). To account for this in TITAN, IndVal scores are standardized by converting the maximum IndVal for a species to a z-score (distance (standard deviation units) from the mean) by determining a null distribution (mean and standard deviation) based on random association through permutations (Baker & King 2010). Purity and reliability are metrics used in selecting potential indicator taxa (Baker & King 2010). Purity is the percentage of bootstrap replicates that have a response direction that is the same as the observed response direction. Reliability is the percentage of bootstrap replicates resulting in an IndVal p-value less than 0.05 indicating the magnitude of response at a given change point differs significantly from random permutation. Taxa with both purity and reliability greater than 0.95 are selected and labeled as indicators. These indicators are defined as either sensitive or tolerant if their abundance values decrease or increase respectively along the environmental gradient. A community level change point is then predicted for both the tolerant and sensitive community by summing the z scores of selected taxa along the gradient. The change point is predicted to occur at the point along the gradient yielding the greatest sum(z) value for each community. Confidence limits for this value are calculated through bootstrap resampling. This analysis was conducted with 250 IndVal permutation replicates, and 500 bootstrap resampling for z score distributions, and a purity and reliability cut-off of 0.95 (Figures 3.6 – 3.8; Tables 3.8 and 3.9; Figure A3.4).

Saline Fen Complex macroinvertebrate Indices of Salinity

In order to visualize the proportion of the macroinvertebrate community represented by sensitive and tolerant taxa along the gradient of specific conductance, and to create an index of salinity tolerance within the community composition the proportion of the community represented by tolerant or sensitive taxa was calculated by summing the taxa's relative abundance values at each site. The saline-sensitive index was calculated for each flark by summing the numbers of individuals identified as sensitive by TITAN and dividing by the total number of animals collected in the flark. Similarly, the saline-tolerant index was calculated by summing the number of individuals identified as tolerant by TITAN and dividing by the total number of animals collected in the flark. Values of the saline sensitive index and the saline tolerant index were each plotted against specific conductance (Figures 3.9 and 3.10 respectively). A generalized linear model was then created for both the tolerant and sensitive taxa to determine the relationship between relative proportion of animals in a sample that were salt-sensitive (Figure 3.9) or salt-tolerant (Figure 3.10) and specific conductance (Log-transformed). I use a quasibinomial probability distribution and the logit function (Table A3.10; Figure A3.5; Table A3.11; Figure A3.6). A quasibinomial family probability distribution is often used when data are bounded between two values, such as proportion data (Demetrio et al. 2014; Gomez-Deniz 2019). A binomial distribution is best fit, when the ratio between residual deviance and degrees of freedom is equal to one. This is not the case for the quasibinomial distribution, which is more capable of handling overdispersion (residual deviance > degrees of freedom) and underdispersion (residual deviance < degrees of freedom; Papanikolaou et al. 2021). Data were plotted alongside the model's predicted values and the 95% confidence interval of the slope (Figures 3.9 and 3.10).

Results

Chloride ion concentration and specific conductance

Salinity in the study site was characterized by specific conductance because of its ease of measurement and high correlation with total dissolved solids. However, toxicity to salts is most commonly characterized by the chloride ion concentration. The guideline for maximum short-term chloride concentration to sustain freshwater aquatic life is 640 mg/L, and the long-term exposure concentration is 120 mg/L (GOA 2018). All samples included in this analysis are from locations where chloride concentration exceeds the CCME short-term guidelines. To predict the specific conductance equivalent to these concentrations of chloride ion, I performed a linear regression between the two variables based on the field conductivity measurements and laboratory analyses of anions from the 52 sites sampled.

Specific conductance was strongly associated with the concentration of chloride ions measured at the 52 study pools (Fig. 3.1). Based on this relationship, the predicted±SD specific conductance corresponding to the long- and short-term exposure guidelines to sustain freshwater life are 1682±406, and 3341±SD 486 μS/cm, respectively.

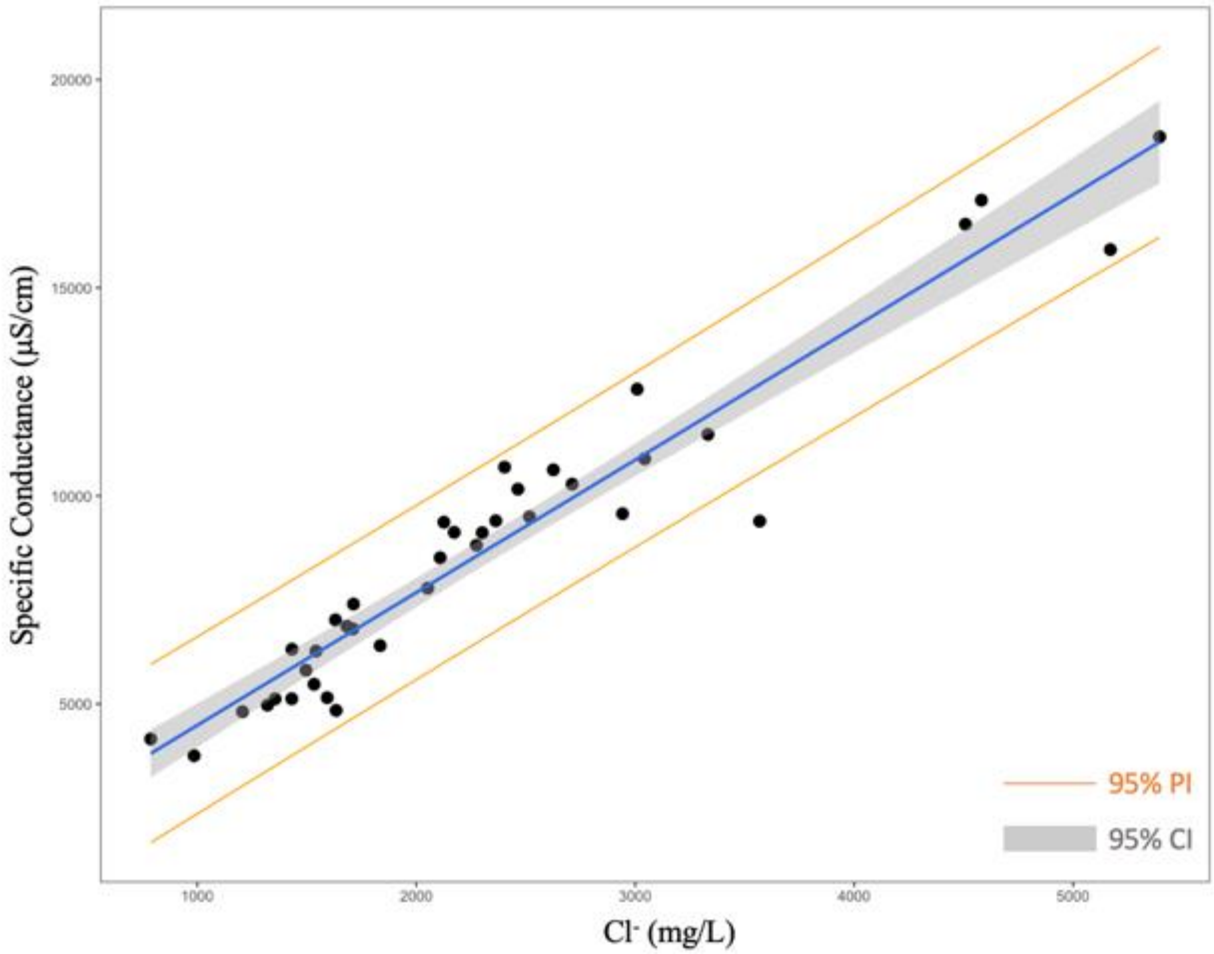

Figure 3.1: Relationship between concentration of chloride and specific conductance measured in 52 waterbodies at the saline fen complex, September 6-8 2020. Equation takes the form: Specific conductance (µS/cm) = 1300.3 +3.1886*([Cl^{-1}] (mg/L)) ($R^2 = 0.93$, p <0.001). CI is the confidence interval of the slope, and PI is the prediction interval of the model.

Abundance and family richness

The abundance of aquatic invertebrates collected from each pool was independent of specific conductance values ($R^2 = 0.01$; $p >> 0.05$); Figure 3.2; Table A3.1).

Richness varied broadly across the salinity gradient, with values ranging from 8 to 28 families (Fig. 3.3). Richness was weakly but marginally significantly negatively associated with specific conductance (p=0.048, R^2 =0.11; Table A3.3; Figure 3.3).

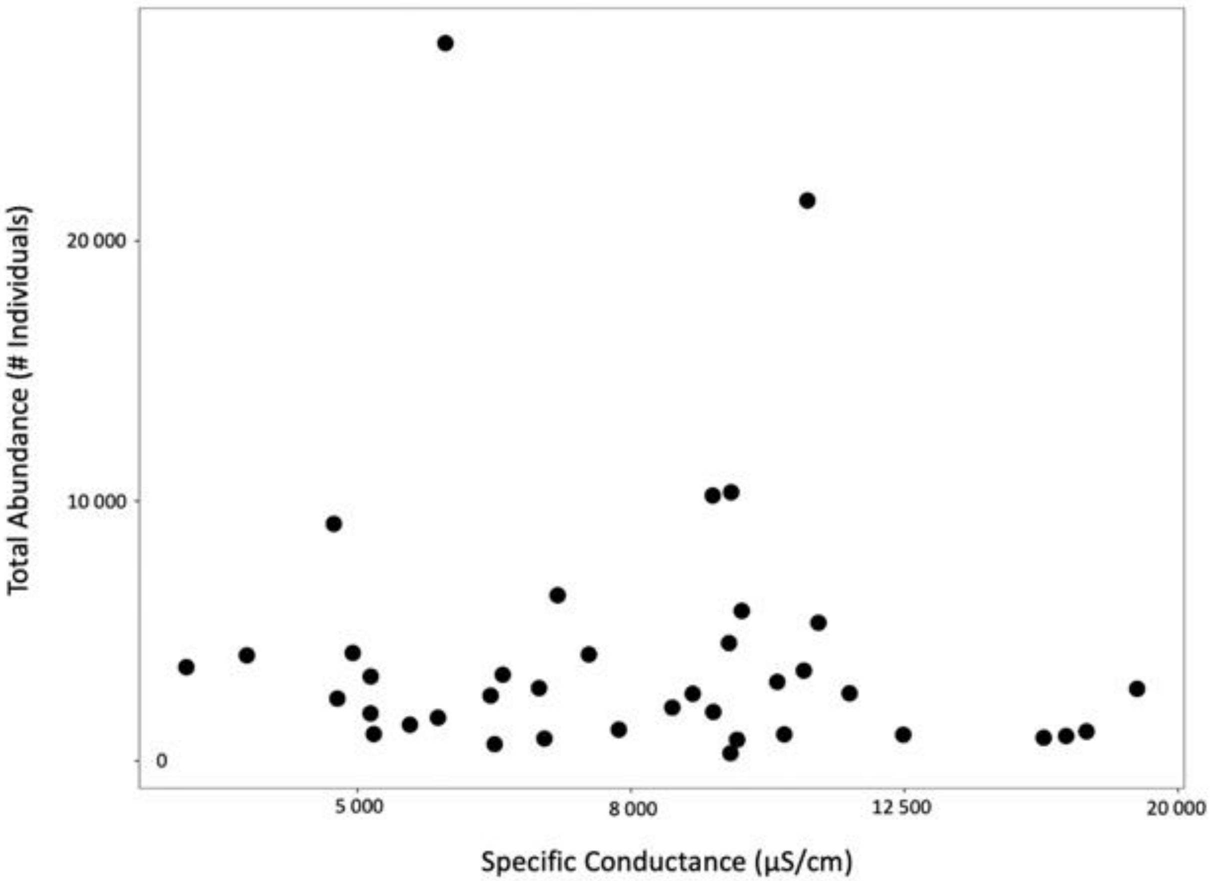

Figure 3.2: Relationship between specific conductance and total number of aquatic invertebrates collected from 38 flarks in the saline fen complex.

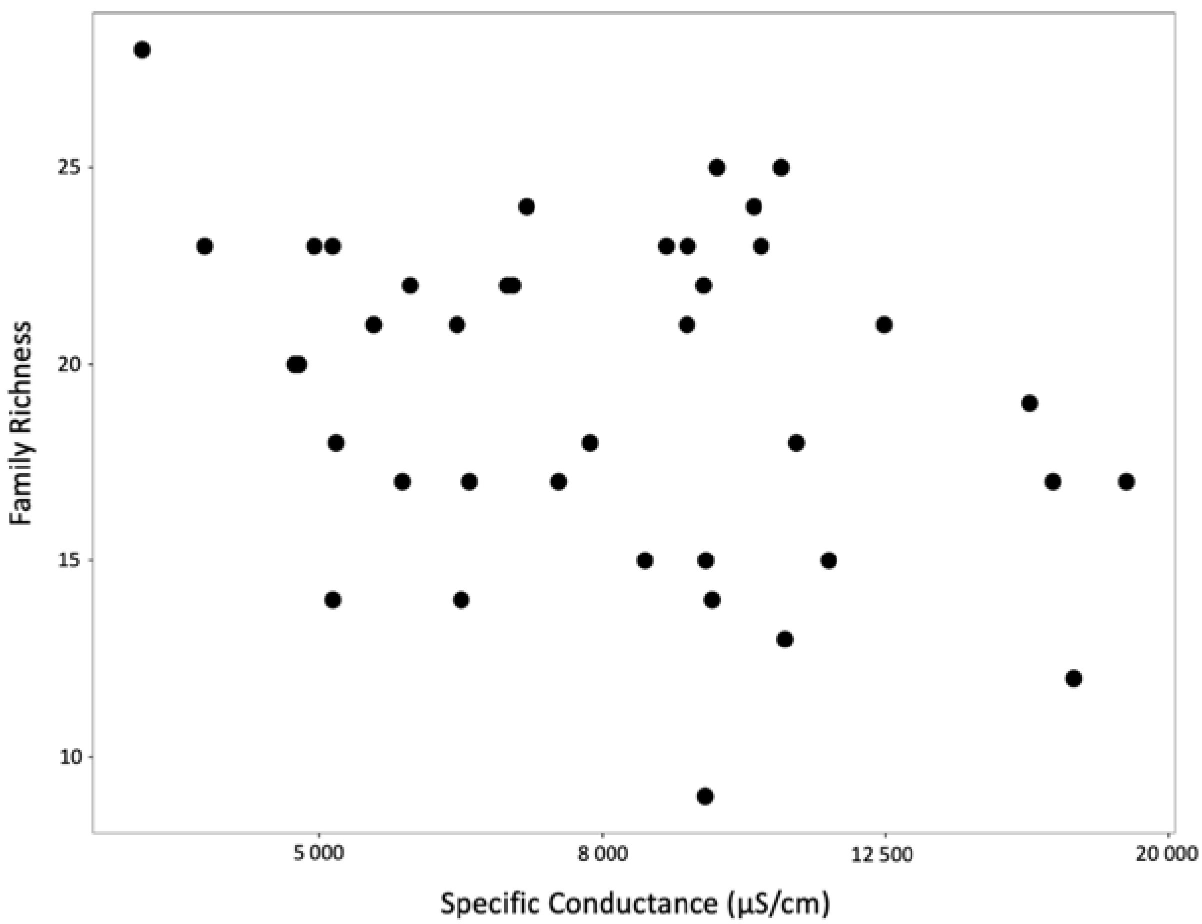

Figure 3.3: Relationship between specific conductance and family richness in 38 flarks in the saline fen complex. Richness = 51.399 -8.136*(Log_{10}(Specific conductance) (uS/cm))

Community composition – Similarities among sites

Eighty-five genera from 40 families of macroinvertebrates were identified within the saline fen complex. Genera present at less than 5 sites were combined to family level (e.g., *Octhera*, *Setacera*, and Ephydridae < 0.5 mm were combined into Ephydridae). Families present at less than 5 sites were removed from the analysis. After conducting these operations, 60 taxa were included in the analysis from a total of 34 families including 29 genera.

Two families were present in all 38 flarks (Chironomidae and Sciomyzidae). Chironomidae was abundant throughout the gradient, with relative abundance values greater than 0.20 in 34 of the 38 flarks. Sciomyzidae was present mostly as pupae, and relative abundance values for Sciomyzidae were below 0.025 in 33 of the 38 flarks. Flarks located in the northern region of the fen typically contained water with lower specific conductance values, and were dominated by Gastropoda (*Lymnaea stagnalis*, *Stagnicola*, Planorbidae) and Odonata (*Nehalennia*, *Aeshna*, *Somatochlora*, *Pachydiplax longipennis*). Flarks in the southern region of the fen typically contained water with greater specific conductance values and were dominated by corixids (*Dasycorixa*) and dipterans, especially mosquitos (*Aedes*, *Culex*, *Culiseta*).

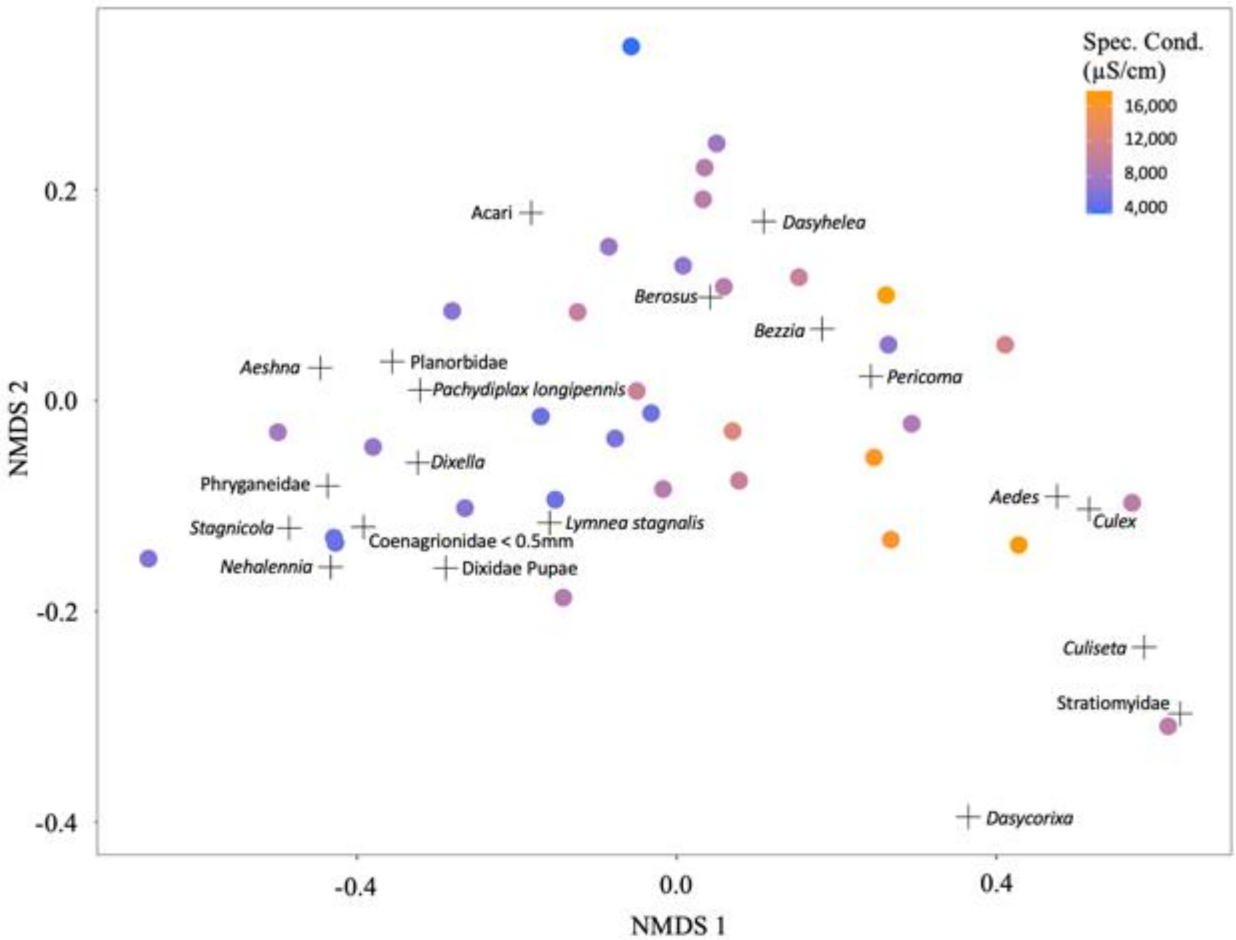

Figure 3.4: Non metric multi-dimensional scaling (NMDS) ordination of relative community composition of aquatic invertebrates in 34 flarks of the saline fen complex. Coloured points represent sites. Points are coloured to correspond with the specific conductance of the sample site. Taxa listed are those identified as indicators of sensitivity to, or tolerance of specific conductance as determined by TITAN (Fig 3.7). Sensitive taxa (ordered by increasing NMDS axis 1 scores) include *Stagnicola*, *Aeshna*, Phryganeidae, *Nehalennia*, Coenagrionidae <0.5 mm, Planorbidae, *Dixella*, *Pachydiplax longipennis*, Dixidae pupae, Acari, and *Lymnaea stagnalis*. Tolerant taxa (ordered by increasing NMDS axis 1 scores) include *Berosus*, *Dasyhelea*, *Bezzia*, *Pericoma*, *Dasycorixa*, *Aedes*, *Culex*, *Culiseta*, and Stratiomyidae.

Table 3.1: Species scores of indicator taxa (Fig 3.7) for NMDS analysis (Figure 3.4)

	MDS1	MDS2	MDS3	TITAN
Stagnicola	-0.485	-0.121	-0.068	Sensitive
Phryganeidae	-0.437	-0.081	0.066	Sensitive
Coenagrionidae<0.5 mm	-0.392	-0.120	0.097	Sensitive
Nehalennia	-0.433	-0.158	0.058	Sensitive
Aeshna	-0.446	0.031	-0.073	Sensitive
Planorbidae	-0.356	0.037	0.095	Sensitive
Pachydiplax longipennis	-0.321	0.010	-0.028	Sensitive
Dixella	-0.324	-0.059	0.085	Sensitive
Dixidae Pupae	-0.289	-0.159	0.094	Sensitive
Lymnaea stagnalis	-0.159	-0.116	0.160	Sensitive
Acari	-0.182	0.178	-0.083	Sensitive
Berosus	0.042	0.098	-0.104	Tolerant
Dasyhelea	0.109	0.170	-0.056	Tolerant
Bezzia	0.182	0.068	0.028	Tolerant
Pericoma	0.243	0.023	-0.184	Tolerant
Dasycorixa	0.365	-0.395	-0.069	Tolerant
Aedes	0.476	-0.091	-0.043	Tolerant
Culex	0.516	-0.103	-0.095	Tolerant
Culiseta	0.585	-0.234	0.140	Tolerant
Stratiomyidae	0.630	-0.297	0.111	Tolerant

The NMDS analysis was able to ordinate the sample sites in three dimensions (Figures 3.4 A3.2, A3.3), with a stress value of 0.08. The order of sites across the first axis broadly corresponded with specific conductance (Fig 3.4). Sites at which specific conductance was low had negative scores of NMD axis 1. These flarks tended to be dominated by snails (*Stagnicola, Lymnaea*, Planorbidae), damselflies (Coenagrionidae), dragonflies (*Aeshna*, *Pachydiplax longipennes*) and phryganeid caddisflies. Flarks in which specific conductance was high had positive scores and were dominated by true flies (Diptera), including mosquitos (*Aedes*, *Culex*, *Culiseta*), moth flies (Psychodidae: *Pericoma*), biting midges (*Dasyhelea*, *Bezzia*), soldier flies (Stratiomyidae) as well as water scavenger beetles (Hydrophilidae: *Berosus*), and water boatmen (*Dasycorixa*) (Figure 3.4; Table A3.4; Table 3.1).

Community Composition – Association with Environmental Variables

The constraining variables used in the redundancy analysis of macroinvertebrate community composition included specific conductance, phosphate concentration, ammonium concentration, manganese concentration, pH, aluminum concentration, water temperature, and maximum depth (Table 2.1). The constraining variables used in the RDA accounted for 43.7% of the variation in invertebrate community composition. The VIF-adjusted proportion of variance explained by the constraining variables was 25.6%. Results of the permutation tests indicated that the analysis was statistically significant ($p<0.001$; Table 3.3), with the first two constrained components being significant (Table 3.5). Specific conductance, phosphate concentration, water temperature, and maximum depth were all statistically significant predictors of aquatic macroinvertebrate community composition, (p=0.001, 0.002, 0.014 and 0.033 respectively (Table 3.4).

The first constrained component exhibited a negative relationship with aluminum concentration, and a positive relationship with phosphate concentration, specific conductance, manganese concentration, and pH (Table 3.7). Additionally, all taxa identified as sensitive to increases in specific conductance had a negative RD1 score, while all taxa identified as tolerant to increased specific conductance had a positive RD1 score, verifying the conductance gradient described by RD1 (Table 3.6; Table 3.7). The second constrained component exhibited a negative relationship with maximum depth (cm), and a positive relationship with ammonium concentration and water temperature (Table 3.7).

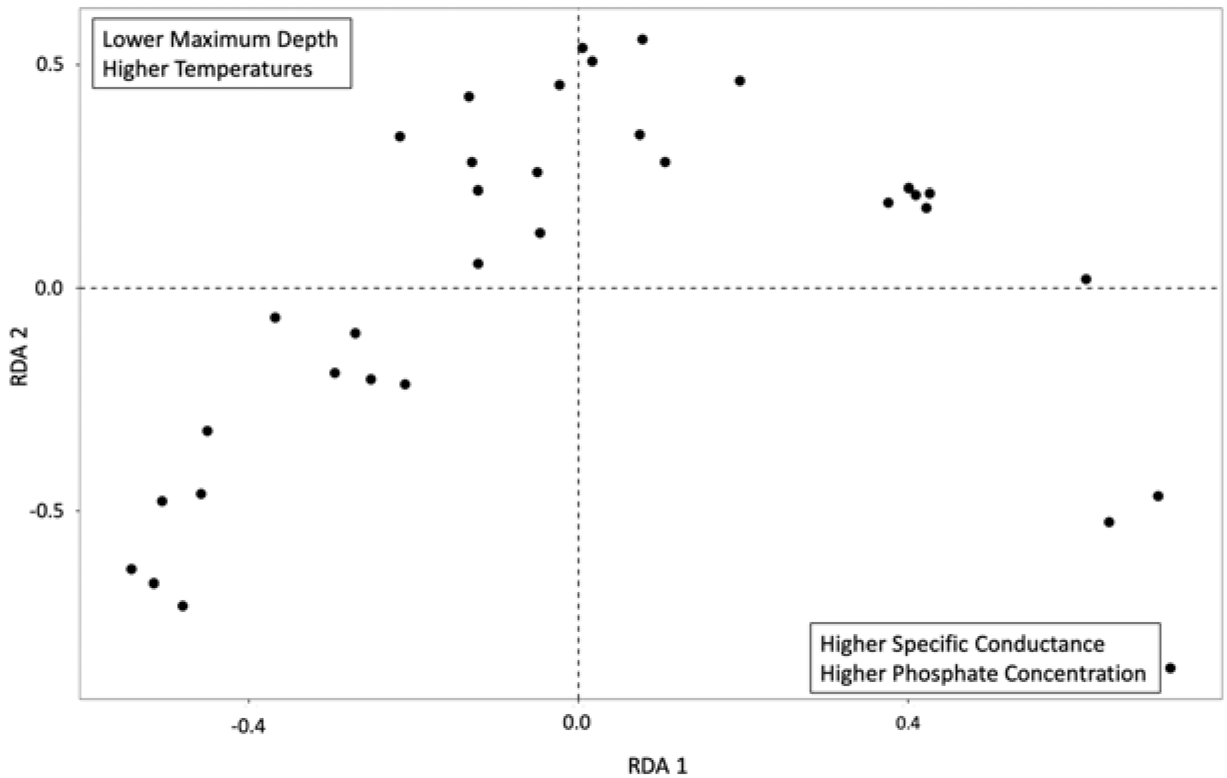

Figure 3.5: Redundancy Analysis (RDA) ordination plot of invertebrate community composition (relative abundance) in 34 flarks. Statistically significant explanatory environmental variables associated with RD axes 1 and 2 are shown

Table 3.2: Redundancy analysis partitioning of variance table (Fig 3.5)

	Variance	Proportion
Total	0.347	1
Constrained	0.152	0.437
Unconstrained	0.196	0.563

Table 3.3: Analysis of variance for redundancy analysis model (Fig 3.5)

	DF	SS	MS	F	p
Model	8	0.152	0.019	2.423	**0.001**
Residual	25	0.196	0.00784		
Total	33	0.348			

Table 3.4: Analysis of variance for redundancy analysis constraining variables (Fig 3.5)

	DF	SS	MS	F	p
Spec. Cond. (μS/cm)	1	0.055	0.055	7.036	**0.001**
PO4-P (μg/L)	1	0.036	0.036	4.547	**0.002**
NH4-N (μg/L)	1	0.004	0.004	0.516	0.886
Mn (mg/L)	1	0.005	0.005	0.684	0.689
pH	1	0.006	0.006	0.765	0.636
Al (mg/L)	1	0.006	0.006	0.779	0.620
Water Temperature (˚C)	1	0.021	0.021	2.669	**0.014**
Maximum Depth (cm)	1	0.019	0.019	2.386	**0.033**
Residual	25	0.196	0.00784		
Total	33	0.348			

Table 3.5: Analysis of variance for redundancy analysis axes (Fig 3.5)

	DF	SS	MS	F	p
RDA1	1	0.081	0.081	10.359	**0.001**
RDA2	1	0.033	0.033	4.234	**0.044**
RDA3	1	0.013	0.013	1.616	0.864
RDA4	1	0.011	0.011	1.353	0.909
RDA5	1	0.006	0.006	0.734	1.000
RDA6	1	0.004	0.004	0.561	0.999
RDA7	1	0.002	0.002	0.282	1.000
RDA8	1	0.002	0.002	0.243	0.999
Residual	25	0.196	0.00784		
Total	33	0.348			

Table 3.6: Species scores of indicator taxa (Fig 3.7) for the first six constrained components of the redundancy analysis, ordered by increasing RDA1 values (Figure 3.5).

	RDA1	RDA2	RDA3	RDA4	RDA5	RDA6	TITAN
Stagnicola	-0.415	-0.142	-0.174	-0.003	-0.057	0.039	Sensitive
Nehalennia	-0.168	-0.092	-0.066	-0.030	-0.019	-0.020	Sensitive
Planorbidae	-0.126	-0.005	0.058	0.073	0.043	0.104	Sensitive
Acari	-0.125	0.172	0.001	0.213	0.009	-0.070	Sensitive
Dixella	-0.125	-0.048	0.001	0.020	0.016	0.044	Sensitive
Coenagrionidae<0.5 mm	-0.070	-0.017	0.008	-0.046	0.006	-0.042	Sensitive
Pachydiplax longipennis	-0.067	-0.010	-0.024	-0.001	-0.006	-0.028	Sensitive
Lymnaea stagnalis	-0.039	-0.021	0.044	-0.020	-0.035	-0.011	Sensitive
Phryganeidae	-0.031	-0.016	0.002	-0.011	0.005	0.007	Sensitive
Dixidae Pupae	-0.030	-0.009	0.004	-0.009	0.009	0.006	Sensitive
Aeshna	-0.017	-0.005	-0.012	0.006	-0.025	-0.004	Sensitive
Berosus	0.010	0.022	0.003	0.002	-0.007	0.003	Tolerant
Dasycorixa	0.062	-0.045	-0.029	-0.015	0.019	-0.030	Tolerant
Culex	0.062	-0.033	-0.003	0.024	0.036	-0.041	Tolerant
Stratiomyidae	0.075	-0.045	-0.006	0.006	0.008	-0.014	Tolerant
Dasyhelea	0.112	0.301	-0.015	-0.076	-0.038	0.051	Tolerant
Bezzia	0.163	0.067	0.062	0.026	-0.088	0.004	Tolerant
Pericoma	0.197	0.223	-0.190	-0.012	0.013	0.033	Tolerant
Culiseta	0.326	-0.150	0.011	-0.036	-0.047	0.014	Tolerant
Aedes	0.418	-0.063	-0.007	0.034	0.056	-0.002	Tolerant

Table 3.7: Redundancy analysis scores for constraining variables on the first six constrained components. Bolded values load onto the respective axis (Fig 3.5).

	RDA1	RDA2	RDA3	RDA4	RDA5	RDA6
PO4-P (μg/L)	0.818	-0.267	-0.168	0.404	-0.157	-0.030
Specific Conductance (μS/cm)	0.782	0.321	-0.141	-0.347	0.222	-0.065
Al (mg/L)	-0.411	-0.017	-0.035	0.194	0.576	0.006
Mn (mg/L)	0.292	-0.024	-0.348	0.226	0.598	0.213
pH	0.157	0.035	-0.257	-0.599	-0.221	0.570
Water Temperature (˚C)	-0.402	0.680	-0.503	0.184	-0.080	-0.280
Maximum Depth (cm)	0.010	-0.558	-0.633	-0.402	-0.013	-0.236
NH4-N (μg/L)	-0.086	0.293	0.017	-0.301	0.347	-0.610

Taxon Indicator Threshold Analysis (TITAN)

Taxon threshold indicator analysis is a means of determining the presence of a threshold along an environmental gradient, and identifying the taxa involved (Baker & King 2010). I performed this analysis to determine if community composition changes gradually along a gradient of specific conductance, or if there was an abrupt change-point (threshold) at which many species appear or disappear. The taxon indicator threshold analysis identified 20 taxa of importance by selecting taxa with purity and reliability values greater than 0.95. Eleven of these taxa were identified as sensitive, and 9 were identified as tolerant (Figure 3.6; Table 3.8). Sensitive taxa were most likely to be present at lower levels of specific conductance and include *Stagnicola*, Phryganeidae, Coenagrionidae < 0.5 mm, *Nehalennia*, *Aeshna*, Planorbidae, *Pachydiplax longipennis*, *Dixella*, other Dixidae, *Lymnaea stagnalis*, and Acari (Figure 3.6; Table 3.8; Table 3.9; Table A3.9). Tolerant taxa were most likely to be present at higher levels of specific conductance and include *Berosus*, *Dasyhelea*, *Bezzia*, *Pericoma*, *Dasycorixa*, *Aedes*, *Culex*, *Culiseta*, and Stratiomyidae (Figure 3.6; Table 3.9; Table A3.9). Taxa identified as sensitive have a predicted community change point where specific conductance is 8,140 μS/cm, with 5% and 95% confidence limits occurring at 6,357 μS/cm and 9,385 μS/cm, respectively (Table 3.8). Taxa identified as tolerant have a predicted community change point where specific conductivity is 8,141 μS/cm with 5% and 95% confidence limits occurring at 6,335 μS/cm and 9,241 μS/cm respectively (Table 3.8).

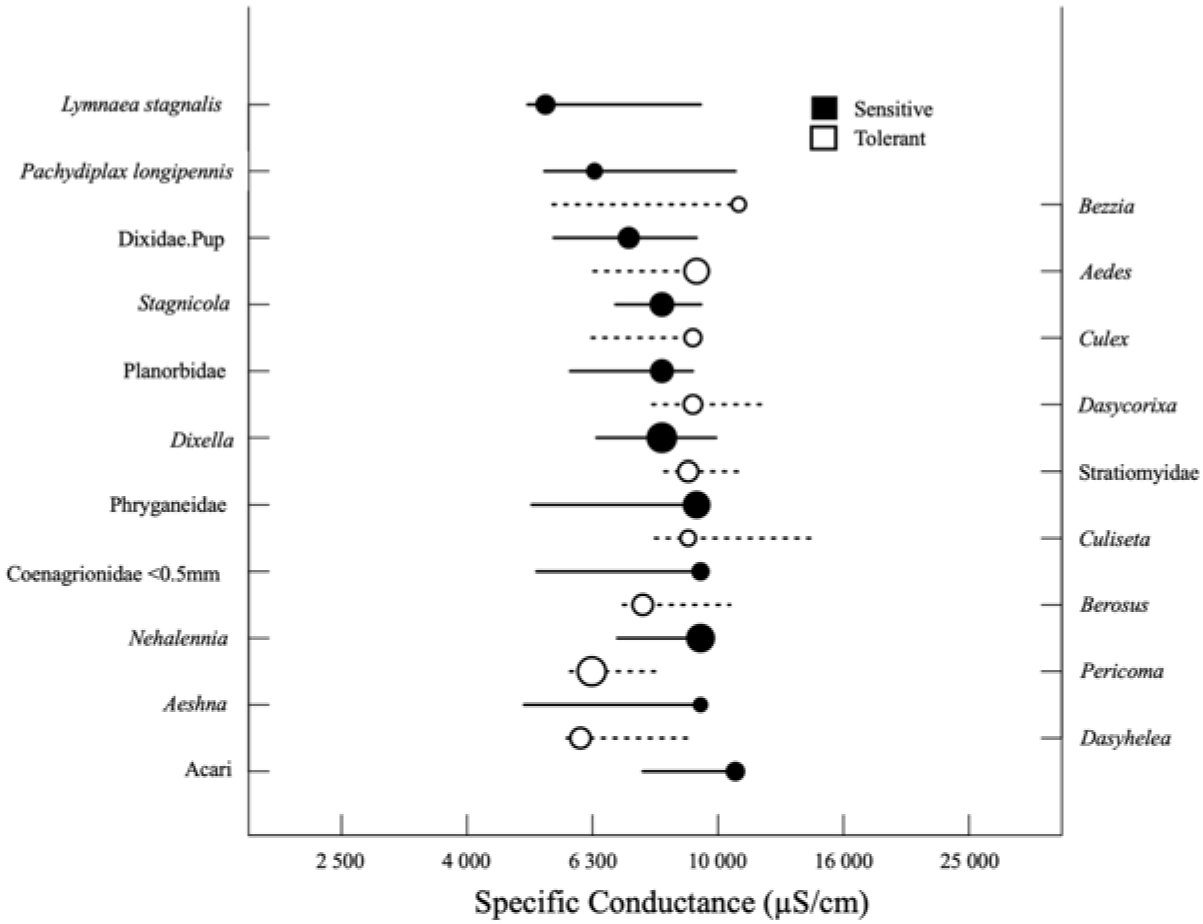

Figure 3.6: Predicted change points and 95% confidence intervals for the occurrence of taxa sensitive to (left y-axis, solid lines and filled circles) or tolerant of salinity (right y axis, open circles and dashed lines) plotted against a log transformed specific conductance scale (x axis). The size of the point is representative of the calculated z score (Table 3.6).

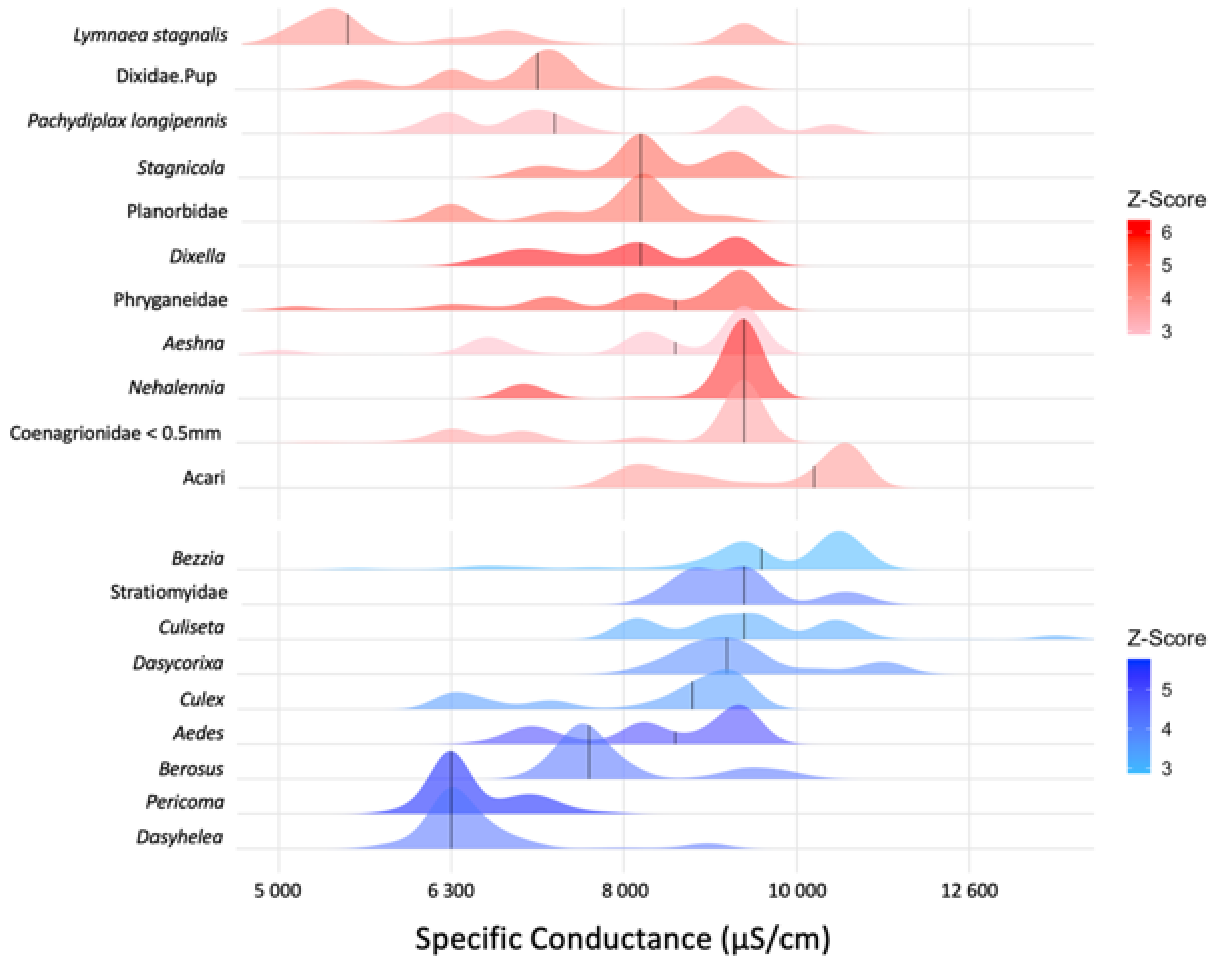

Figure 3.7: Plot of Change point density distributions (number of occurrences) of the taxon-specific predicted change point from bootstrap samples of taxa identified as indicators. Vertical lines represent the predicted change point for each taxon (Figure 3.6). Taxa identified as sensitive are shown in red, and taxa identified as tolerant are shown in blue. Note the different specific conductivity range from Figure 3.6.

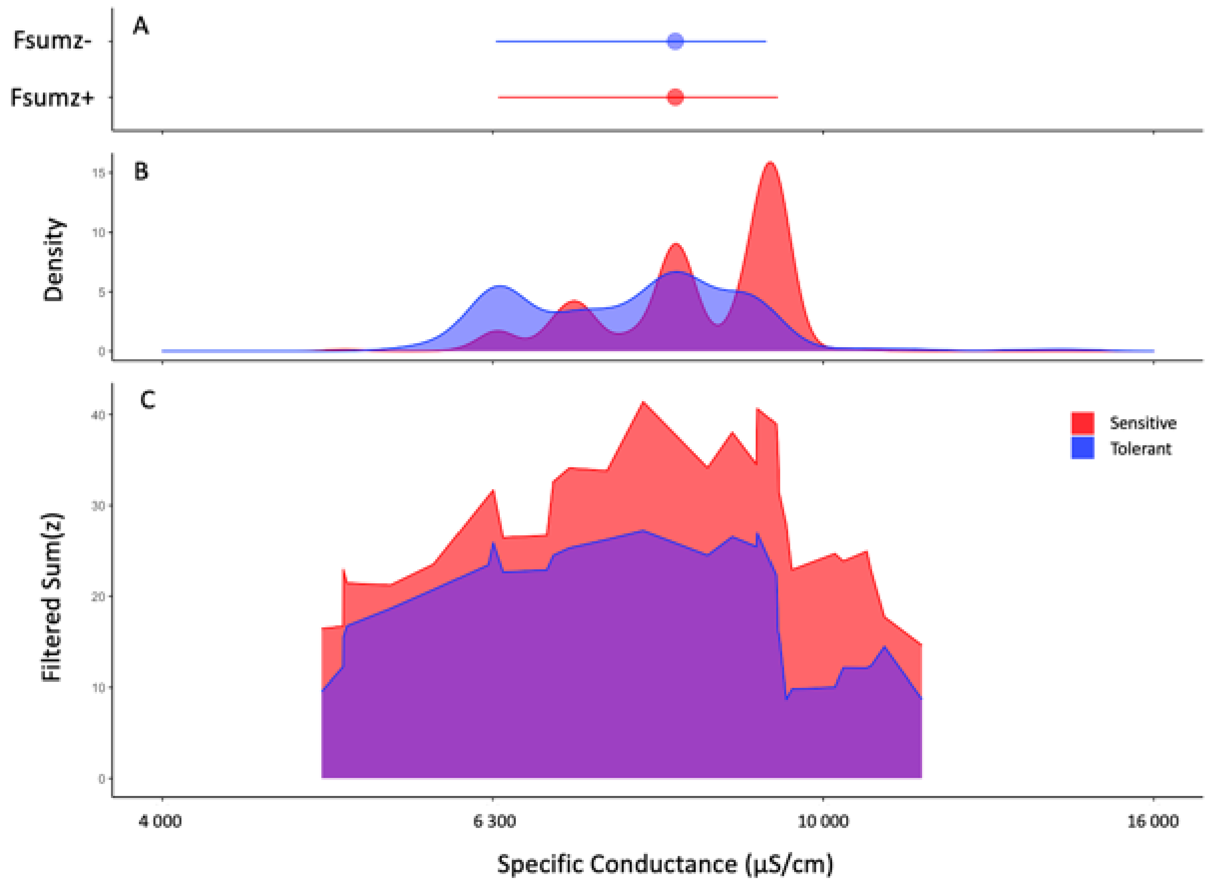

Figure 3.8: Results of TITAN analysis of aquatic invertebrate distribution in 38 flarks varying in specific conductance at the saline fen. A) community level change points (circles) and 95% confidence intervals based on saline-sensitive taxa identified by TITAN (red) and saline-tolerant taxa. B) Sum of change point density distributions from bootstrap samples of TITAN selected tolerant (blue) and sensitive (red) taxa. C) Summed Z scores of all TITAN selected tolerant (blue) and sensitive (red) taxa. All are plotted along the log transformed specific conductance gradient. Note the different specific conductivity range from Figure 3.6.

Table 3.8: Predicted community level change points and confidence limits determined through summing z-scores of sensitive and tolerant taxa along the specific conductance gradient from bootstrap samplings. Values in the table are specific conductance values (µS/cm).

	Change Point	5%	10%	50%	90%	95%
Sensitive	8140.780	6357.348	6943.061	8888.552	9380.500	9385.491
Tolerant	8140.780	6335.662	6357.348	7937.943	9116.455	9241.852

Table 3.9: Summary table for TITAN analysis including taxa's predicted change points, frequency of occurrence, response to salinity, IndVal score, z-score, purity, reliability, and the outcome of the indicator identification test (Filter). (Fig 3.6; Fig 3.7). "Change Point" is the log transformed specific conductance value for the predicted taxon change point. "Filter" determines whether the taxa are identified as sensitive (filter = 1), tolerant (filter = 2), or did not pass the filter test (reliability & purity < 0.95, filter = 0).

	Change Point	**Occurrence**	**Group**	**IndVal**	**z-score**	**Purity**	**Reliability**	**Filter**
Hydracarina	3.960	11	Sensitive	32.14	1.02	0.81	0.514	0
Acari	4.028	31	Sensitive	91.05	3.79	1	0.996	1
Collembola	4.028	36	Sensitive	78.92	2.81	0.926	0.854	0
Oligochaeta	3.842	25	Tolerant	67.38	2.62	0.906	0.81	0
Lymnaeidae.Other	3.960	12	Sensitive	46.48	3.2	0.998	0.94	0
Stagnicola	3.911	30	Sensitive	90.21	5.01	1	1	1
Lymnaea stagnalis	3.725	11	Sensitive	57.39	3.97	0.992	0.952	1
Fossaria	4.048	10	Sensitive	31.25	0.79	0.662	0.39	0
Physa	4.028	8	Sensitive	26.67	1.05	0.782	0.488	0
Planorbidae	3.911	24	Sensitive	79.90	4.82	1	0.998	1
Hydrobiidae	3.725	7	Tolerant	23.33	0.81	0.606	0.326	0
Coenagrionidae<.5 mm	3.972	19	Sensitive	66.18	3.58	0.994	0.978	1
Nehalennia	3.972	25	Sensitive	84.62	5.94	1	1	1
Aeshna	3.972	10	Sensitive	43.48	2.9	0.99	0.954	1
Sympetrum	4.028	6	Sensitive	20.00	0.61	0.536	0.276	0
Somatochlora	3.966	16	Sensitive	36.79	1.08	0.718	0.57	0
Pachydiplax longipennis	3.803	23	Sensitive	67.61	3.23	1	0.982	1
Libellulidae	3.803	3	Tolerant	11.54	0.57	0.526	0.174	0
Corixidae.Other	4.079	10	Tolerant	57.22	4.21	0.93	0.744	0
Dasycorixa	3.960	13	Tolerant	58.67	3.75	0.994	0.972	2
Trichocorixa	4.048	4	Tolerant	48.02	5.52	0.938	0.744	0
Mesovelia	3.858	6	Sensitive	22.31	1.21	0.72	0.696	0
Notonectidae	3.710	6	Sensitive	54.23	4.56	0.92	0.906	0

Gerridae	3.710	8	Sensitive	61.11	4.86	0.966	0.906	0
Saldidae	4.079	4	Tolerant	34.86	3.21	0.836	0.574	0
Phryganeidae	3.966	16	Sensitive	67.02	5.68	1	1	1
Dytiscidae.Other	4.010	10	Tolerant	38.04	1.88	0.834	0.722	0
Dytiscus	4.079	3	Tolerant	38.25	4.91	0.944	0.762	0
Hydaticus	3.938	10	Tolerant	40	3.03	0.948	0.828	0
Agabus	3.858	12	Sensitive	38.24	2.21	0.896	0.716	0
Ilybius	3.960	11	Sensitive	33.19	1.75	0.902	0.708	0
Liodessus	4.079	17	Tolerant	75.43	3.23	0.91	0.73	0
Laccophilus	4.079	10	Tolerant	56.37	3.83	0.854	0.78	0
Hydrophilidae.Other	3.911	9	Tolerant	34.95	2.99	0.99	0.892	0
Cymbiodyta	4.048	17	Tolerant	73.46	3.5	0.88	0.806	0
Berosus	3.880	12	Tolerant	50.83	4.18	0.988	0.96	2
Hydraenidae	3.979	13	Tolerant	39.01	1.69	0.828	0.612	0
Chironomidae	3.751	38	Sensitive	56.53	1.04	0.68	0.51	0
Ceratopogonidae.Other	3.703	24	Tolerant	58.44	1.37	0.794	0.532	0
Dasyhelea	3.781	38	Tolerant	82.73	4.16	0.994	0.982	2
Bezzia	4.033	34	Tolerant	85.72	2.87	0.964	0.954	2
Atrichopogon	4.048	19	Sensitive	47.49	0.63	0.57	0.34	0
Forcipomyia	3.979	6	Tolerant	30.69	2.77	0.852	0.664	0
Culicidae<0.5mm	3.803	21	Tolerant	55.61	1.83	0.908	0.742	0
Aedes	3.966	27	Tolerant	91.02	4.97	1	1	2
Culiseta	3.952	22	Tolerant	73.25	3.13	0.99	0.976	2
Culex	3.960	16	Tolerant	66.19	3.44	0.998	0.984	2
Ephydridae	3.725	33	Tolerant	71.48	1.97	0.8	0.766	0
Psychodidae.Other	3.979	10	Tolerant	45.43	2.94	0.978	0.862	0
Psychoda	3.711	13	Tolerant	38.36	0.81	0.62	0.334	0
Pericoma	3.799	32	Tolerant	92.34	5.77	1	0.998	2
Sciomyzidae	3.975	38	Tolerant	61.96	1.59	0.766	0.628	0

Dixidae Pupae	3.858	19	Sensitive	64.39	4.4	0.984	0.966	1
Dixella	3.911	28	Sensitive	82.62	6.36	1	1	1
Dolichopodidae	3.960	8	Tolerant	32.33	2.34	0.868	0.718	0
Muscidae	3.975	25	Tolerant	65.31	3.19	0.986	0.948	0
Tipulidae	4.033	13	Tolerant	67.62	4.55	0.73	0.986	0
Tabanidae	3.979	24	Tolerant	46.63	0.58	0.568	0.482	0
Stratiomyidae	3.952	14	Tolerant	60.03	4.1	0.994	0.978	2
Empididae	3.703	8	Sensitive	35.68	1.7	0.746	0.542	0

Saline Fen Complex macroinvertebrate Indices of Salinity

20 of the 60 taxa common enough to be analyzed for their diagnostic value as indicators of salinity were identified as being sensitive to (halophobic; 11 taxa) or tolerant of (halophilic; 9 taxa) elevated specific conductance (Figure 3.6; Figure 3.7; Table 3.9). The remaining 40 taxa were not identified as indicators of salinity and were present along the entirety of the gradient either abundantly (Chironomidae, Ephydridae) or sparsely (Muscidae, Empididae, Gerridae, Dytiscidae) (Table 3.9).

In an effort to create a composite zoobenthic bioindicator index of sensitivity to or tolerance of salinity, I assessed two measures. The saline-sensitive index was calculated for each flark by summing the numbers of individuals identified as sensitive by TITAN and dividing by the total number of animals sampled in the flark. Similarly, the saline-tolerant index was calculated by summing the number of individuals identified as tolerant by TITAN, and dividing by the total number of animals sampled in the flark. Values of the saline sensitive index and the saline tolerant index were each plotted against specific conductance (Figure 3.9 and Figure 3.10 respectively).

Values for the sensitive-saline index ranged haphazardly between 0.05 and 0.88 among sites where specific conductance was less than the TITAN-derived threshold's 5% confidence limit. Of the 15 flarks whose specific conductance was greater than the TITAN-derived threshold's 95% confidence limit, 4 flarks had a saline-sensitive index value of zero, and 14 flarks contained saline-sensitive index values less than 0.11.

Values for the tolerant-saline index ranged between 0.09 and 0.62 in sites where specific conductance was greater than the TITAN-derived threshold's 95% confidence limit. In flarks with specific conductance values less than the TITAN-derived threshold's 5% confidence limit, tolerant-saline index values were below 0.11.

The models used for both the sensitive and tolerant taxa predicted values of summed relative abundance using the log-transformed specific conductance scale and a quasi-binomial logistic regression. Specific conductance was highly significantly associated with the summed relative abundance values for both sensitive ($p<0.0006$ and tolerant ($p<0.0004$) communities (Table A3.10; Table A3.11).

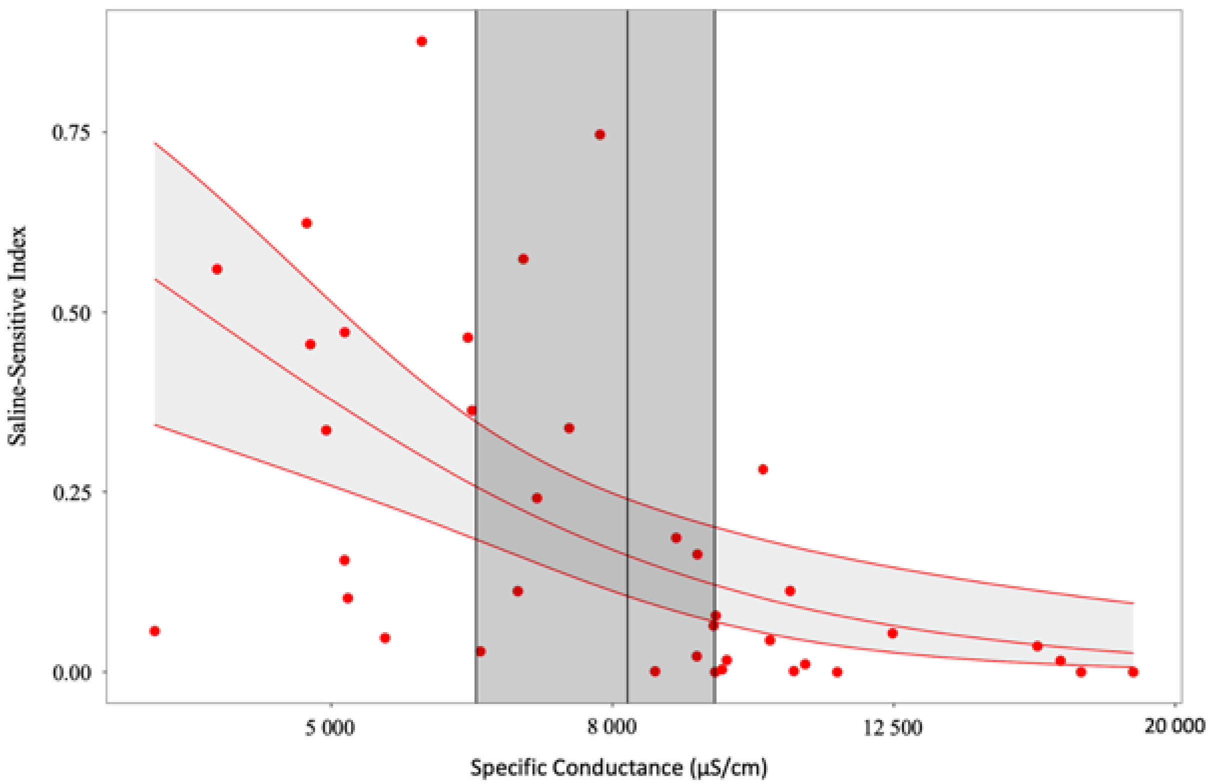

Figure 3.9: Relationship between specific conductance and saline-sensitive index values from 38 flarks in the saline fen complex. Vertical line and shaded region represent the community level change point and 95% confidence interval estimated from TITAN. The fitted red line represents results of quasi-binomial logistic regression and 95% confidence interval of the slope.

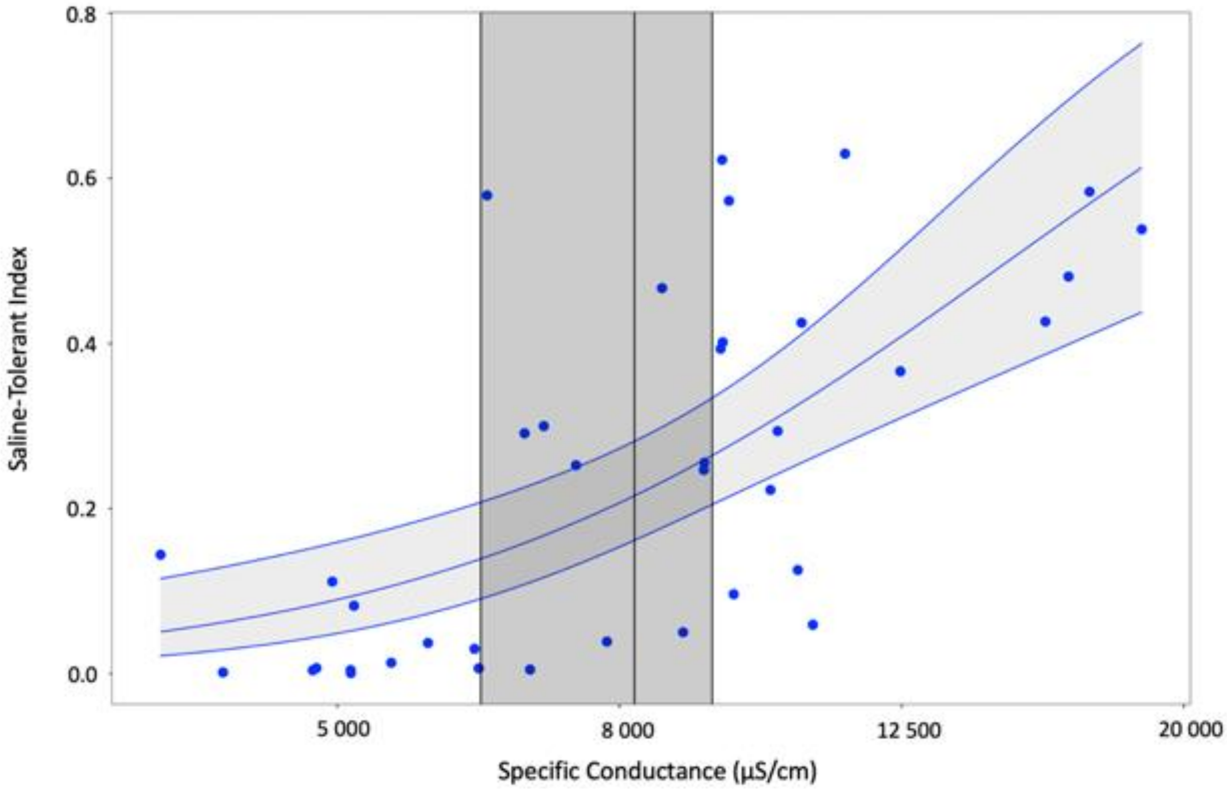

Figure 3.10: Relationship between specific conductance and saline-tolerant index values from 38 flarks in the saline fen complex. Vertical line and shaded region represent the community level change point and 95% confidence interval estimated from TITAN. The fitted blue line represents results of quasi-binomial logistic regression and 95% confidence interval of the slope.

Discussion

Community composition of aquatic macroinvertebrates varies along a gradient of salinity (Kovalenko et al. 2013; Mushet et al. 2015; Lancaster & Scudder 1986). However, it has been unclear whether increasing salinity results in a gradual loss of species and shift in community composition or whether salinity thresholds exist that may regulate community richness and composition. The goal of this analysis was to elucidate the relationship between salinity and aquatic macroinvertebrate community composition of a suite of naturally saline waterbodies. Key questions for these analyses encompass the influence of salinity on the macroinvertebrate community and include variations in abundance (Lancaster & Scudder 1986; Mushet et al. 2015; Van Meter et al. 2011), richness (Lancaster & Scudder 1986; Bendell-Young et al. 2000) and the transition of taxa from one community state to the next along the gradient. Specifically, I aimed to determine whether a gradual replacement of species occurs, or if there is a change-point within the gradient yielding an abrupt transition between states (threshold; Baker & King 2010; Mushet et al. 2015; Lancaster & Scudder 1986; Bendell-Young et al. 2000). In addition, other water chemistry and environmental parameters influencing community composition within the saline fen complex were identified. I found that salinity had little effect on overall abundance among flarks, but that there were marked differences in the relative abundance of the 60 taxa observed in the saline fen complex. Specifically, 11 taxa were identified as sensitive to increased specific conductance, and 9 taxa were identified as tolerant of increased specific conductance. Salinity did not significantly influence the relative abundance of the remaining 40 taxa analysed. The Threshold Indicator Taxon Analysis provided strong evidence of a threshold regulating community composition rather than a gradual replacement.

Specific conductance vs chloride

Specific conductance is a measure of the combined conductance of ions dissolved in a water body corrected to 25˚C and thus can serve as a simple proxy for total dissolved salts, or salinity (Wetzel, 2001; ECCC 2018). Ions that tend to be the most abundant in aquatic ecosystems are chloride, sulfate, sodium, magnesium, and calcium (Wetzel 2001; Price and Wells 2015). While cations such as sodium and calcium are often used in organisms' metabolic processes, chloride is not and so the concentration of chloride in a water body typically reflects the water inputs and outputs (precipitation, evaporation, or groundwater discharge) but is independent of organism density within the ecosystem (Wetzel 2001; Dugan et al. 2017). As a result, specific conductance can also be used as a proxy for chloride concentration when the relationship between specific conductance and chloride for the study area has been identified (Wallace & Biastoch 2016; Howard & Haynes 1993). At the saline fen complex chloride concentration was strongly linearly associated with specific conductance. Specific conductance, conductivity and chloride concentrations are widely used in the literature (Wallace & Biastoch 2016; Howard & Haynes 1993; Wells & Price 2015; Purdy et al. 2005; Rooney & Bayley 2011; Hartsock et 2021). Chloride has well defined lethal concentrations for various organisms and has been used in many toxicology studies (Dugan et al. 2017; Brungs 1973; Stewart et al. 1996). Specific conductance is used in the Alberta Wetland Classification System to differentiate types of wetlands (AESRD 2015), and specific conductance is easier to use for rapid bioassessment monitoring programs (ECCC 2018). As a result, further discussion on this topic will refer primarily to specific conductance. CCME water quality guidelines (GOA 2018) for the protection of aquatic life in freshwater systems cite long-term and short-term exposure values for chloride concentration of 120 mg/L and 640 mg/L, respectively (GOA 2018). According to the regression equation and 95% prediction interval of the model relating chloride concentration to specific conductance, these exposure limits correspond to specific conductance±SD values of 1,682±406 and 3,341±486 μS/cm, respectively. These values are much lower than the concentrations recorded in the saline fen complex. However, taxa generally indicative of freshwater ecosystems (Odonata) were present in the saline fen complex in waterbodies with specific conductance values up to 10,000 μS/cm. This finding is similar to observations in studies conducted in similar regions (Cannings & Cannings 1987; Mushet et al. 2015).

Total Abundance & Family Richness

Macroinvertebrate abundance was unaffected by specific conductance along the salinity gradient. Based on published literature, abundance was expected to increase as specific conductance values increased along with a decline in body size thus maintaining community biomass (Mushet et al. 2015; Van Meter et al. 2011; Bendell-Young et al. 2000). At higher specific conductance, individuals must expend energy on osmotic regulation, resulting in less energy available to be stored as biomass (Mushet et al. 2015; Lancaster & Scudder 1986; Chapman 1975). Body size was not measured in this analysis, but since abundance values were not influenced by specific conductance values, if body size did in fact decrease as stated in the literature, community biomass would likely decrease as specific conductance values increase. The number of species and trophic levels an ecosystem can support is often related to the stability and the health of that ecosystem (Aoki & Mizushima 2001; Cummins 1973). An ecosystem with many trophic levels requires a large biomass present in lower trophic levels to support the requirements of individuals in higher trophic levels (Pimm & Lawton 1977; Gullan & Cranston 2010; Cummins 1973). Because of this, biomass, or secondary productivity may be a better metric to use than total abundance when comparing reference condition wetlands to reclaimed or opportunistic wetlands on the mining lease area.

Richness was expected to decline as salinity increased (Mushet et al. 2015; Lancaster & Scudder 1986), which was observed, albeit with a weak correlation. A linear model comparing family richness to the log transformed specific conductance gradient, explained about 10% of the variation within the richness data. While this seems like a minor amount of the variation explained, using family richness as opposed to genus or species richness possibly masked the true decline in diversity. Families such as Chironomidae and Dytiscidae, were present across the entire gradient, although transitions in genera likely occurred along the gradient (Mushet et al. 2015; Zheng et al. 2021; Lancaster & Scudder 1986). Zheng et al. (2021) found that specific conductance was a statistically significant ($p < 0.01$) determinant of diversity of the Chironomidae community in various lakes. As a result, beta diversity possibly changes along a specific conductance gradient, while alpha diversity remains minimally affected when using broader taxonomic levels. Measures of diversity are typically based on species richness and abundances, but functional diversity may be a better metric to use to measure the functional capabilities of an ecosystem (Schleuter et al. 2010; Tilman 2001; Petchey & Gaston 2006). Functional diversity is the diversity of a community based on functional groups of phenotypes (Schleuter et al. 2010; Tilman 2001; Petchey & Gaston 2006; Cummins 1974). Common functional diversity groups include functional feeding groups (Cummins 1973; Merritt et al. 2002; Gholizadeh & Heydarzadeh 2017), which can be used to assess the diversity and evenness of an ecosystem's trophic system or food web (Petchey & Gaston 2006). A distribution of species within a community comprised of various functional groups can increase the stability of the ecosystems during times of disturbance, decrease unused resources, and increase community biomass (Tilman 2001). Diversity is an inherently and intrinsically valid metric that is simple to measure and should be analyzed and compared when monitoring wetlands on the Alberta oil sands reclaimed landscape.

Community Composition – Association with Environmental Variables

The Redundancy analysis identified specific conductance (μS/cm), water temperature (˚C), maximum depth (cm), and phosphate concentration (μg/L) as significantly in influencing community composition. These variables, along with aluminum concentration (mg/L), ammonium concentration ((μg/L), manganese concentration (mg/L), and pH explained over 25% of the variation in community composition.

Specific conductance ranged from 3,757 μS/cm (moderately brackish) to 18,628 μS/cm (subsaline) within the saline fen complex, and a change in composition across a gradient of this breadth was expected (Kovalenko et al. 2013; Mushet et al. 2015; Lancaster & Scudder 1986). Maximum depth of sampled flarks ranged from 6 cm to 27.5 cm. During preliminary data exploration, no patterns were observed between flark maximum depth and either abundance, or richness; however, semi-aquatic invertebrates such as mites are more likely to occur in very shallow areas, while larger aquatic invertebrates may be constrained to deeper areas by their larger size and mobility. Phosphate concentration was also significantly associated with community composition. Phosphate concentration covaried with concentrations of iron, silica, and oxygenated nitrogen, collectively forming a nutrient gradient. Community composition was expected to vary as a function of nutrient concentrations. Higher levels of silica concentration are likely a representation of diatom abundance, as diatoms accumulate silica when forming their frustules (Wetzel 2001). As a result, areas with greater nutrient availability would likely be able to support more organisms and more trophic levels.

Taxon Indicator Threshold Analysis (TITAN)

Threshold indicator taxa analysis (TITAN) is a statistical analysis using indicator values (IndVal) (Dufrêne & Legendre 1997) of all taxa present along the gradient, standardized to z scores (standard deviations from a mean; Baker & King 2010). IndVal scores are used to determine the strength of a taxon's association relative to environmental variables (Dufrêne & Legendre 1997). IndVals account for both the proportions of individuals associated with an environmental class (i.e., fidelity), and the relative abundance of the population associated with the environmental class (Baker & King 2010). For TITAN, a permutation test shuffles the values of the gradient so that a mean and standard deviation associated with random variation can be calculated for each taxon, and a z-score is formed as the number of standard deviations to the observed mean from the permuted random variation mean (Baker & King 2010). This allows rare but informative taxa be included in determining a community level threshold (Baker & King 2010; King & Baker 2010).

Of the 60 genera of aquatic invertebrates observed in the saline fen complex, TITAN analysis identified 11 taxa that were sensitive to salinity and 9 that were tolerant of increased specific conductance on the basis of their relative abundance. Relative abundances of remaining 40 taxa did not significantly vary across the salinity gradient. These included taxa that were consistently abundant along the gradient (Chironomidae) those that were consistently present at low proportions across the gradient (Ephydridae), and those that occurred sporadically along the gradient (Oligochaeta). The taxon-specific thresholds were markedly synchronized, providing strong evidence of the presence of community level thresholds for both the sensitive and tolerant communities aligned at 8,141 μS/cm, with bootstrapped 95% confidence limits of 6,335 - 9,385 μS/cm. These findings are broadly consistent with literature reports of aquatic invertebrate tolerance for gastropods and Hemiptera. Mushet et al. (2015), found a salinity threshold of between 5000 μS/cm and 10,000 μS/cm in prairie lakes and large wetlands of south-central North Dakota. Similar limits were described for Hemiptera in saline lakes in British Columbia, Canada (Lancaster & Scudder 1986), and for the entire aquatic invertebrate community of saline lakes in Saskatchewan and Alberta, Canada (Timms et al. 1986). Gastropods have well-studied conductivity tolerance ranges, with *Lymnaea stagnalis* and *Stagnicola* being present below 5,000 μS/cm and between 5,000 μS/cm and 10,000 μS/cm respectively (Mushet et al. 2015), while halophilic Corixidae species typically appear around 8,000 μS/cm (Lancaster & Scudder 1986). Additionally, Odonata species have been studied in saline lakes across British Columbia, where only 2 taxa (*Lestes congener* & *Enallagma boreale)* were found in lakes with conductivity values above 9,000 μS/cm (Cannings & Cannings 1987). All of these trends are consistent with findings of the current study. Furthermore, the same taxa were identified by the TITAN analysis as being important indicator taxa. Some of the indicator taxa identified via TITAN, such as the genera of Culicidae (specifically *Aedes* and *Culiseta)* were present across the entire gradient, albeit at very low densities in lower salinity flarks. *Aedes* can survive a wide range of conductivity values (Chapman 1975; Grueber & Bradley 1994). Its restriction to the most saline areas could well be an indirect effect of the distribution of Odonata - its chief predators. Four genera of dragonflies and one family of damselflies were abundant in lower salinity wetlands but were absent at locations where specific conductance was 10,000 μS/cm or greater. So, it is possible, although unstudied in this analysis, that *Aedes* is exploiting unused resources and minimizing competition by avoiding pools with (or being extirpated by) predatory species such as Odonata, thereby associating with more saline sites.

Based on existing literature and the results of this analysis, specific conductance values below 6,000 μS/cm to 10,000 μS/cm are likely to support communities identified as saline-sensitive taxa. Reclaimed landscapes on the Alberta mining lease area are expected to gradually increase in conductivity as salts leach to the surface from the overburden below (Giesy et al. 2010). Conductivity of the surface waters of Syncrude Canada's Sandhill watershed have gradually risen between 2015 and 2019, with mean±SD values reaching around 2,560±305 μS/cm (n=5) in 2019 (Hartsock et al. 2021b). While these values are well below those observed at the saline fen complex, if this trend continues, some species may be lost. It is important to further analyze the drivers of species loss with respect to conductivity, as complicating features may be present in the reclaimed landscape, such as naphthenic acids in upwelling groundwater (Bartlett et al. 2017) or synergistic effects among multiple stressors (Howland et al. 2019).

Using TITAN as an analytical tool across various gradients present within the AOS wetlands (salinity, age, permanence, OSPW contamination), will create subsets of taxa indicative of various environmental transition points along a continuum of reclaimed wetland systems, allowing researchers to identify reclaimed and opportunistic wetlands within the AOS that may mimic natural wetlands as well as those that may warrant further monitoring or possibly intervention as indicated by macroinvertebrate community composition. This would allow for efficient allocation of resources to wetlands that require more monitoring.

Saline Fen Complex macroinvertebrate Indices of Salinity

Combining the relative abundances of saline-sensitive taxa, or saline-tolerant taxa, provides a simple, integrated measure of the effects of specific conductance on the aquatic invertebrate community. As expected, since only taxa deemed informative via TITAN were used in this analysis, both of these models effectively predicted the summed relative abundances of both sensitive and tolerant taxa, which were both altered across the salinity threshold's confidence interval. The logistic regression does not fit these data well, as is expected with thresholds due to the abrupt change associated with a threshold (Hugget 2005). This type of pattern can be modeled using piecewise quantile regression (Tomal & Ciborowski 2020) to identify the threshold boundaries evident in the intolerance index. Based on the calculated standard errors associated with the logistic regression for the sensitive community, at the 5% confidence limit of the TITAN predicted community threshold, the predicted saline-sensitive index values are between 0.18 and 0.34 of the community, while at the 95% confidence limit, the predicted saline-sensitive index values are between 0.07 and 0.20 (Figure 3.9). For the tolerant taxa, at the 5% confidence limit of the TITAN predicted community threshold, the predicted saline tolerant index values are between 0.09 and 0.21, and at the 95% confidence limit, the predicted saline-tolerant index values are between 0.20 and 0.33. Based on these models' predictions including only specific conductance values in the explanation, the 0.20 value of the saline-sensitive index, and the saline-tolerant index can suggest which side of the threshold zone these taxa are on (Figures 3.11 and 3.12). These values were then used to populate the Punnett Square decision diagram (Figure 3.13). This information could potentially be applied to determine a metric to use when assessing the biota of reclaimed or opportunistic wetlands to naturally occurring wetlands. Saline wetlands do occur in northern Alberta, and a focus on creating exclusively freshwater wetlands in the reclaimed landscape would result in overlooking the contribution of unique ecosystems such as the saline fen complex to regional biodiversity. These provisional salinity-indicating metrics must be validated before they can be recommended for general use. Typically, when creating a metric, datasets are split into training and testing sub-datasets. Because I used all available data to create the metric, an independent dataset using information from other saline systems is needed to determine their applicability and identify an accurate scope of use.

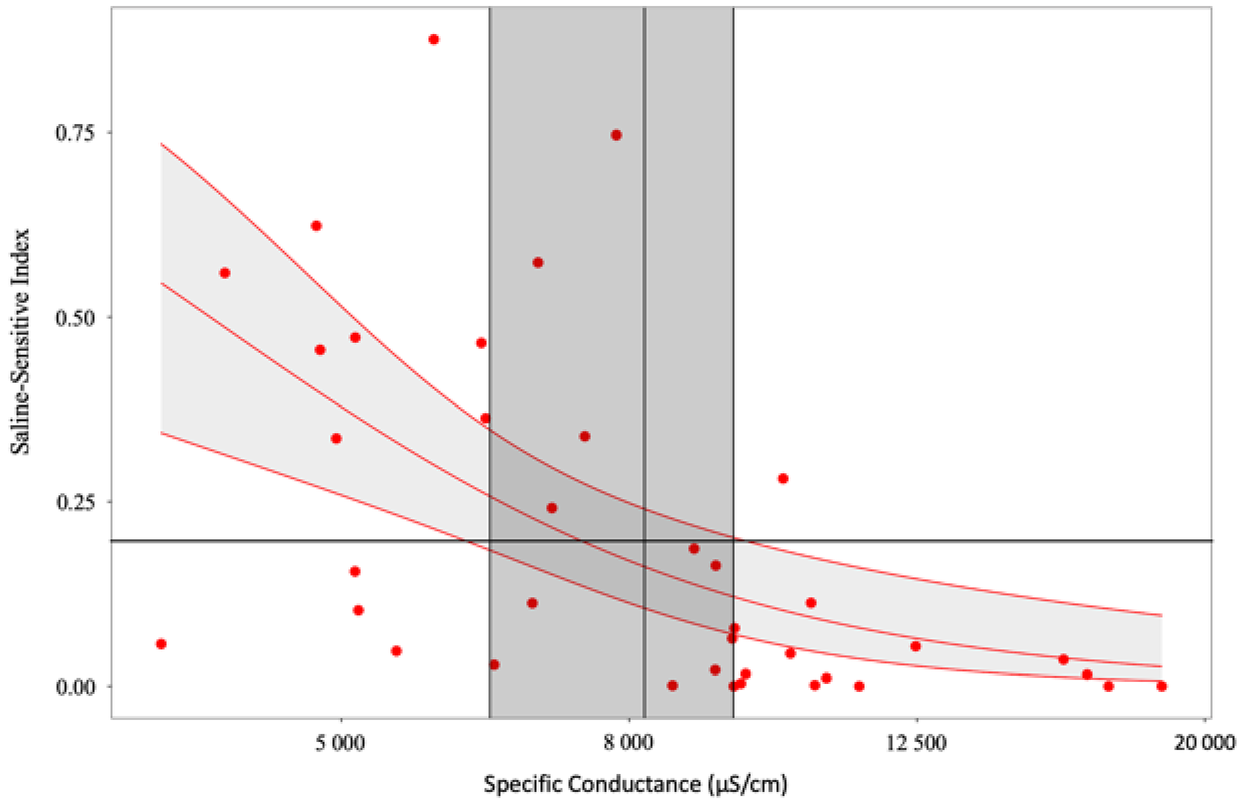

Figure 3.11: Relationship between specific conductance and saline-sensitive index values from 38 flarks in the saline fen complex. Vertical line and shaded region represent the community level change point and 95% confidence interval estimated from TITAN. The fitted red line represents results of quasi-binomial logistic regression and 95% confidence interval of the slope. The horizontal black line represents the 0.20 value used to populate the Punnet Square decision diagram (Figure 3.13)

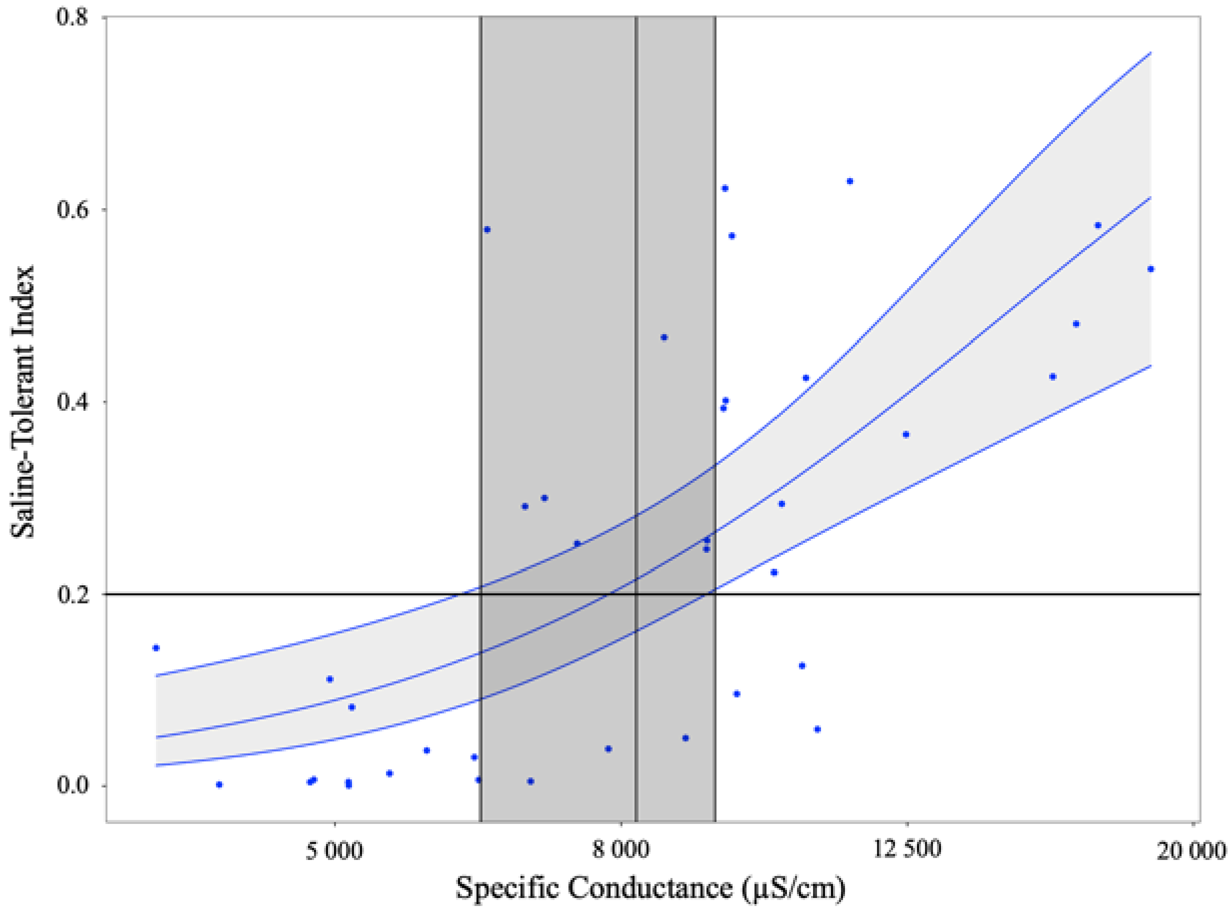

Figure 3.12: Relationship between specific conductance and saline-tolerant index values from 38 flarks in the saline fen complex. Vertical line and shaded region represent the community level change point and 95% confidence interval estimated from TITAN. The fitted red line represents results of quasi-binomial logistic regression and 95% confidence interval of the slope. The horizontal black line represents the 0.20 value used to populate the Punnet Square decision diagram (Figure 3.13)

		Saline-Sensitive Index	
		< 0.20	> 0.20
Saline-Tolerant Index	< 0.20	**Inconclusive** 8/38 flarks Spec. Cond. Range: 3,757 – 10,892	**Not Salt-Stressed** 9/38 flarks Spec. Cond. Range: 4,160 – 6,866
	> 0.20	**Salt-Stressed** 17/38 flarks Spec. Cond. Range: 6,401 – 18,628	**Salt-Stressed** 4/38 flarks Spec. Cond. Range: 7,021 – 10,163

Figure 3.13: Punnet Square decision diagram for possible outcome combinations of the saline-sensitive and saline-tolerant indices, with the proportion of flarks and the respective specific conductive ranges (μS/cm) of sampled flarks in the saline fen complex for each possible outcome.

Conclusion

Three postulates were posed for this study. I predicted that 1) macroinvertebrate abundance would be greater in locations with higher specific conductance than in less saline flarks within the fen system. 2) family richness would be lower in locations where specific conductance was high 3) A threshold would be detected distinguishing waterbodies containing a subset of taxa indicative of relatively low specific conductance, and a complementary subset that dominates in pools with relatively high levels of specific conductance, while euryhalic taxa were present along the entirety of the gradient.

Abundance was independent of the salinity gradient. Family richness varied only slightly along the specific conductance gradient. Water temperature, depth, specific conductance, and phosphate concentration accounted for a significant amount of the variation in community composition. Of these, specific conductance appeared to be the main regulator of community composition. A threshold, occurring between 6,335 and 9,385 μS/cm distinguished saline sensitive taxa (*Stagnicola*, *Aeshna*, Phryganeidae, *Nehalennia*, small Coenagrionidae, Planorbidae, *Dixella*, *Pachydiplax longipennis*, Dixidae pupae, Acari, and *Lymnaea stagnalis*) from saline tolerant taxa (*Berosus*, *Dasyhelea*, *Bezzia*, *Pericoma*, *Dasycorixa*, *Aedes*, *Culex*, *Culiseta*, and Stratiomyidae).

The relative abundances of all sensitive or all tolerant taxa in a sample have potential value as an index of saline stress that may have applications in assessing the importance of salinity in reclaimed wetlands.

Chapter 4: General Discussion

Objectives

The oil reserves present in the AOS contain 1.71 trillion barrels of bitumen, and the region is the second largest proven reserve globally. As of 2017, mining practices in the AOS have created a degraded land area of roughly 900 km^2 (GOA 2009; GOA 2017). Mining companies in the AOS are required to reclaim land degraded in the mining process to equivalent pre-mining land capabilities. The reclaimed landscape should encompass a mixture of upland forests and wetlands (GOA 2021, AEP 2017). Reclaimed wetlands in the AOS are expected to increase in salinity over time as salts from materials used in reclamation rise to the surface (Giesy et al. 2010; Purdy et al. 2005; Kovalenko et al. 2013; Hartsock et al. 2021b). To predict and understand the potential biological effects of salinity on wetland ecosystems in the reclaimed AOS landscape, natural analogues should be used as a frame of reference (Purdy et al. 2005; Wells & Price 2015).

Saline wetland systems such as the complex that I studied can provide a frame of reference against which to compare the fauna in reclaimed AOS wetlands (Volik et al. 2017; Wells & Price, 2015; Purdy et al. 2005). Several studies have been conducted to identify variation of macroinvertebrate community composition in opportunistic and constructed wetlands in the AOS (Whelly 1999; Leonhardt 2003; Kovalenko et al. 2013; Moore 2021; Bendell-Young et al. 2000), all of which, identified reduced diversity at higher levels of conductivity and differences in community composition relative to reference wetlands. Moore (2021) described an absence of well-defined salt-sensitive taxa including species of *Enallagma* (Odonata: Coenagrionidae), *Caenis* (Ephemeroptera: Caenidae), Planorbidae (Gastropoda) and Physidae (Gastropoda), from opportunistic and constructed wetlands with conductivities exceeding 1,500 μS/cm. However, naturally saline systems often support a variety of taxa to much greater levels of conductivity. Cannings and Cannings (1987) studied the adult and larval presence of Odonata species in a suite of saline lakes in British Columbia, Canada. Similar to what has been observed in reclaimed wetlands on the post-mining landscape, 13 of the 19 observed species in larval form were present in lakes with specific conductance values below 1,500 μS/cm and only 5 of the 19 observed species were present in lakes with specific conductance values above 8,000 μS/cm (Cannings & Cannings 1987).

The objective of this study was to summarize water chemistry variation across a series of flarks along the salinity gradient of a boreal saline fen complex in northeastern Alberta to identify how macroinvertebrate community composition covaries with salinity. In particular, I aimed to determine whether the aquatic invertebrate assemblages reflected a gradual replacement of species, each with its own unique optimum and range of salinity tolerance, or whether abrupt changes in community composition were evident, possibly representing broad limits of physiological accommodation to osmotic stress. Broad-scale ability of salt tolerance in aquatic insect taxa of distantly related phylogenetic groups may be due to the convergent evolution of osmoregulatory capabilities, from ancestral salt-sensitive lineages, in salt-tolerant organisms inhabiting inland waters (Grueber & Bradley 1994; Palleres et al. 2015). Adaptations allowing individuals to live in saline areas may allow individuals to exploit unused resources and minimize interspecific competition (Grueber & Bradley 1994; Palleres et al. 2015).

Major Findings and Applications

The salinity gradient within the saline fen complex increases in a northwest-to-southeast direction. Conductivity and associated ions accounted for roughly 35% of the variation of measured environmental variables within the saline fen complex. Other features that were identified as independent of salinity were a suite of nutrients (phosphate, nitrate, silica); dissolved oxygen and ammonium; manganese and barium; and pH and reduction oxidation potential. Aluminum concentration, water temperature and maximum depth were all independent of each other, and of the other suites of variables.

Macroinvertebrate community composition and family richness were found to vary with respect to salinity across the saline fen complex. However, abundance was independent of salinity. In total, 60 genera in 34 families of aquatic invertebrates were collected in the saline fen complex. The family richness observed in the saline fen complex is consistent with what has been observed in reference condition wetlands, where Leonhardt (2003) observed aquatic invertebrate family richness values between 3 and 30 across 31 reference wetlands in the AOS. Of the 60 taxa observed, a subset of 20 taxa were identified as being diagnostic of the specific conductance of the waterbody in which they occurred (11 saline sensitive and 9 saline tolerant). I observed a loss of salt-sensitive taxa including snails, dragonflies, damselflies, and caddisflies between specific conductance values of 6,335 and 9,385 μS/cm (95% CI), corresponding to chloride ion concentrations of roughly 1,500 mg/L and 2,500 mg/L. This is roughly 300 percent greater than the CCME guideline for maximum short-term concentration to sustain freshwater aquatic life (640 mg/L; GOA 2018). The absence of these taxa was counterbalanced by a greater richness and abundance of salt-tolerant taxa, primarily mosquitos and other Diptera, as well as water boatmen (Corixidae) and water scavenger beetles (Hydrophilidae). The euryhaline capacity of mosquitos is well known (Chapman 1975; Grueber & Bradley 1994), so perhaps the high salinity flarks provide mosquitos with a refuge from predation in the complex. Silberbush and Blaustein (2011), studied mosquito (*Culiseta longiareolata*) oviposition patterns using a set of 15 artificial pools containing 0, 1, or 4 adult *Notonecta maculata* (predatory backswimmers), and consistently found greater mosquito oviposition rates in pools that had lower predator density, suggesting mosquitos will selectively oviposit in areas with decreased predators. Regardless of the mechanism that accounts for the observed dichotomy of community composition, the two sets of indicator taxa identified using TITAN have potential application as bioindicators of condition for assessment of constructed wetlands, and opportunistic wetlands, found in reclaimed landscapes.

I created a provisional saline-tolerant index by summing the number of individuals belonging to taxa identified as tolerant by TITAN and dividing by the total number of animals sampled in the flark. A saline-sensitive index was similarly calculated. In flarks where conductivity exceeded the TITAN-derived community change point, the saline-tolerant index score was consistently greater than 0.20, reflecting increased dominance of taxa tolerant to higher levels of specific conductance, and a paucity of the saline-sensitive taxa. Flarks in which the saline-tolerant index was less than 0.20 were either dominated by euryhaline taxa (i.e., the saline-sensitive index was also <0.20), or the specific conductance was less than the TITAN-derived community change point, and fauna are unlikely subjected to salt stress. Clearly, these indices require validation using independently-collected data. However, they have potential for use in assessment of salt-stress associated with the aquatic macroinvertebrate community in reclaimed and opportunistic wetlands.

Limitations

Despite the strong evidence that salinity thresholds regulate aquatic invertebrate community composition in the saline fen complex, several aspects of this study limit the interpretation of the results. The invertebrate samples were collected over a 3-day period. As a result, seasonal variation in water chemistry was not accounted for, and insect taxa that may have completed life cycles and emerged during spring or summer would not necessarily have been detected or included in this analysis.

Water chemistry in the saline fen complex varies through the year due to snowmelt, precipitation, and evaporation. During the two-week period between August 27 and September 9 in 2020, 48.8 mm of precipitation was recorded at the Fort McMurray weather station (ECCC 2020). Perhaps counterintuitively, in wetlands located within a groundwater discharge zone (such as the saline fen complex), precipitation is expected to cause an increase in salinity, as precipitation promotes ground water recharge, thus increasing groundwater flow and causing an increase of saline groundwater upwelling (Volik et al. 2017). As a result, the specific conductance values observed in this study are possibly higher than the seasonal averages of all sites sampled. This could result in an overestimation of the chronic salinity limits of taxa inferred by this analysis, and an overestimation of the predicted community-based change points. Seasonal variability in conductivity could be assessed by repeatedly sampling a set of focal ponds and flarks over the course of the ice-free period. Loggers could be deployed to provide a continuous record of specific conductance and other parameters. Collecting additional synoptic samples from the 52 selected sites during June and July, when local wetland biodiversity is the greatest (Kovalenko et al. 2013) would complement the existing data.

Future Research

Mean±SD specific conductance values in Sandhill fen watershed, a constructed wetland on Syncrude’s mining lease area, have increased gradually from the date of its construction in 2013 to 2019, reaching an average value of 2,560±305 μS/cm (n=5) in surface waters in 2019 (Hartsock et al. 2021b; J.J.H Ciborowski, unpublished). These values are well below those observed in the saline fen complex and the community change point estimated from this analysis.

Future research should aim to clarify the influence of salinity on macroinvertebrate community composition in AOS reclaimed landscapes (e.g., Moore 2021), since such wetlands may be additionally affected by complementary factors in the reclaimed landscape such as naphthenic acid concentration (McQueen et al. 2017), the potential buffering of naphthenic acid toxicity by carbonate (Kavanagh et al. 2012), synergistic effects among multiple constituents of concern (Howland et al. 2019), and differences among ionic concentrations (e.g. sodium, chloride or sulfate) rather than specific conductance (total ionic content) (Kovalenko et al. 2013; Hall & Anderson 1995). Complex interactions among constituents of concern and the resulting toxicity to flora and fauna in the AOS remain unclear and need further analysis.

Despite the limitations associated with this study, my research has described the biodiversity of a unique, little-studied boreal habitat and has identified key change points along a salinity gradient at which abrupt, marked changes in macroinvertebrate community composition occur. These findings provide a frame of reference for assessing the potential role of salinity in opportunistic and reclaimed wetlands in the post-mining landscape. Ultimately, these data could contribute to current guidelines for salt effects that are useful to regulators and ecologists constructing and evaluating wetlands in the AOS.

References

Acal, C., Aguilera, A.M., & Escabias, M. 2020. New Modeling Approaches Based on Varimax Rotation of Functional Principal Components. Mathematics. 2020(8): Article #: 2085

Aickin, M., & Gensler, H. 1996. Adjusting for multiple testing when reporting research results. The Bonferroni vs Holm methods. American Journal of Public Health. 86(5): 726-728

Alberta Environment and Parks (AEP). 2017. Reclamation critera for wellsites and associated facilities for peatlands.

Alberta Environment and Sustainable Resource Development (AESRD). 2015. Alberta Wetland Classification System. Water Policy Branch, Policy and Planning Division, Edmonton, AB.

Antweiler, R.C. 2015. Evaluation of Statistical Treatments of Left-Censored Data Using Coincident Uncensored Data Sets. II. Group Comparisons. Environmental Science and Technology. 49: 13439-13446

Aoki, I., & Mizushima, T. 2001. Biomass diversity and stability of food webs in aquatic ecosystems. Ecological Research. 16: 65-71

Baker, M.E., & King, R.S. 2010. A new method for detecting and interpreting biodiversity and ecological community thresholds. Methods in Ecology and Evolution. 1(1): 25-37

Bartlett, A.J., Frank, R.A., Gillis, P.L., Parrott, J.L., Marentette, J.R., Brown, L.R., Hooey, T., Vanderveen, R., McInnis, R., Brunswick, P., Shang, D., Headley, J.V., Peru, K.M., & Hewitt, L.M. 2017. Toxicity of naphthenic acids to invertebrates: Extracts from oil sands process-affected water versus commercial mixtures. Environmental Pollution. 227: 271-279

Bauer I.E., & Vitt D.H. 2011. Peatland dynamics in a complex landscape: Development of a fen-bog complex in the Sporadic Discontinuous Permafrost Zone of northern Alberta, Canada. Boreas. 40(4): 10.1111/j.1502-3885.2011.00210.x.

Bendell-Young L.I., Bennett K.E., Crowe A., Kennedy C.J., Kermode A.R., Moore M.M., Plant A.L., & Wood A. 2000. Ecological characteristics of wetlands receiving an industrial effluent. Ecological Applications. 10(1): 310-322

BGC Engineering Inc. 2010. Review of reclamation options for oil sands tailings substrates. Oil Sands Research and Information Network, University of Alberta, School of Energy and the Environment, Edmonton, Alberta. OSRIN Report No. TR-2. 59pp

Biagi K.M., Oswald, C.J., Nicholls E.M., & Carey S.K. 2019. Increases in salinity following a shift in hydrologic regime in a constructed wetland watershed in a post-mining oil sands landscape. Science of the Total Environment. 653: 1445-1457

Borcard, D., Gillet, F., & Legendre, P. 2018.Numerical Ecology With R. 2nd Edition.

Borkenhagen, A., & Cooper, D.J. 2016. Creating fen initiation conditions: A new approach for peatland reclamation in the oil sands region of Alberta. Journal of Applied Ecology. 53: 550-558

Borkenhagen, A., & Cooper, D.J. 2019. Establishing vegetation on a constructed fen in a post-mined landscape in Alberta's oil sands region: A four-year evaluation after species introduction. Ecological Engineering. 130: 11-22

Brungs, W.A. 1973. Effects of residual chlorine on aquatic life. Water Pollution Control Federation. 45(10): 2180-2193

Canada's Oil Sands Innovation Alliance (COSIA). 2017. Guide for in situ reclamation in the Oil Sands Region of Alberta: Reclaiming in situ pads and roads to peatlands.

Cannings, R.A., & Cannings, S.G. 1987. The Odonata of some saline lakes in British Columbia, Canada: Ecological distribution and zoogeography. Advances in Odonatology. 3(1): 7-21

Chapman R.F. 1975. "Nitrogenous Excretion and Salt and Water Regulation." *In* The Insects: Structure and Function. New York, NY. American Elsevier Publishing Company, 1975: 490-512

Ciborowski, J.J.H. 1991. Estimating processing time of stream benthic samples. Hydrobiologia. 222(2): 101-107

Clark M.G., Humphreys E., & Carey S.K. 2019. The initial three years of carbon dioxide exchange between the atmosphere and reclaimed oil sand wetland. Ecological Engineering, 135: 116-126

Clifford, H.F. 1990. Aquatic invertebrates of Alberta. University of Alberta Press, Edmonton, AB.

Cummins, K.W. 1973. Trophic relations of aquatic insects. Annual Review of Entomology. 18: 183-206

Cummins, K.W. 1974. Structure and function of stream ecosystems. BioScience. 24(11): 631-641

Cumulative Environmental Management Association (CEMA). 2003. Creating wetlands in oil sands reclamation workshop proceedings, October 2003, Fort McMurray, Alberta.

Daly C.A. 2011. "History of wetland reclamation in the Alberta oil sands", Proceedings of the Sixth International Conference on Mine Closure. Ed. Fourie A.B., Tibbett M., & Beersing A. Australian Centre for Geomechanics, Perth, Australia. pages 535-544

Demetrio, C.G.B, Hinde, J., & Moral, R.A. 2014. Models for overdispersed data in Entomology. *In* Ferreira, C., & Godoy, W. (eds) Ecological Modelling Applied to Entomology in Focus, vol 1. Springer, Cham.

Dufrêne, M., & Legendre, P. 1997. Species assemblages and indicator species: The need for a flexible asymmetrical approach. Ecological Monographs. 67(3): 345-366

Dugan, H.A., Helmueller, G., & Magnuson, J.J. 2017. Ice formation and the risk of chloride toxicity in shallow wetlands and lakes. Limnology and Oceanography Letters. 2: 150-158

Environment and Climate Change Canada (ECCC), Canadian Aquatic Biomonitoring Network (CABIN). 2018. CABIN wetland macroinvertebrate protocol. Gatineau (QC).: Environment and Climate Change Canada. Web http://publications.gc.ca/collections/collection_2019/eccc/CW66-571-2019-eng.pdf

Environment and Climate Change Canada (ECCC). 2020. Weather Data. Fort McMurray CS, Alberta (2020). Climate ID 3062696

Foote L. 2012. Threshold considerations and wetland reclamation in Alberta's mineable oil sands. Ecology and Society. 17(1): 35

Foote L., & Krogman N. 2006. Wetlands in Canada's western boreal forest: Agents of Change. The Forestry Chronicle. 82(6): 825-833

Gholizadeh, M., & Heydarzadeh, M. 2020. Functioanl feeding groups of macroinvertebrates and their relationhip with environmental parameters, case study: in Zarin-Gol River. Iranian Journal of Fisheries Sciences. 19(5): 2532-2543

Gibbs J.P. 2000. Wetland loss and Biodiversity Conservation. Conservation Biology. 14(1): 314-317

Giesy J.P., Anderson J.C., & Wiseman S.B. 2010. Alberta oil sands development. Proceesings of the National Academy of Sciences of the United States of America. 107(3): 951-952

Government of Alberta (GOA). 2009. Responsible Actions: A Plan for Alberta's Oil Sands.

Government of Alberta (GOA). 2015. Lower Athabasca region tailings management framework for the mineable Athabasca oil sands.

Government of Alberta (GOA). 2017. Oil Sands Facts and Statistics. Web: https://open.alberta.ca/dataset/b6f2d99e-30f8-4194- b7eb-76039e9be4d2/resource/063e27cc-b6d1-4dae-8356- 44e27304ef78/download/fsoilsands.pdf

Government of Alberta (GOA). 2018. Environmental Quality Guidelines for Alberta Surface Waters. Water Policy Branch, Alberta Environment and Parks. Edmonton, Alberta.

Government of Alberta (GOA). 2021. Environmental Protection and Enhancement Act. Revised Statutes of Alberta 2000 Chapter E-12. Updated December 2021.

Golterman, H.L. 1995. Theoretical aspects of the adsorption of ortho-phosphate onto iron-hydroxide. Hydrobiologia. 315: 59-68

Gomez-Deniz, E., Gallardo, D.I., Gomez, H.W. 2019. Quasi-binomial zero-inflated regression model suitable for variables with bounded support. Journal of Applied Statistics. 47(12): 2208-2229

Grueber, W.B., & Bradley, T.J. 1994. The Evolution of Increased Salinity Tolerance in Larvae of *Aedes* Mosquitos: A Phylogenetic Analysis. Physiological Zoology. 67(3): 566-579

Gullan P.J., & Cranston P.S. 2010. The insects: An outline of entomology. 4th ed. West Sussex(UK): Wiley-Blackwell.

Hall, L.W., & Anderson, R.D. 1995. The Influence of Salinity on the Toxicity of Various Classes of Chemicals to Aquatic Biota. Critical Reviews in Toxicology. 25(4): 281-346

Halsey L.A., Vitt D.H., & Bauer I.E. 1998. Peatland Initiation During the Holocene in Continental Western Canada. Climatic Change. 40: 315-342

Harenda K.M., Lamentowicz M., Samson M., & Chojnicki H. 2018. The Role of Peatlands and Their Carbon Storage Function in the Context of Climate Change. *In* Interdisciplinary Approaches for Sustainable Development Goals. *Edited by* T. Zielinski, I. Sagan, W. Surosz. Springer International Publishing. Cham, Switzerland. p. 169-187

Hartsock J. 2020. Characterizations of key performance measures at the reclaimed sandhill wetland: implications for achieving wetland reclamation success in the Athabasca oil sands region. PhD thesis. Southern Illinois University, Carbondale, IL, USA.

Hartsock J.A., House, M., Clark, M.G., & Vitt, D.H. 2021a. A comparison of plant communities and water chemistry at Sandhill Wetland to natural Albertan peatlands and marshes. Ecological Engineering. 169: 106313

Hartsock J.A., Piercey, J., House, M.K., & Vitt, D.H. 2021b. An evaluation of water quality at Sandhill Wetland: Implications for reclaiming wetlands above soft tailings deposits in northern Alberta, Canada. Wetlands Ecological Management. 29: 111-127

Hawkes, V.C., Miller, M.t., Novoa, J., Ibeke, E., & Martin, J.P. 2020. Opportunistic wetland formation, characterization and quantification on lanforms reclaimed to upland ecosites in the Athabasca Oil Sands Region. Wetlands Ecology and Management. 28: 953-970

Heffernan, L., Estop-Aragones, C., Knorr, K., Talbot, J., & Olefeldt, D. 2020. Long-term impacts of permafrost thaw on carbon storage peatlands: Deep losses offset by surficial accumulation. Journal of Geophysical Research: Biogeosciences. 125(3): e2019JG005501
Herbert E.R., Boon P., Burgin A.J., Neubauer S.C., Franklin R.B., Ardon M., Hopfenspreger K.N., Lamers L.P.M., & Gell P. (2015). A global perspective on wetland salinization: ecological consequences of a growing threat to freshwater wetlands. Ecosphere, 6(10): 1-43

Herbert, E.R., Boon, P., Burgin, A.J., Neubauer, S.C., Franklin, R.B., Ardon, M., Hopfensperger, K.N., Lamers, L.P.M., & Gell, P. 2015. Ecosphere. 6(10): Article 206

Hilsenhoff W.L. 1982. Using a biotic index to evaluate water quality in streams. Madison Wisconsin: Department of Natural Resources.

Hilsenhoff, W.L. 1988. Rapid field assessment of organic pollution with a family-level biotic index. Journal of the North American Benthological Society. 7(1): 65-68

Holm, S. 1979. A Simple Sequentially Rejective Multiple Test Procedure. Scandinavian Journal of Statistics. 6: 65-70

Howard, K.W.F., & Haynes, J. 1993. Groundwater contamination due to road de-icing chemicals: Salt balance implications. Geoscience Canada. 20(1): 1-8

Howland, J.R., Alexander, A.C., Milani, D., Culp, J.M., & Peru, K.M. 2019. Effects of oil sands process water mixtures on the mayfly *Hexagenia* and field-collected aquatic macroinvertebrate communities. Ecotoxicology. 28: 658-668

Hugget, A.J. 2005. The concept and utility of ecological thresholds in biodiversity conservation. Biological Conservation. 124(2005): 301-310

Hutton M.J., MacDonald G.M., & Mott R.J. 1994. Postglacial vegetation of the Mariana Lake region, Alberta. Canadian Journal of Earth Sciences. 31: 418-425

Jonusaite, S., Donini, A., & Kelly, S.P. 2017. Salinity alters snakeskin and mesh transcript abundance and permeability in midgut and Malpighian tubules of larval mosquito, *Aedes aegypti*. Comparative Biochemistry and Physiology Part A: molecular & Integrative Physiology. 205: 58-67

Kannel P.R., & Gan, T.Y. 2012. Napthenic acids degredation and toxicity mitigation in tailings wastewater systems and aquatic environments: A review. Journal of Environmental Science and Health, Part A. 47(1): 1-21

Karr, J.R. 1981. Assessment of Biotic Integrity Using Fish Communities. Fisheries. 6(6): 21-27

Kavanagh, R.J., Frank, E.A., Burnison, B.K., Young, R.F., Fedorak, O.M., Solomon, K.R., & Kraak G.V.D. 2012. Fathead minnow (*Pimephales promelas*) reproduction is impaired when exposed to a naphthenic acid extract. Aquatic Toxicology. 116-117: 34-42

Kerans, B.L. & Karr, J.R. 1994. A Benthic Index of Biotic Integrity (B-IBI) for Rivers of the Tennessee Valley. Ecological Applications. 4(4): 768-785

Ketcheson S.J., Price J.S., Carey S.K., Petrone R.M., Mendiza C.A., & Devito K.J. 2016. Constructing fen peatlands in post-mining oil sands landscapes: Challenges and opportunites from a hydrological perspective. Earth Science Reviews. 161: 130-139

King, R.S., & Baker, M.E. 2010. Considerations for analyzing ecological community thresholds in response to anthropogenic environmental gradients. Journal of North American Benthological Society. 29(3): 998-1008

Kovalenko K.E., Ciborowski J.J.H., Daly C., Dixon D.G., Farwell A.J., Foote A.L., Frederick K.R., Gardner Costa J.M., Kennedy K., Liber K., Roy M.C., Slama C. A., & Smits J.E.G. 2013. Food web structure in oil sands reclaimed wetlands. Ecological Applications. 23(5): 1048-1060

Lancaster J., & Scudder G.G.E. 1986. Aquatic Coleoptera and Hemiptera in some Canadian saline lakes: patterns in community structure. Canadian Journal of Zoology. 65: 1383-1390

Legendre, P., & Gallagher, E.D. 2001. Ecologically meaningful transformation for ordination of species data. Oecologia. 129: 271-280

Legendre, P., & Legendre, L. 2012. Numerical Ecology. 3rd ed. Elsevier. Oxford, UK.

Leonhardt, C.L., 2003. Zoobenthic succession in Constructed Wetlands of the Fort McMurray Oil Sands Region: Developing a Measure of Zoobenthic Recovery. M.Sc. Thesis, University of Windsor, Windsor, ON, Canada.

Little-Devito, M., Mendoza, C.A., Chasmer, L., Kettridge, N., & Devito, K.J. 2019. Opportunistic wetland formation on reconstructed landforms in a sub-humid climate: Influence of landscape-scale factors. Wetlands Ecology and management. 27: 587-608

McQueen A.D., Kinley, C.M., Hendriske,, M., Gaspari, D.P., Calomeni, A.J., Iwinski, K.J., Castle, J.W., Haakensen, M.C., Peru, K.M., Headley, J.V., & Rodgers, J.H. 2017. A risk-based approach for identifying constituents of concern in oil sands process-affected water from the Athabasca Oil Sands region. Chemosphere. 173: 340-350

Menard, K. 2017. Community development of terrestrial and semi-terrestrial invertebrates along environmental gradients in a reclaimed watershed. M.Sc. University of Windsor, Windsor, ON, Canada

Merritt R.W., Cummins K.W., & Berg M.B. 2019. An introduction to the aquatic insects of North America. Ed. 5. Dubuque, Iowa: Kendall/Hunt Pub Co.

Mitsch W.J., & Gosselink J.G. 2015. Wetlands. 5th ed. Hoboken (NJ): John Wiley & Sons

Moore, J.C., Berlow, E.L., Coleman, D.C., de Ruiter, P.C., Dong, Q., Hastings, A., Johnson, N.C., McCann, K.S., Melville, K., Morin, P.J., Nadelhoffer, K., Resomond, A.D., Post. D.M., Sabo, J.L., Scow, K.M., Vanni, M.J., & Wall, D.H. 2004. Detritus, trophic dynamics and biodiversity. Ecology Letters, 7: 584-600

Moore, E. 2020. Successional and disturbance controls on macroinvertebrate community composition in young boreal wetlands. Undergraduate Honours Thesis in Environmental Science, University of Calgary, Calgary, AB, Canada

Mushet, D.M., Goldhaber, M.B., Mills, C.T., McLean, K.I., Aparicio, V.M., McCleskey, R.B., Stockwell, C.A. 2015. Chemical and biotic characteristics of prairie lakes and large wetlands in south-central North Dakota: Effects of a changing climate. U.S. Geological Survey Scientific Investigation Report 2015-5126.

Natural Resources Canada (NRCAN), Energy Reports and Publications. 2016. Oil Sands: Indigenous peoples. Web < https://www.nrcan.gc.ca/energy/publications/18736 >

Nwaishi F., Petrone, R.M., Price, J.S., & Anderson, R. 2015. Towards developing a functional-based approach for constructed peatlands evaluation in the Alberta Oil Sands Region, Canada. Wetlands. 35: 211-225

Papanikolaou, N.E., Kavellieratos, N.G., Boukouvala, M.C., & Malesios, C. 2021. (Quasi)-Binomial vs Gaussian models to evaluate Thiamethoxam, Pirimiphos-Methyl, Alpha-Cypermethrin and Deltamethrin on different types of storage bag materials against *Ephestia kuehniella* zeller (Libidoptera: Pyralidae) and *Tribolium confusum* Jacquelin du Val (Coleoptera: Tenebrionidae). Insects. 12(2): 182

Pallarés S, Arribas P, Bilton DT, Millán A, Velasco J. 2015. The comparative ssmoregulatory ability of two water beetle genera whose species span the fresh-hypersaline gradient in inland waters (Coleoptera: Dytiscidae, Hydrophilidae). PLoS ONE 10(4): e0124299.

Petchey, O.L., & Gaston K.J. 2006. Functional diversity: Back to basics and looking forward. Ecology Letters. 9(6): 741-758

Pimm, S.L., & Lawton, J.H. 1977. Number of trophic levels in ecological communities. Nature, 268: 329-331

Popovic, N., Petrone, R.M., Green, A., Khomik, M., & Price, J.S. 2022. A temporal snapshot of ecosystem functionality during the initial stages of reclamation of an upland-fen complex. Journal of Hydrology: Regional Studies. 41: Article 101078

Preston T.M., Borgreen, M.J., & Ray, A.M. 2018. Effects of brine contamination from energy development on wetland macroinvertebrate community structure in the Prairie Pothole Region. Environmental Pollution. 239: 722-732

Price J.S., McLaren R.G., & Rudolph D.L. 2010. Landscape restoration after oil sands mining: conceptual design and hydrological modelling for fen reconstruction. International Journal of Mining, Reclamation and Environment. 24(2): 109-123

Purdy B.G., Macdonald S.E., & Lieffers V.J. 2005. Naturally saline boreal communities as models of reclamation of saline oil sands tailings. The Journal of the Society for Ecological Restoration. 13(4): 667-677

Quagrine E.K., Peterson, H.G., & Headley, J.V. 2005. In situ bioremediation of naphthenic acids contaminated tailing pond waters in the Athabasca Oil Sands Region – demonstrated field studies and plausible options: A review. Journal of Environmental Science and Health, Part A. 40(3): 685-722

R Core Team. 2021. R: A language and environment for statistical computing. *R Foundation for Statistical Computing*. Vienna, Australia. URL: https://www.R-project.org/

Risacher, F.F., Morris, P.K., Arriaga, D., Goad, C., Nelson, T.C., Slater, G.F., & Warren, L.A. 2018. The interplay of methane and ammonia as key oxygen consuming constituents in early stage development of Mase Mine Lake, the first demonstration oil sands pit lake. Applied Geochemistry. 93: 49-59

Rooney R.C., & Bayley S.E. 2011. Setting reclamation targets and evaluating progress: Submersed aquatic vegetation in natural and post-oil sands mining wetlands in Alberta, Canada. Ecological Engineering 37(4): 569 – 579

Schleuter, D., Daufresne, M., Massol, F., & Argillier, C. 2010. A user's guide to functional diversity indices. Ecological Monographs 80(3): 469-484

Silberbush, A., & Blaustein, L. Mosquito females quantify risk predation to their progeny when selecting an oviposition site. Functional Ecology. 25(5): 1091-1095

Simhayov R.B., Price J.S., Smeaton C.M., Parsons C., Rezanezhad F., & Cappellen P.V. 2017. Solute pools in Nikanotee Fen watershed in the Athabasca oil sands region. Environmental Pollution. 225: 150-162

Sjogersten, S., Caul, S., Daniell, T.J., Jurd, A.P.S., O'Sullivan, O.S., Stapleton, C.S., & Titman, J.J. 2016. Organic matter chemistry controls greenhouse gas emissions from permafrost peatlands. Soil Biology and Biochemistry. 98: 42-53

Stewart, A.J., Hill, W.R., Ham, K.D., Christensen, S.W., & Beauchamp, J.J. 1996. Chlorine dynamics and amient toxicity in receiving streams. Ecological Applications. 6(2): 458-471

Storm, S.L., Harvey, E.L., Fredrickson, K.A., & Menden-Deuer, K.A. 2013. Broad salinity tolerance as a refuge from predation in the harmful raphidophyte alga *Heterosigma akashiwo* (Raphidophyceae). Journal of the Physiological Society of America 49: 20-31

Swindlers, G.T., Morris, P.J., Mullan, D., Watson, E.J., Turner, T.E., Roland, T.P., Amesbury, M.J., Kokfelt, U., Schloning, K., Pratte, S., Gallego-Sala, A., Charman, D.J., Sanderson, N., Garneau, M., Carrivick, J.L., Woulds, C., Holden, J., Parry, L., & Galloway, J.M. 2015. The long-term fate of permafrost peatlands under rapid climate warming. Scientific Reports 5: 17951

Syncrude Canada Limited. 2020. Composite tailings capping knowledge synthesis.

Tilman, D. 2001. "Functional Diversity" *In* Encyclopedia of Biodiversity (Vol. 3). Ed. Levin, S.A. pages 109-120

Timms, B.V., Hammer, U.T., & Sheard, J.W. 1986. A study of benthic communities in some saline lakes in Saskatchewan and Alberta, Canada. International Review of Hydrobiology. 71(6): 759-777

Tomal, J.H. & Ciborowski, J.J.H. 2020. Ecological models for estimating breakpoints and prediction intervals. R\Ecology and Evolution. 2020(10): 13500-13517

Trites M., & Bayley S.E. 2009. Vegetation communities in continental boreal wetlands along a salinity gradient: Implications for oil sands mining reclamation. Aquatic Botany. 91: 27-39

U.S. EPA. 2002. Methods for Evaluating Wetland Condition: Developing metrics and Indexes of biological Integrity. Office of Water, U.S. Environmental Protection Agency, Washington, DC. EPA-822-R-02-016

Van Meter, R.J., Swan, C.M., Leips, J., & Snodgrass, J.W. 2011. Road salt stress induces novel food web structure and interactions. Wetlands. (31): 843-851

Vitt D. 2018. Interview with *Peatlands*: "Expert Q&A: Dr. Dale Vitt". Fall Equinox 2018, 16:3. https://www.biohabitats.com/newsletter/peatlands/expert-qa-dr-dale-vitt/

Vitt D.H., Weider, R.K., Scott, K.D., & Faller S. 2009. Decomposition and peat accumulation in rich fens of Boreal Alberta, Canada. Ecosystems. 12: 360-373

Vitt D.H., & House M. 2015. Establishment of bryophytes from indigenous sources after disturbance from oil sands mining. The Bryologist. 118(2): 123-129

Vitt D.H., House M., Hartsock J.A. 2016. Sandhill Fen, an initial trial for wetland species assembly on in-pit substrates: Lessons after three years. Botany. 94: 1015-1025

Volik O., Petrone R.M., Hall R.I., Macrae M.L., Wells C.M., Elmes M.C., & Price J.S. 2017. Long-term precipitation-driven salinity change in a saline peat-forming wetland in the Athabasca Oil Sands Region, Canada: a diatom-based paleolimnological study. Journal of Paleolimnology. 58: 533-550

Volik O., Petrone, R.M., Hall, R.I., Macrae, M.L., & Wells, C.M. 2018. Organic matter accumulation and salinity change in open water areas within a saline boreal fen in the Athabasca Oil Sands Region, Canada. Catena 165: 425-433

Volik O., Petrone R.M., Quanz A., Macrae M.L., Rooney R., & Proce J.S. 2019. Environmental controls in CO_2 exchange along a salinity gradient in a saline boreal fen complex in the Athabasca oil sands region. Wetlands. 40(5): 1353-1366

Wallace, A.M., & Biastoch, R.G. 2016. Detecting changes in the benthic invertebrate community in response to increasing chloride in streams in Toronto, Canada. Freshwater Science. 35(1): 353-363

Wells C.M., & Price J.S. 2015. A hydrologic assessment of a saline-spring fen in the Athabasca oil sands region, Alberta, Canada: A potential analogue for oil sands reclamation. Hydrological Processes. 29(20): 4533-4548

Wetzel R.G. 2001. "Salinity of Inland Waters." *In* Limnology: Lake and River Ecosystems. 3rd ed. San Diego, CA. Academic Press, 2001: 169-187

Whelly, M.P. 1999. Aquatic invertebrates in wetlands of the oil sands region of northeast Alberta, Canada, with emphasis on Chironomidae (Diptera). M.Sc. Thesis, University of Windsor, Windsor, ON, Canada.

Wissinger, S.A. 1999. Ecology of Wetland Invertebrates: Synthesis and Applications for Cnservation and Management. *In*: Batzer, D.P., Rader, R.B., & Wissinger, S.A. (eds). Invertebrates in Freshwater Wetlands of North America: Ecology and Management. New York: John Wiley: 1043-1086

Wytrykush C., Vitt D.H., McKenna G., & Vassov R. 2012. Designing landscapes to support peatland development on soft tailings deposits. *In* Restoration of boreal ecosystems. *Edited by* D.H. Vitt and J. Bhatti. Cambridge University Press, Cambridge. p. 161-178

Zheng, W., Wang, R., Zhang, E., Yang, H., & Xu, M. 2021. Declining chironomid diversity in relation to human influences in southwest China. Anthropocene 36(2021): 100308.

Appendix A1: The Influence of Waterbody Morphometry on the Community Composition of Aquatic Macroinvertebrates and Environmental Conditions in a Saline Fen Complex

Introduction

This section details the potential influence of morphometry on macroinvertebrate community composition and water chemistry of waterbodies within the saline fen complex. Benthic invertebrate samples, water samples, standard water quality parameter measurements (dissolved oxygen concentration, specific conductance, pH and reduction oxidation potential), maximum depth, water temperature, and qualitative estimates of length and width were collected from 52 waterbodies within the saline fen. Upon arrival, waterbodies were identified as flarks (n=38), flark/ponds (n=9), and ponds (n=5). Flarks are typically observed in patterned fens, and are landforms characterized as a shallow depression filled with water containing emergent vegetation (AEP 2017). In this analysis, the depth of flark sites was typically between 8 and 15 cm. The primary emergent vegetation present in flarks were *Juncus balticus* and *Triglochin maritima*. Ponds were also common in the saline fen complex, although less-so than flarks. Ponds were waterbodies of variable depths (typically between 15 and 30 cm) and contained emergent vegetation only around the periphery of the waterbody. The open water zone of ponds typically contained some submerged aquatic vegetation, or no vegetation at all. Flark/ponds contained similarities of both flarks, and ponds, with the majority of their wetted area containing emergent vegetation, and a small open water zone in the center, with minimal, or no submerged aquatic vegetation. In this appendix's two sections, I contrast environmental and water chemistry conditions and then macroinvertebrate community composition among the three wetland types. Tables A1.1 to A1.3 contain environmental variables and water chemistry data collected for this analysis. All statistical analyses were conducted using R version 3.6.1 (R Core Team 2021).

Table A1.1: Site name, location, collection date and environmental parameters measured at 52 sampling sites and incorporated into analysis for Appendix A1. Sites and entries that are italicized were identified as outliers using Dixon's Q-test (Table A2.5) and were excluded from the principal component analysis (Figure A1.1), the Pearson's correlation coefficient calculations (Table A1.6). NMDS (Figure A1.2), and Indval (Table A1.15) analyses.

Site Code	**Collection Date 2020)**	**Northing**	**Easting**	**Water Temp. (˚C)**	**DO (mg/L)**	**Spec. Cond. (µS/cm)**	**pH**	**ORP (mV)**	**Max. Depth(cm)**
SFC-A-003	09-08	56.57316	-111.27444	13.5	5.11	6866	6.73	129.6	15
SFC-A-004	09-07	56.57318	-111.27422	14.4	6.55	6271	7.12	197.4	9
SFC-A-007	09-06	56.57314	-111.27393	13.8	8.79	4972	7.41	171.2	13
SFC-A-009	09-08	56.57275	-111.27375	13.4	5.76	7021	7.2	181.2	10
SFC-A-010	09-08	56.57265	-111.27384	14.1	5.07	6804	6.66	144.6	6
SFC-A-012	09-06	56.57183	-111.27394	15.2	9.03	10283	7.24	217.2	16.5
SFC-A-015	09-07	56.57182	-111.27396	15.5	5.58	12564	6.95	202.8	17
SFC-A-019	09-07	56.57159	-111.27364	13.9	6.71	8515	7.18	193.8	17.5
SFC-A-020	09-08	56.57164	-111.27283	17	3.5	7400	6.27	122.2	8
SFC-A-026	09-06	56.57115	-111.27268	13.2	9.34	6401	7.64	207.8	10.33
SFC-A-027	09-08	56.571	-111.27268	14	8.31	9125	7.27	206.9	24
SFC-A-033	09-08	56.57089	-111.27288	13.2	8.03	10692	7.11	173.6	7.5
SFC-A-036	09-08	56.57064	-111.2727	15.6	9.02	6314	6.8	106.9	20
SFC-A-039	09-08	56.57049	-111.2727	16	7.97	9369	6.8	135.3	24
SFC-A-041	09-06	56.57033	-111.27235	14.3	11.62	5739	7.8	201.1	25.83
SFC-A-042	09-07	56.57028	-111.27209	13.7	10.03	5812	6.85	102.4	22
SFC-A-043	09-07	56.57003	-111.27197	13	9.71	7783	6.89	102.9	14
SFC-A-051	09-07	56.56809	-111.27072	12.1	7.45	16529	7.06	91.3	6.5
SFC-A-056	09-06	56.56739	-111.26942	12.9	6.22	11478	7.33	107.6	12.5
SFC-A-068	09-06	56.56746	-111.2696	14.9	11.23	11173	7.35	198.5	20
SFC-A-074	09-07	56.56805	-111.26871	11	8.23	17045	7.37	173.7	22
SFC-A-076	09-07	56.57143	-111.27413	11.5	6.48	9095	7.62	183.9	21
SFC-A-077	09-07	56.57154	-111.27426	13.2	4.74	8814	7.37	179.8	24

SFC-A-078	09-08	56.56747	-111.26964	11.2	6.03	14590	6.5	234.2	15
SFC-A-079	09-08	56.56783	-111.27033	11.3	4.41	20170	6.98	201.1	28
SFC-A-080	09-08	56.56941	-111.27325	13.3	5.84	9116	7.15	182.2	9
SFC-A-081	09-08	56.57037	-111.27412	14.4	7.28	10627	7.15	216.9	9
SFC-A-082	09-08	56.57059	-111.27438	15.3	7.7	10163	7.15	209.7	12
SFC-B-003	09-07	56.57433	-111.27753	14.1	7.3	4816	7.16	205.3	20
SFC-B-004	09-08	56.5743	-111.27704	10	6.6	5125	6.88	116.6	16
SFC-B-005	09-08	56.57436	-111.27631	10.1	6.32	5151	7.01	98.9	9.5
SFC-B-006	09-08	56.57412	-111.27622	11	6.15	5474	6.96	110.2	12
SFC-B-010	09-08	56.57359	-111.27655	11.6	5.48	5123	6.8	109.7	11.5
SFC-B-011	09-06	56.57352	-111.27621	13.9	5.44	4845	*3.9*	125.8	6
SFC-B-026	09-05	56.57455	-111.27743	14.8	8.55	4160	*4.2*	91.3	17.5
SFC-B-035	09-08	56.57154	-111.27443	14.1	4.62	6888	6.7	77.2	22
SFC-B-038	09-08	56.57129	-111.27414	13.5	7.54	9868	7.44	116.4	18
SFC-B-039	09-08	56.57092	-111.27441	14.6	4.94	6646	6.91	109.9	24
SFC-B-049	09-07	56.56965	-111.27278	11.5	4.05	10892	7.18	80.5	14
SFC-B-051	09-07	56.56939	-111.27316	13.5	7.3	9812	6.87	8	23
SFC-B-052	09-07	56.5693	-111.2732	13.4	7.66	9402	6.65	54.4	6.5
SFC-B-055	09-06	56.5689	-111.27265	13.9	8.11	3757	6.78	185.4	12.5
SFC-B-058	09-06	56.56798	-111.27065	13.6	5.91	15918	6.99	199.5	11
SFC-B-059	09-07	56.56796	-111.27061	11.5	5.93	18328	6.83	97.6	31
SFC-B-060	09-07	56.56786	-111.27037	10.7	6.76	18628	7.36	187.6	27.5
SFC-B-062	09-08	56.56786	-111.27	11.3	3.57	17759	6.84	172.5	19
SFC-B-063	09-07	56.56792	-111.26964	12.8	9.52	13274	7.15	106.6	16
SFC-B-064	09-07	56.5682	-111.26982	10	9.3	15556	7	98.4	18
SFC-B-065	09-07	56.56812	-111.26936	10.7	3.65	9392	6.46	47.4	18.5
SFC-B-068	09-07	56.56795	-111.26873	8.5	3.33	17106	7.26	126.2	14.5
SFC-B-069	09-07	56.56759	-111.26923	9.4	7.59	9498	6.92	158.8	22.5
SFC-B-070	09-06	56.56906	-111.27283	13.7	3.59	9572	7.32	189.9	13

Table A1.2: Site name, morphometry and major anion concentrations measured at 52 sampling sites and incorporated into analysis for Appendix A1. Sites and entries that are italicized were identified as outliers using Dixon's Q-test (Table A2.5) and were excluded from the principal component analysis (Figure A1.1), the Pearson's correlation coefficient calculations (Table A1.6). NMDS (Figure A1.2), and Indval (Table A1.15) analyses. Values shown in red were below the limit of detection, and adjusted using the R2D method (Antweiler 2015).

Site Code	Morphometry	Cl (mg/L)	SO4-S (mg/L)	NH4-N (µg/L)	PO4-P (µg/L)	TON-N (µg/L)	S (mg/L)
SFC-A-003	Flark	1683	7.120	89.91	2.828	39.21	8.085
SFC-A-004	Flark	1542	0.283	254.7	4.802	17.56	4.265
SFC-A-007	Flark	1320	0.283	19.84	5.963	12.02	4.019
SFC-A-009	Flark	1631	0.283	222.7	5.470	18.64	3.048
SFC-A-010	Flark	1710	0.283	76.92	4.832	29.53	2.397
SFC-A-012	Flark	2712	0.283	208.8	4.961	20.27	1.884
SFC-A-015	Flark	3009	0.283	180.3	4.513	22.82	4.523
SFC-A-019	Flark	2109	1.210	35.43	7.954	21.43	8.346
SFC-A-020	Flark	1713	1.184	293.3	8.806	26.99	2.401
SFC-A-026	Flark	1835	0.283	50.81	5.510	16.61	2.047
SFC-A-027	Flark	2173	0.283	180.5	4.478	16.61	2.497
SFC-A-033	Flark	2403	17.96	171.08	2.828	55.01	19.683
SFC-A-036	Flark	1432	0.283	25.06	5.574	15.58	2.267
SFC-A-039	Flark	2126	0.283	372.3	2.828	16.03	2.854
SFC-A-041	Flark/Pond	1626	0.283	52.19	6.395	17.99	2.610
SFC-A-042	Flark	1496	0.283	89.92	4.599	36.02	2.411
SFC-A-043	Flark	2052	0.283	22.85	4.705	21.38	7.044
SFC-A-051	Flark	4508	36.84	302.7	10.42	26.63	33.618
SFC-A-056	Flark	3332	3.759	53.75	21.41	49.11	7.585
SFC-A-068	Flark/Pond	3010	10.02	34.50	13.89	28.81	11.285
SFC-A-074	Flark/Pond	4496	19.87	44.36	13.09	25.53	17.159
SFC-A-076	Pond	2374	19.03	138.7	2.828	305.6	16.121
SFC-A-077	Flark	2275	15.33	205.0	4.147	24.30	12.874

SFC-A-078	Flark/Pond	3577	8.744	74.54	13.07	55.92	19.892
SFC-A-079	Pond	5550	63.62	94.70	4.519	32.27	63.295
SFC-A-080	Flark	2301	0.283	112.5	2.828	11.09	6.356
SFC-A-081	Flark	2626	17.38	210.6	4.195	18.60	17.364
SFC-A-082	Flark	2464	16.90	24.61	4.193	10.29	13.040
SFC-B-003	Flark	1206	0.283	289.0	2.828	19.44	2.073
SFC-B-004	Flark	1431	0.283	24.17	5.131	22.41	2.491
SFC-B-005	Flark	1593	0.283	23.01	2.828	11.50	4.343
SFC-B-006	Flark	1533	4.448	287.2	2.828	16.99	5.294
SFC-B-010	Flark	1355	0.283	85.30	4.012	37.64	2.836
SFC-B-011	Flark	1634	2.596	121.9	2.828	17.92	5.456
SFC-B-026	Flark	787	0.283	76.57	2.828	18.39	1.962
SFC-B-035	Flark/Pond	1577	0.283	82.76	4.919	16.84	4.900
SFC-B-038	Flark/Pond	2675	18.90	258.8	8.013	70.34	17.033
SFC-B-039	Pond	1834	0.283	31.67	4.181	8.461	2.964
SFC-B-049	Flark	3043	27.36	*1591*	*133.1*	*590.0*	23.897
SFC-B-051	Pond	2537	19.49	68.18	4.375	15.73	15.751
SFC-B-052	Flark	2363	8.072	34.89	4.287	8.830	9.128
SFC-B-055	Flark	985	0.283	24.83	4.842	10.16	4.408
SFC-B-058	Flark	5170	54.44	34.64	5.087	10.32	45.806
SFC-B-059	Flark/Pond	5264	54.45	80.05	4.933	26.13	48.293
SFC-B-060	Flark	5395	51.35	29.80	5.652	10.43	46.613
SFC-B-062	Pond	4603	39.43	242.3	6.249	18.33	36.897
SFC-B-063	Flark/Pond	3839	12.19	413.5	9.368	40.39	19.380
SFC-B-064	Flark/Pond	4453	16.14	46.20	14.33	299.3	22.212
SFC-B-065	Flark	3568	9.973	66.73	12.38	31.37	19.321
SFC-B-068	Flark	4581	1.726	37.78	16.47	23.43	16.957
SFC-B-069	Flark	2517	28.34	44.74	15.80	37.38	31.162
SFC-B-070	Flark	2942	25.71	*1558*	*140.2*	*422.3*	24.352

Table A1.3: Site name and major cation concentrations measured at 52 sampling sites and incorporated into analysis for Appendix A1. Sites and entries that are italicized were identified as outliers using Dixon's Q-test (Table A2.5) and were excluded from the principal component analysis (Figure A1.1), the Pearson's correlation coefficient calculations (Table A1.6). NMDS (Figure A1.2), and Indval (Table A1.15) analyses. Values shown in red were below the limit of detection, and adjusted using the R2D method (Antweiler 2015).

Site Code	Al mg/L	B mg/L	Ba mg/L	Ca mg/L	Fe mg/L	K mg/L	Li mg/L	Mg mg/L	Mn mg/L	Na mg/L	S mg/L	Si mg/L	Sr mg/L
SFC-A-003	2.994	2.204	0.041	53.516	0.313	6.484	0.508	29.307	0.061	977.290	8.085	2.327	2.974
SFC-A-004	3.455	2.517	0.042	46.539	0.543	5.225	0.449	26.132	0.093	911.090	4.265	2.830	2.555
SFC-A-007	3.516	2.337	0.089	95.860	0.239	7.517	0.557	48.745	0.150	1663.930	4.019	1.732	5.245
SFC-A-009	2.942	2.080	0.042	45.882	1.083	5.836	0.438	25.134	0.114	1763.587	3.048	2.147	2.469
SFC-A-010	3.457	1.991	0.043	50.055	0.453	3.046	0.329	27.141	0.045	976.393	2.397	1.943	2.773
SFC-A-012	4.071	2.530	0.042	66.751	0.434	4.929	0.363	28.497	0.090	1043.162	1.884	2.054	2.896
SFC-A-015	3.472	2.874	0.096	103.130	0.262	6.233	0.515	53.850	0.251	1810.690	4.523	2.482	5.837
SFC-A-019	2.633	2.173	0.041	49.433	0.197	4.119	0.318	26.356	0.044	1180.340	8.346	2.595	2.879
SFC-A-020	4.575	2.435	0.040	49.638	1.478	2.504	0.258	25.159	0.093	1036.734	2.401	3.379	2.701
SFC-A-026	3.206	1.867	0.042	45.125	0.786	3.918	0.249	19.623	0.129	728.357	2.047	2.118	1.895
SFC-A-027	2.964	2.089	0.042	64.372	0.242	4.139	0.358	35.195	0.036	1269.549	2.497	2.189	3.632
SFC-A-033	3.715	2.254	0.047	76.712	0.276	6.016	0.381	42.332	0.048	1562.504	19.683	3.745	4.505
SFC-A-036	2.837	1.980	0.042	42.909	0.435	3.689	0.346	21.624	0.033	901.282	2.267	2.847	2.149

SFC-A-039	2.815	1.945	0.066	73.196	0.421	4.090	0.438	39.540	0.156	1390.034	2.854	3.033	4.039
SFC-A-041	3.664	2.447	0.042	52.221	0.914	3.365	0.291	26.552	0.115	1016.212	2.610	4.904	2.872
SFC-A-042	3.852	2.090	0.042	34.959	0.389	2.651	0.235	21.020	0.024	847.351	2.411	3.892	2.209
SFC-A-043	3.572	2.292	0.051	62.484	0.416	3.945	0.355	35.905	0.033	1320.825	7.044	3.323	3.709
SFC-A-051	2.777	2.997	0.042	99.202	0.589	11.143	0.533	62.194	0.072	2708.529	33.618	2.209	6.768
SFC-A-056	3.017	2.433	0.042	63.634	2.643	5.133	0.368	38.855	0.049	1772.226	7.585	3.300	4.677
SFC-A-068	4.465	2.870	0.042	72.705	1.321	9.387	0.361	40.130	0.086	1812.690	11.285	1.880	4.485
SFC-A-074	4.323	2.360	0.043	108.399	1.768	11.064	0.474	63.379	0.071	2956.558	17.159	3.735	6.975
SFC-A-076	2.643	2.363	0.047	74.158	0.226	5.501	0.275	40.915	0.111	1459.408	16.121	2.886	4.014
SFC-A-077	3.550	2.358	0.051	65.538	0.255	4.448	0.229	36.442	0.100	1271.341	12.874	2.531	3.655
SFC-A-078	3.376	3.141	0.042	85.448	1.677	7.439	0.345	49.801	0.142	2241.282	19.892	2.307	5.728
SFC-A-079	4.293	3.731	0.044	141.791	0.273	25.950	0.826	90.855	0.047	3712.840	63.295	2.469	9.835
SFC-A-080	3.259	2.209	0.059	71.958	0.208	5.077	0.317	39.769	0.055	1374.806	6.356	1.653	4.006
SFC-A-081	5.264	2.140	0.064	84.009	0.263	6.801	0.365	46.605	0.053	1627.990	17.364	3.264	4.624
SFC-A-082	2.879	2.224	0.051	81.096	0.261	5.780	0.353	43.786	0.058	1449.039	13.040	3.386	4.051
SFC-B-003	2.975	2.484	0.043	40.605	0.425	3.403	0.211	21.284	0.088	709.679	2.073	2.622	1.902

SFC-B-004	5.193	2.074	0.070	49.059	0.726	2.408	0.209	24.352	0.167	835.613	2.491	3.628	2.329
SFC-B-005	2.771	1.940	0.044	52.215	0.423	1.174	0.193	23.771	0.027	823.755	4.343	2.310	2.207
SFC-B-006	4.066	1.935	0.042	43.251	0.404	1.174	0.232	25.617	0.025	850.373	5.294	2.253	2.232
SFC-B-010	3.493	2.011	0.042	40.861	0.538	1.174	0.231	23.301	0.053	795.363	2.836	2.481	1.993
SFC-B-011	3.776	2.179	0.047	44.869	0.462	1.841	0.229	26.055	0.075	837.151	5.456	2.768	2.284
SFC-B-026	1.898	2.410	0.048	38.230	0.378	2.151	0.157	18.607	0.045	623.262	1.962	2.867	1.781
SFC-B-035	2.912	2.373	0.065	58.710	0.673	1.174	0.224	30.909	0.429	985.706	4.900	2.676	2.892
SFC-B-038	2.297	2.074	0.065	80.974	0.186	5.643	0.421	45.173	0.061	1573.416	17.033	2.295	4.235
SFC-B-039	3.730	1.981	0.050	68.118	0.133	2.744	0.284	36.150	0.062	963.105	2.964	2.371	2.895
SFC-B-049	3.940	2.550	0.046	78.978	0.826	7.219	0.398	45.669	0.105	1701.535	23.897	6.527	4.511
SFC-B-051	2.784	2.321	0.052	72.597	0.296	4.345	0.306	40.362	0.107	1450.132	15.751	2.486	4.147
SFC-B-052	2.943	2.239	0.064	75.772	0.317	4.244	0.290	41.896	0.066	1431.588	9.128	1.700	3.976
SFC-B-055	3.176	1.980	0.042	39.057	0.380	1.863	0.151	19.624	0.040	633.723	4.408	2.723	1.413
SFC-B-058	3.578	2.989	0.042	121.682	0.384	12.429	0.562	77.949	0.052	3157.420	45.806	2.173	7.987
SFC-B-059	2.733	3.037	0.041	115.695	0.327	12.578	0.496	74.941	0.058	3110.040	48.293	2.406	7.955
SFC-B-060	2.996	3.139	0.049	120.195	0.306	12.985	0.471	72.886	0.043	3131.340	46.613	2.290	8.019

SFC-B-062	2.791	2.999	0.047	109.996	1.233	10.763	0.444	68.231	0.165	2850.160	36.897	2.109	7.139
SFC-B-063	5.460	2.434	0.051	112.078	1.457	6.689	0.372	66.437	0.248	2399.060	19.380	1.980	6.290
SFC-B-064	2.754	2.434	0.059	123.147	1.756	4.330	0.375	71.881	0.161	2474.140	22.212	2.403	6.761
SFC-B-065	2.756	2.392	0.078	147.692	5.194	5.999	0.562	85.440	0.175	3195.040	19.321	4.730	8.931
SFC-B-068	2.596	2.516	0.070	115.414	3.273	13.302	0.443	67.172	0.119	2799.060	16.957	3.810	7.155
SFC-B-069	3.093	2.430	0.070	94.639	1.985	2.965	0.312	49.891	0.129	1706.057	31.162	3.445	4.791
SFC-B-070	7.186	2.099	0.052	84.730	0.970	6.769	0.309	48.612	0.140	1787.623	24.352	6.602	4.731

Environmental Conditions

Methods

Sampling locations were selected as described in chapters 2 and 3, samples of flarks were collected from the deepest region of the flark, and samples from flark/ponds or ponds were collected at the boundary between the emergent vegetation and the open water zone. A water sample was collected at each of these locations by submersing a 250-mL bottle midway between the surface and the substrate. The 3 samples were then combined to form a composite sample for each site. Using the composite sample, specific conductance, dissolved oxygen, pH, water temperature and reduction-oxidation potential were measured using a YSI Proplus multiparameter meter. Two water samples (20mL) were filtered through a 0.45-μm mesh glass fibre filter into scintillation vials. One of these samples was acidified by adding 1.0 mL of 2.0 M nitric acid to the sample to be preserved for major cation analysis. The other sample was stored for analysis of anions and nutrients.

Water samples were analysed for major cations, anions, and nutrients by the Natural Resources Analytical Laboratory (NRAL) facility at the University of Alberta (Edmonton, AB) as described in Chapter 2.

Outliers were determined using Dixon's Q-test (Table A2.5), and sites containing outliers were removed from the analyses. Pearson's correlation coefficients were calculated to test correlations between water chemistry variables and the morphometry classification (Table A1.6). Morphometry types were adjusted so that flark =1, flark /pond = 2 and pond = 3. Associated p-values were adjusted for multiple comparisons using Holm's method (Aickin & Gensler 1996; Holm 1979)

Principle component analysis was conducted using water chemistry data to elucidate patterns of environmental variables across morphometry classes (Figure A1.1). Morphometry type was excluded from the principal component analysis to avoid bias, as including morphometry type could promote clustering due to the included values of morphometry. Points were then labelled as their respective morphometry classification. The principal components were rotated using varimax rotation to increase interpretability of environmental loadings onto the plotted axes (Acal et al. 2020; Figure A1.1; Table A1.8; Table A1.9)

Results

A suite 27 water chemistry and environmental variables were used to characterize sites within the saline fen complex (Table A1.4; Table A1.5), as well as make comparisons among morphometry types present at the complex (Table A1.6). To be used in Pearson's correlation coefficient analysis, the morphometry classification of each waterbody was converted to numerical data such that flark =1, flark/pond = 2 and pond = 3. The strongest correlation with morphometry is depth (Pearson's correlation coefficient = 0.512). Other variables associated weakly (Pearson's correlation coefficient > 0.3 and < 0.5) with morphometry include northing, conductivity, and concentrations of chloride, sulfate, boron, calcium, magnesium, sodium, sulfur and strontium (Table A1.6); however, no correlations with morphometry class were significant (Table A1.6). When comparing mean and standard deviation values of variables across morphometry types, value ranges overlap amongst all the environmental variables except for phosphate concentration (μg/L), which is greatest in flark/ponds, and is lowest in ponds (Table A1.5).

Table A1.4: Summary statistics of environmental and water chemistry variables. Values below limit of detection (Table A1.2; Table A1,3) were accounted for using the R2D method (Antweiler 2015). Outliers were removed using Dixon's Q test (Table A.2.5; Table A1.1; Table A2.2; Table A2.3).

Variable (Units)	Minimum	First Quartile	Median	Third Quartile	Maximum	Mean	Sd
Northing	56.56739	56.56806	56.57054	56.571775	56.57436	56.57041	0.002168
Easting	-111.27753	-111.27414	-111.27286	-111.27043	-111.26871	-111.27265	0.002296
Water Temp. (˚C)	8.5	11.35	13.4	14.1	17	12.98	1.86
DO (mg/L)	3.33	5.625	6.735	8.2	11.62	6.944	1.975
Spec. Cond. (µS/cm)	3757	6462.3	9247	12292.5	20170	9963.6	4343.4
pH	6.27	6.833	7.005	7.255	7.8	7.04	0.311
Redox (mV)	8	107.08	165	198.23	234.2	149.22	52.75
Max. Depth (cm)	6	11.125	16.25	22	31	16.493	6.415
Cl (mg/L)	985	1627.5	2332	3509	5550	2657.6	1269.8
SO4-S (mg/L)	0.283	0.283	2.7427	17.8162	63.6191	11.747	16.7496
NH4-N (µg/L)	19.84	35.024	78.484	207.888	413.455	121.838	106.166
PO4-P (µg/L)	2.828	4.1934	4.9261	7.9978	21.4115	6.6698	4.2891
TON-N (µg/L)	8.461	16.171	21.407	32.046	305.588	35.985	57.701
Al (mg/L)	2.297	2.8205	3.191	3.7023	5.46	3.3892	0.7301
B (mg/L)	1.867	2.0823	2.3475	2.508	3.731	2.3899	0.397
Ba (mg/L)	0.04	0.042	0.044	0.059	0.096	0.0513	0.0134
Ca (mg/L)	34.959	49.7423	72.2775	98.3665	147.692	75.8849	29.3669
Fe (mg/L)	0.133	0.2738	0.422	1.0408	5.194	0.8079	0.9399
K (mg/L)	1.174	3.3745	5.003	6.773	25.95	5.9753	4.3879
Li (mg/L)	0.151	0.2773	0.3565	0.4438	0.826	0.3671	0.1263
Mg (mg/L)	19.623	26.188	39.6545	52.8603	90.855	42.7523	19.1929
Mn (mg/L)	0.024	0.0483	0.0715	0.1265	0.429	0.0965	0.0731

Na (mg/L)	633.723	976.6173	1440.3135	2134.134	3712.84	1638.7669	820.3999
S (mg/L)	1.884	2.8815	7.835	18.8318	63.295	13.684	14.479
Si (mg/L)	1.653	2.194	2.4815	3.291	4.904	2.7094	0.742
Sr (mg/L)	1.413	2.719	4.01	5.8098	9.835	4.3626	2.1108

Table A1.5: Mean and standard deviation for environmental variables and water chemistry variables separated by morphometry. Data used is the same as from Table A1.4.

Variable (Units)	Flark (n=38)		Flark/Pond (n=9)		Pond (n=5)	
	Mean	**SD**	**Mean**	**SD**	**Mean**	**Sd**
Northing	56.57094	0.00216	56.56891	0.00166	56.56949	0.00168
Easting	-111.27313	0.00221	-111.27099	0.00212	-111.2724	0.0021
Water Temp. (˚C)	13.17	1.96	12.59	1.72	12.44	1.52
Dissolved Oxygen (mg/L)	6.841	1.734	8.224	2.422	5.34	1.525
DO	68.27	68.27	68.27	68.27	68.27	68.27
Spec. Cond. (µS/cm)	8891.4	3726.8	12495.7	4399.2	12696.4	5903
pH	7.016	0.286	7.127	0.409	7.044	0.326
Redox (mV)	152.45	48.69	144.86	57.12	135.08	78.94
Maximum Depth (cm)	14.38	5.9	20.87	5.06	23	3.39
Cl (mg/L)	2357.4	1125.5	3390.8	1282.4	3379.7	1605.9
SO4-S (mg/L)	8.2683	14.3948	15.654	16.1936	28.3691	24.082
NH4-N (µg/L)	123.11	105.833	120.766	129.185	115.119	81.122
PO4-P (µg/L)	6.1762	4.3244	9.7784	3.8928	4.4304	1.2194
TON-N (µg/L)	22.518	11.35	64.585	89.809	76.077	128.591
Al (mg/L)	3.3664	0.6554	3.5538	1.0249	3.2482	0.7271
B (mg/L)	2.2985	0.3238	2.5744	0.3562	2.679	0.6936
Ba (mg/L)	0.0521	0.015	0.05	0.0103	0.048	0.0031
Ca (mg/L)	69.6012	28.3065	89.9308	25.9627	93.332	31.8563
Fe (mg/L)	0.7806	1.0454	1.1199	0.6156	0.4322	0.452
K (mg/L)	5.1719	3.1684	6.8521	3.7004	9.8606	9.4836
Li (mg/L)	0.3567	0.1172	0.3732	0.0848	0.427	0.2333
Mg (mg/L)	38.4234	17.6878	52.1337	17.8328	55.3026	23.6017
Mn (mg/L)	0.0815	0.0527	0.1523	0.1202	0.0984	0.0465
Na (mg/L)	1460.4724	735.8887	2063.2338	771.9432	2087.129	1149.824
S (mg/L)	10.56	12.0927	18.0849	13.2099	27.0056	23.6532
Si (mg/L)	2.7395	0.7308	2.7318	0.975	2.4642	0.2799
Sr (mg/L)	3.9171	1.9634	5.3548	1.8241	5.606	2.8393

Table A1.6: Pearson's correlation coefficient for environmental variables and morphometry with Holm's adjusted p-value (Aickin & Gensler 1996; Holm 1979). Sites containing outliers were removed using Dixon's test (Table A2.5). Specific conductance values, and concentrations of nutrients, cations and anions were log transformed before the analysis.

	Pearson's Correlation Coefficient (r)	**Holm's Adjusted p-value**
Northing	-0.33	1
Easting	0.238	1
Water Temperature (˚C)	-0.152	1
Dissolved Oxygen (mg/L)	-0.072	1
Specific Conductance (µS/cm)	0.346	1
pH	0.083	1
Redox (mV)	-0.108	1
Maximum Depth (cm)	0.512	0.116
Cl (mg/L)	0.346	1
SO4-S (mg/L)	0.376	1
NH4-N (µg/L)	0.044	1
PO4-P (µg/L)	0.076	1
TON-N (µg/L)	0.299	1
Al (mg/L)	-0.019	1
B (mg/L)	0.348	1
Ba (mg/L)	-0.076	1
Ca (mg/L)	0.343	1
Fe (mg/L)	-0.026	1
K (mg/L)	0.254	1
Li (mg/L)	0.142	1
Mg (mg/L)	0.358	1
Mn (mg/L)	0.264	1
Na (mg/L)	0.315	1
S (mg/L)	0.375	1
Si (mg/L)	-0.087	1
Sr (mg/L)	0.326	1

The principal component analysis extracted seven components with eigenvalues greater than 1, and an eighth principal component with an eigenvalue of 0.95 (Table A1.7). These 8 components account for 83.6% of the total variance. After varimax rotation of these 8 components, 8 factors associated with various chemical parameters were identified (Table A1.8). The first rotated component explains the salinity gradient. The second component describes a correlation between phosphate (μg/L) and iron concentration (mg/L). The third component explains a gradient amongst pH, dissolved oxygen (mg/L), and reduction oxidation potential (mV). The fourth component includes a correlation between manganese and barium concentrations (mg/L). The fifth component contains a gradient between water temperature (˚C) and total oxygenated nitrogen concentration (μg/L), in which water temperature is negatively associated with the component. The sixth component accounts for ammonium concentration (μg/L). The seventh component includes a correlation between maximum depth (cm) and silicone concentration (mg/L). The final component accounts for aluminum concentration (mg/L).

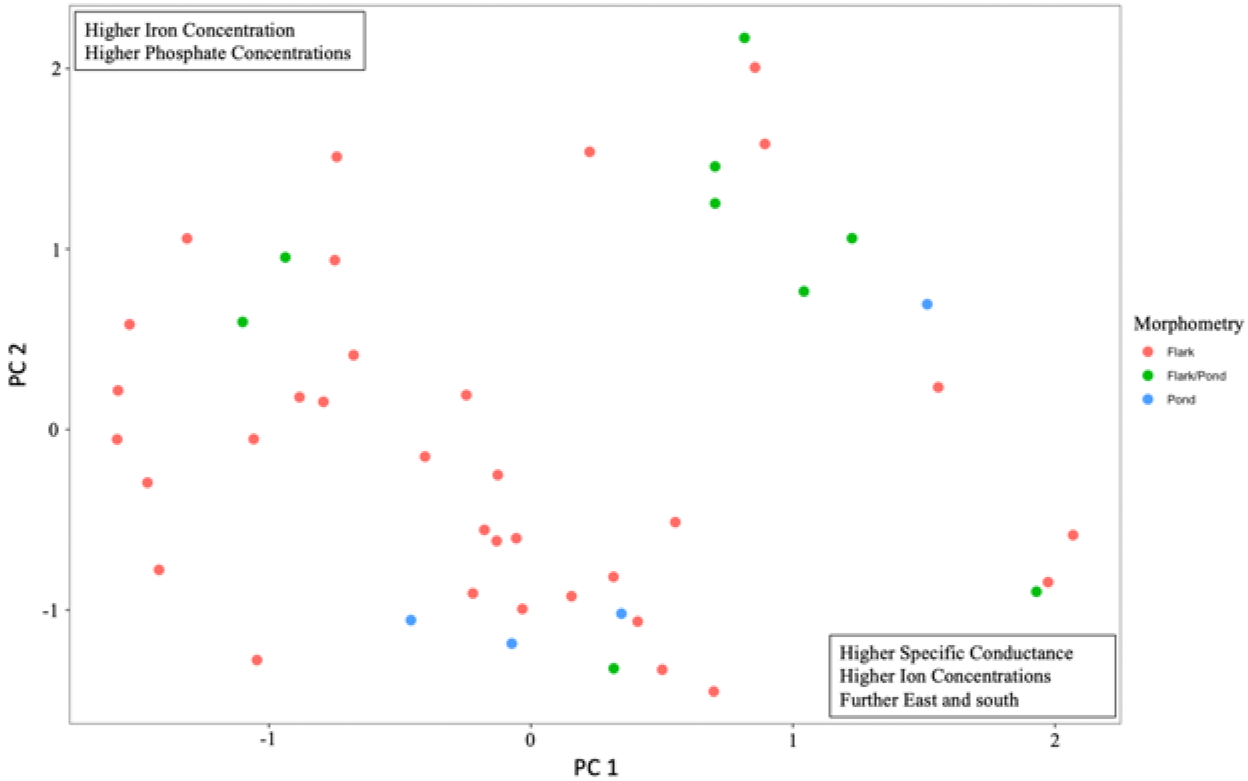

Figure A1.1: Scatterplot of the distribution of 48 sample sites relative to scores of rotated principal components 1 (summarizing salinity) and 2 (summarizing nutrient concentrations).Point colour depicts morphometry class: flark (red), flark/pond (green), and pond (blue).

Table A1.7: Eigenvalues and proportion of variance of principal component analysis used to determine the number of components to use in rotated principal component analysis (Figure A1.1). The first 8 principal components are shown here.

	PC1	PC2	PC3	PC4	PC5	PC6	PC7	PC8
Eigenvalue	10.844	2.510	2.014	1.649	1.452	1.343	1.036	0.952
Prop. Var. Expl.	0.417	0.097	0.077	0.063	0.056	0.052	0.040	0.037
Cum. Var. Expl.	0.417	0.514	0.591	0.655	0.711	0.762	0.802	0.839

Table A1.8: Varimax rotated component loadings of environmental data along with factors' variance sums of squares after extraction, and proportions of variance explained by 8 rotated components. Bold-faced values indicate the strongest association of each variable with a component. Variables are sorted in decreasing order of their strength of association with their most highly-associated component. Cations, anions, nutrients, and specific conductance values were log-transformed before the analysis.

Variable (Unit)	PC1	PC2	PC3	PC4	PC5	PC6	PC7	PC8
Sr (mg/L)	**0.944**	0.119	<0.001	0.214	<0.001	0.119	<0.001	<0.001
Na (mg/L)	**0.942**	0.194	<0.001	0.123	<0.001	0.119	<0.001	<0.001
Mg (mg/L)	**0.932**	<0.001	<0.001	0.240	<0.001	0.162	<0.001	<0.001
Cl (mg/L)	**0.932**	0.183	<0.001	<0.001	<0.001	0.142	<0.001	<0.001
Spec. Cond.	**0.930**	0.151	<0.001	<0.001	0.115	<0.001	<0.001	<0.001
Ca (mg/L)	**0.904**	<0.001	<0.001	0.328	<0.001	0.139	<0.001	<0.001
K (mg/L)	**0.886**	<0.001	0.233	<0.001	<0.001	-0.110	<0.001	<0.001
S (mg/L)	**0.861**	<0.001	<0.001	<0.001	<0.001	0.382	<0.001	<0.001
B (mg/L)	**0.798**	<0.001	<0.001	<0.001	0.164	<0.001	<0.001	0.130
Li (mg/L)	**0.797**	<0.001	<0.001	0.155	<0.001	-0.186	<0.001	<0.001
SO4-S (mg/L)	**0.775**	<0.001	<0.001	-0.189	<0.001	0.390	<0.001	<0.001
Northing	**-0.728**	-0.486	<0.001	0.147	0.205	<0.001	-0.170	<0.001
Easting	**0.692**	0.639	<0.001	-0.100	-0.131	<0.001	0.129	<0.001
Fe (mg/L)	<0.001	**0.894**	-0.149	0.133	<0.001	0.182	<0.001	0.111
PO4-P (µg/L)	0.329	**0.850**	<0.001	<0.001	<0.001	0.104	<0.001	<0.001
pH	<0.001	-0.105	**0.898**	<0.001	<0.001	0.149	<0.001	<0.001
Dissolved Oxygen (mg/L)	-0.188	0.173	**0.688**	-0.133	-0.221	-0.146	0.162	<0.001
Redox (mV)	0.130	-0.153	**0.604**	<0.001	0.184	-0.200	-0.146	0.384
Ba (mg/L)	0.119	<0.001	<0.001	**0.906**	-0.189	<0.001	<0.001	<0.001
Mn (mg/L)	0.113	0.319	<0.001	**0.740**	0.351	<0.001	<0.001	<0.001
Water Temp. (˚C)	-0.275	-0.175	<0.001	<0.001	0.169	**-0.800**	<0.001	<0.001
TON-N (µg/L)	0.108	0.291	0.147	<0.001	0.539	**0.542**	0.148	-0.154
NH4-N (µg/L)	<0.001	-0.125	<0.001	<0.001	**0.872**	-0.122	<0.001	<0.001
Maximum Depth (cm)	0.273	-0.106	0.140	<0.001	<0.001	<0.001	**0.829**	-0.194
Si (mg/L)	-0.139	0.293	<0.001	<0.001	<0.001	0.233	**0.641**	0.287

Al (mg/L)	<0.001	<0.001	<0.001	<0.001	<0.001	<0.001	<0.001	**0.904**
Factor Var.	9.991	2.696	1.828	1.780	1.609	1.464	1.256	1.181
Prop. Var. Expl.	0.384	0.104	0.070	0.068	0.062	0.056	0.048	0.045
Cum. Var. Expl.	0.384	0.488	0.558	0.626	0.744	0.682	0.792	0.837

Table A1.9: Site scores for varimax rotated principal component analysis (Figure A1.1).

Site Code	PC1	PC2	PC3	PC4	PC5	PC6	PC7	PC8
SFC-A-003	-0.241	-0.999	-0.833	-0.676	0.813	0.101	-0.342	-0.520
SFC-A-004	-0.600	-0.005	0.248	-0.105	1.223	-0.812	-0.811	0.683
SFC-A-007	0.006	-0.798	1.515	2.842	-1.645	-0.729	-1.502	-0.016
SFC-A-009	-0.621	0.498	0.353	0.126	1.199	-0.629	-1.570	-0.516
SFC-A-010	-0.795	0.072	-0.899	-0.574	0.215	-0.297	-1.766	-0.026
SFC-A-012	-0.211	-0.011	1.152	-0.155	1.042	-1.425	-0.438	0.655
SFC-A-015	0.602	-0.889	-0.015	2.778	0.866	-1.476	-0.091	0.511
SFC-A-019	-0.371	-0.306	0.632	-0.909	-0.410	-0.157	-0.086	-0.969
SFC-A-020	-0.819	1.369	-2.445	-0.740	1.636	-1.336	-0.134	1.749
SFC-A-026	-1.222	0.867	2.052	0.015	-0.186	-0.206	-1.287	-0.435
SFC-A-027	-0.152	-0.585	1.004	-0.651	0.272	-1.079	0.410	-0.824
SFC-A-033	0.241	-0.821	0.285	-0.599	0.657	1.213	-0.064	1.132
SFC-A-036	-0.945	0.425	-0.179	-1.074	-1.146	-1.511	0.809	-1.127
SFC-A-039	-0.201	-0.375	-0.409	1.325	0.903	-1.998	1.410	-0.938
SFC-A-041	-0.928	0.845	2.334	0.110	-0.258	-0.630	2.399	0.754
SFC-A-042	-1.231	0.386	-0.106	-1.532	-0.272	-0.217	1.978	0.342
SFC-A-043	-0.309	0.130	-0.063	-0.442	-1.656	-0.063	0.472	0.319
SFC-A-051	1.326	0.624	-0.282	-0.840	0.750	0.054	-1.510	-0.927
SFC-A-056	0.041	2.331	0.208	-0.973	-0.075	0.315	-0.270	-0.613
SFC-A-068	0.602	1.571	1.798	-0.789	-0.455	-1.126	-0.223	0.610
SFC-A-074	1.053	1.192	0.909	-0.406	-0.726	0.635	0.844	1.323
SFC-A-076	-0.117	-1.140	1.530	0.044	2.054	2.445	0.850	-1.097
SFC-A-077	-0.033	-1.225	0.255	0.124	1.018	0.639	0.824	0.307
SFC-A-078	0.843	1.591	-0.463	-0.640	0.779	0.051	-0.637	0.497
SFC-A-079	2.574	-1.380	-0.342	-0.844	0.295	-0.023	0.940	1.379
SFC-A-080	0.149	-0.992	0.140	0.332	-0.506	-0.543	-1.740	-0.215
SFC-A-081	0.454	-1.070	0.326	0.360	0.052	0.481	-0.382	2.704
SFC-A-082	0.293	-0.917	0.471	-0.079	-1.203	-0.260	-0.032	0.266
SFC-B-003	-1.296	-0.908	0.516	-0.069	1.544	-0.380	0.532	-0.050
SFC-B-004	-1.549	-0.243	-0.441	1.798	-0.896	1.717	0.568	2.327
SFC-B-005	-1.402	-0.956	-0.603	-0.534	-1.551	1.720	-1.047	-0.575
SFC-B-006	-1.152	-1.172	-0.898	-1.060	0.411	1.647	-0.630	0.857
SFC-B-010	-1.563	-0.257	-0.932	-0.445	0.412	1.229	-0.518	0.130
SFC-B-035	-1.017	0.182	-1.507	1.822	0.502	-0.707	1.046	-0.856
SFC-B-038	0.155	-0.767	0.940	0.531	1.034	0.868	-0.160	-2.197
SFC-B-039	-0.462	-1.127	-0.849	0.204	-1.255	-1.024	0.856	-0.020
SFC-B-051	0.141	-0.536	-1.108	-0.007	-0.459	-0.253	1.144	-1.551
SFC-B-052	0.116	-0.355	-1.142	0.268	-1.657	-0.375	-1.613	-0.970

SFC-B-055	-1.522	0.464	-0.150	-1.249	-1.562	-0.457	0.003	0.048
SFC-B-058	1.925	-0.592	-0.243	-0.863	-1.045	-0.516	-1.168	0.827
SFC-B-059	1.789	-0.838	-0.875	-1.046	0.007	-0.096	1.522	-1.204
SFC-B-060	1.914	-1.053	0.634	-0.601	-1.391	0.206	0.651	-0.270
SFC-B-062	1.519	0.227	-0.974	-0.048	1.074	-0.197	-0.456	-0.486
SFC-B-063	0.782	1.261	0.407	0.634	1.121	-0.054	-0.405	1.202
SFC-B-064	0.503	1.686	0.629	0.702	0.532	1.926	-0.024	-1.571
SFC-B-065	0.736	1.586	-2.311	1.839	-0.436	0.622	1.035	-0.212
SFC-B-068	0.862	1.573	-0.268	1.303	-0.891	1.242	-0.381	-0.427
SFC-B-069	0.134	1.439	-0.001	0.791	-0.728	1.465	0.996	-0.012

Discussion

Flarks are much more abundant in the data, as the sample size for flarks is 38, while flark/ponds and ponds have sample sizes of 9 and 5 respectively (Table A1.5). Flark sites contained the minimum values for all but four environmental variables (Redox: pond, total oxygenated nitrogen: pond, iron concentration: pond, aluminum concentration: flark/pond), while the maximum values of environmental variables were distributed evenly throughout morphometry classifications. The greatest values of water temperature, phosphate concentration, barium concentration, calcium concentration and iron concentration all occur in flark sites. The greatest values of specific conductance, chloride concentration, sulfate concentration, total oxygenated nitrogen, boron concentration, potassium concentration, lithium concentration, magnesium concentration, sodium concentration, sulfur concentration and strontium concentration occurred in pond sites.

Pearson's correlation coefficient analysis (Table A1.6) showed no significant correlations associated with morphometry after adjusting p-values using Holm's correction method (Aickin & Gensler 1996; Holm 1979). The strongest correlation with morphometry was depth (Pearson's correlation coefficient =0.512; adjusted p-value = 0.116; Table A1.6). This is expected, as maximum depth was a component of the morphometry classification process. Other environmental variables weakly correlated with morphometry (Pearson's correlation coefficient between 0.25 and 0.5) include a negative correlation to northing, and positive correlations to specific conductance, chloride concentration, sulfate concentration, boron concentration, magnesium concentration, sodium concentration, sulfur concentration, and strontium concentration, all of which have a non-significant p-value (Table A1.6). These variables are all associated with the salinity gradient, as outlined in the varimax rotated principal component analysis (Table 2.2; Figure 2.4; Table A1.8; Figure A1.1). These correlations may be a result of ponds increased connectivity to groundwater, however, correlation coefficients and p-values for these correlations are weak, and so should be considered accordingly.

The varimax rotated principal components yielded similar factor loadings to the principal component analysis conducted in chapter 2 (Table 2.2; Figure 2.4; Table A1.8). Environmental differences among morphometry types were not visually distinct while viewing the rotated principal component analysis, as sites of differing morphometries were not ordinated in clusters (Figure A1.1).

Macroinvertebrate Community Composition

Methods

At each of the three locations where water samples were collected (stated above), benthic invertebrate samples were collected roughly following CABIN's jab and sweep method (ECCC 2018) using a D-frame sweep net with 0.25 mm mesh. To standardize sampling effort, a total of 20 jabs were used to collect the sample. Fine silt and organics less than 0.25 mm were removed from the sample in the field by rinsing the sample in a 0.25 mm mesh sieve bag. Each sample was then stored in a polyethylene soil bag and preserved with 70% ethanol.

In the laboratory, sampled material was separated into its constituent size fractions by rinsing the sample through a set of soil sieves with 4.00, 1.00, 0.50 and 0.25-mm mesh (Ciborowski 1991). The resulting size fractions were then viewed under a dissecting microscope where the benthic invertebrates were sorted from the detritus, identified using taxonomic keys by Merritt et al. (2019) and Clifford (1990), and enumerated. Genera present in less than 5 sites were combined to form family abundance, and a families present in less than 5 sites were removed from the calculations of community composition, but not the calculations of family richness and total abundance.

To determine patterns of the invertebrate community associated with morphometry, total abundance and family richness were first compared across morphometric types. A one-way Analysis of Variance (ANOVA) test were conducted to determine if differences of total abundance (Table A1.13) or family richness (Table A1.14) existed among morphometry classifications. Values were tested for normal distribution using the Shapiro-Wilks test (Table A1.), and equality of variance was tested using Bartlett's test (Table A1.12). Total abundance values were log transformed to meet ANOVA's assumption of normal distribution.

Dufrêne and Legendre's (1997) indicator value (IndVal) scores were calculated to identify taxa uniquely indicative of a particular morphometry type (Table A1.15). IndVal scores are calculated based on both the taxa's frequency of occurrence in a site type, and the relative abundance of the taxa in a site type (Dufrêne & Legendre 1997). Thus, a high IndVal score indicates a taxon that occurs frequently in a site type, and has high relative abundance in that site type (Dufrêne & Legendre 1997). IndVal scores are calculated for a given taxon for each morphometry classification, and the morphometry yielding the maximum IndVal score for that taxon was noted. Associated p-values were calculated through a permutation test as the probability that a greater IndVal score could occur given random variation (Dufrêne & Legendre 1997). These p-values were adjusted using Holm's correction method (Aickin & Gensler 1996; Holm 1979).

Non-metric multidimensional scaling (NMDS) analysis was conducted using Hellinger transformed abundance values (calculating the square root of relative abundance of each taxon) to determine similarities of community composition among morphometries (Figure A1.2). The

NMDS analysis ordinated sites in 2 dimensions (stress=0.118). Environmental variables associated with the rotated principal components (Table A1.8) were regressed onto the unconstrained ordination and plotted as vectors (Figure A1.2; Table A1.16). Only vectors for environmental variables that were statistically significant were plotted with the NMDS ordination (Figure A1.2; Table A1.16).

Results

Both total abundance and family richness varied greatly across the saline fen complex and within morphometry types (Table A1.10). While value ranges for both total abundance and family richness overlapped among morphometry types, flarks tended to have the most individual invertebrates and greatest family richness. Mean (SD) values of total abundance for flarks, flark/ponds and ponds were 4,221 (5,777) individuals, 1,931 (1,434) individuals, and 3,048 (2,118) individuals respectively. Mean (SD) values of family richness for flarks, flark/ponds and ponds were 19.2 (4.3) families, 15.7 (2.5) and 16.6 (4.2) respectively. Results from the one-way ANOVA analyses used to determine if total abundance differed among wetland type was insignificant (F=0.846; p=0.436; Table A1.13). Results from the one-way ANOVA used to determine if family richness differed among wetland type was nearly significant (F=3.039, p=0.055; Table A1.14).

Table A1.10: Total abundance, family richness and morphometry classifications for sites included in Appendix A1 analyses.

Site Code	Morphometry	Total Abundance (# of Individuals)	Family Richness (# of Families)
SFC-A-003	Flark	807.6	22
SFC-A-004	Flark	2490.6	21
SFC-A-007	Flark	4144.5	23
SFC-A-009	Flark	6319.8	24
SFC-A-010	Flark	2790.3	22
SFC-A-012	Flark	1020	23
SFC-A-015	Flark	1001	21
SFC-A-019	Flark	2051.9	15
SFC-A-020	Flark	4089.6	17
SFC-A-026	Flark	3311.8	17
SFC-A-027	Flark	1850.5	23
SFC-A-033	Flark	21556.5	13
SFC-A-036	Flark	617	14
SFC-A-039	Flark	4523.9	22
SFC-A-041	Flark/Pond	1625	17
SFC-A-042	Flark	27456	22
SFC-A-043	Flark	1155.1	18
SFC-A-051	Flark	956.7	17
SFC-A-056	Flark	2599.5	15
SFC-A-068	Flark/Pond	901.8	15
SFC-A-074	Flark/Pond	2163.4	18
SFC-A-076	Pond	4047	20
SFC-A-077	Flark	2540.8	23
SFC-A-078	Flark/Pond	518	12
SFC-A-079	Pond	820	10
SFC-A-080	Flark	10204.6	21
SFC-A-081	Flark	3466.8	25
SFC-A-082	Flark	3018	24
SFC-B-003	Flark	8511.5	20
SFC-B-004	Flark	2995.8	14
SFC-B-005	Flark	1033	18
SFC-B-006	Flark	1385.8	21
SFC-B-010	Flark	1774.1	23
SFC-B-035	Flark/Pond	5075.8	19
SFC-B-038	Flark/Pond	3177.1	17
SFC-B-039	Pond	5009.3	18

SFC-B-051	Pond	4664.1	20
SFC-B-052	Flark	10332.4	15
SFC-B-055	Flark	3599	28
SFC-B-058	Flark	892.3	19
SFC-B-059	Flark/Pond	655.6	17
SFC-B-060	Flark	2770.5	17
SFC-B-062	Pond	699	15
SFC-B-063	Flark/Pond	1631.2	12
SFC-B-064	Flark/Pond	1632.8	14
SFC-B-065	Flark	294	9
SFC-B-068	Flark	1134.6	12
SFC-B-069	Flark	809.7	14

Table A1.11: Summary table for Shapiro Wilk's test of normal distribution for total abundance (number of individuals collected from a site) and family richness (number of unique taxonomic families identified from a site). Abundance values were log-transformed.

Variable	Shapiro-Wilk's Test Statistic	p-Value
Abundance	0.977	0.471
Family Richness	0.98	0.593

Table A1.12: Summary table for Bartlett's test of equal variance. Abundance values were log-transformed.

Variable	Bartlett's K^2	DF	p-Value
Abundance	1.0759	2	0.5839
Family Richness	2.7661	2	0.2508

Table A1.13: Summary table for one-way Analysis of Variance (ANOVA) test comparing the means of total abundance among morphometry classifications. Abundance values were log-transformed.

	DF	SS	MS	F-Value	p-Value
Morphometry	2	0.294	0.1471	0.846	0.436
Residuals	45	7.821	0.1738		

Table A1.14: Summary table for one-way Analysis of Variance (ANOVA) test comparing the means of family richness among morphometry classifications.

	DF	SS	MS	F-Value	p-Value
Morphometry	2	102.9	51.43	3.093	0.0551
Residuals	45	748.1	16.63		

The IndVal analysis of distribution of among morphometry classes failed to identify any significant associations between taxa and wetland class once probability values had been adjusted for multiple comparisons using Holm's method (Table A1.15; Aickin & Gensler 1996; Holm 1979).

Table A1.15: Indicator Value (IndVal) scores calculated across morpheme wetland types, with the class yielding the maximum value, p-value and adjusted p-value included. Adjusted p-values were corrected using Holm's correction method (Aickin & Gensler 1996; Holm 1979).

Taxa	Flark	Flark/Pond	Pond	Max Class	p-unadj	p-adj
Lymnaea stagnalis	0.224	0	0.009	Flark	0.326	1
Physa	0.082	0	0.24	Pond	0.219	1
Atrichopogon	0.067	0	0.502	Pond	0.053	1
Hydracarina	0.011	0.001	0.382	Pond	0.122	1
Psychoda	0.271	0.002	0.012	Flark	0.332	1
Planorbidae	0.426	0.002	0.102	Flark	0.14	1
Agabus	0.106	0.003	0.114	Pond	0.837	1
Lymnaeidae.Other	0.16	0.003	0.171	Pond	0.688	1
Acari	0.356	0.004	0.324	Flark	0.69	1
Hydrobiidae	0.008	0.005	0.182	Pond	0.303	1
Hydraenidae	0.33	0.007	0	Flark	0.144	1
Ilybius	0.028	0.01	0.317	Pond	0.118	1
Phryganeidae	0.302	0.011	0.023	Flark	0.239	1
Pachydiplax longipennis	0.435	0.014	0.055	Flark	0.266	1
Empididae	0.077	0.016	0.097	Pond	0.892	1
Dolichopodidae	0.197	0.018	0	Flark	0.369	1
Hydrophilidae.Other	0.164	0.023	0	Flark	0.391	1
Dytiscidae.Other	0.237	0.023	0	Flark	0.282	1
Forcipomyia	0.131	0.025	0	Flark	0.552	1
Laccophilus	0.193	0.026	0.007	Flark	0.55	1
Oligochaeta	0.29	0.035	0.296	Pond	0.772	1
Coenagrionidae.Other	0.163	0.038	0.294	Pond	0.35	1
Notonectidae	0.076	0.039	0	Flark	0.967	1
Nehalennia	0.4	0.041	0.171	Flark	0.429	1
Sympetrum	0.105	0.045	0	Flark	0.765	1
Cymbiodyta	0.05	0.047	0.642	Pond	0.013	0.743
Dytiscus	0.067	0.048	0	Flark	1	1
Tabanidae	0.263	0.053	0.236	Flark	0.71	1
Muscidae	0.329	0.058	0.112	Flark	0.33	1
Pericoma	0.321	0.061	0.549	Pond	0.158	1
Psychodidae.Other	0.102	0.063	0.075	Flark	0.972	1
Collembola	0.633	0.067	0.094	Flark	0.044	1
Dasyhelea	0.194	0.069	0.725	Pond	0.086	1
Liodessus	0.171	0.072	0.506	Pond	0.092	1
Somatochlora	0.13	0.073	0.071	Flark	0.992	1
Trichocorixa	0.07	0.073	0	Flark/Pond	0.961	1

Dixidae.Pup	0.19	0.076	0.051	Flark	0.835	1
Aeshna	0.154	0.076	0	Flark	0.57	1
Gerridae	0.046	0.077	0.135	Pond	0.617	1
Berosus	0.052	0.078	0.294	Pond	0.222	1
Libellulidae	0.03	0.083	0	Flark/Pond	0.763	1
Fossaria	0.001	0.085	0.294	Pond	0.152	1
Hydaticus	0.064	0.113	0.099	Flark/Pond	0.959	1
Stagnicola	0.412	0.122	0.031	Flark	0.607	1
Dixella	0.232	0.136	0.234	Pond	0.96	1
Bezzia	0.288	0.142	0.49	Pond	0.369	1
Chironomidae	0.276	0.144	0.563	Pond	0.119	1
Corixidae.Other	0.035	0.148	0.223	Pond	0.594	1
Stratiomyidae	0.042	0.172	0.336	Pond	0.295	1
Ephydridae	0.421	0.189	0.197	Flark	0.682	1
Dasycorixa	0.032	0.195	0.339	Pond	0.48	1
Ceratopogonidae.Other	0.175	0.205	0.175	Flark/Pond	0.998	1
Mesovelia	0.038	0.225	0	Flark/Pond	0.188	1
Sciomyzidae	0.351	0.23	0.368	Pond	0.808	1
Culex	0.103	0.247	0.187	Flark/Pond	0.644	1
Culiseta	0.093	0.311	0.265	Flark/Pond	0.719	1
Culicidae.Other	0.099	0.382	0.145	Flark/Pond	0.354	1
Tipulidae	0.096	0.383	0.019	Flark/Pond	0.116	1
Saldidae	0.002	0.427	0	Flark/Pond	0.009	0.558
Aedes	0.129	0.491	0.258	Flark/Pond	0.137	1

A total of 60 taxa were included in the analysis of community composition. There were not any taxonomic families or genera present in flark/ponds or ponds that were absent from previous analyses of community composition (Chapter 3). The NMDS analysis was able to ordinate the sample sites in two dimensions (stress=0.118). Vectors associated with supplementary environmental variables were fitted onto the unconstrained ordination via regression analysis (Table A1.16). Specific conductance, phosphate concentration, water temperature, and maximum depth all regressed onto the unconstrained ordination points with p-values less than 0.05. Only environmental variables with statistically significant regressions were plotted as vectors (Figure A1.2). The first dimension of the NMDS analysis correspond to variations of community composition due to the nutrient and salinity gradients present in the saline fen complex, where sites with lower levels of specific conductance tended to have negative scores on NMD axis 1 (Table A1.17). The second dimension of the NMDS analysis corresponds to a negative relationship between water temperature and depth, where deeper, cooler waterbodies tended to have positive scores of NMD axis 2 (Table A1.17). As a result, the majority of pond sites have positive NMD axis 2 scores.

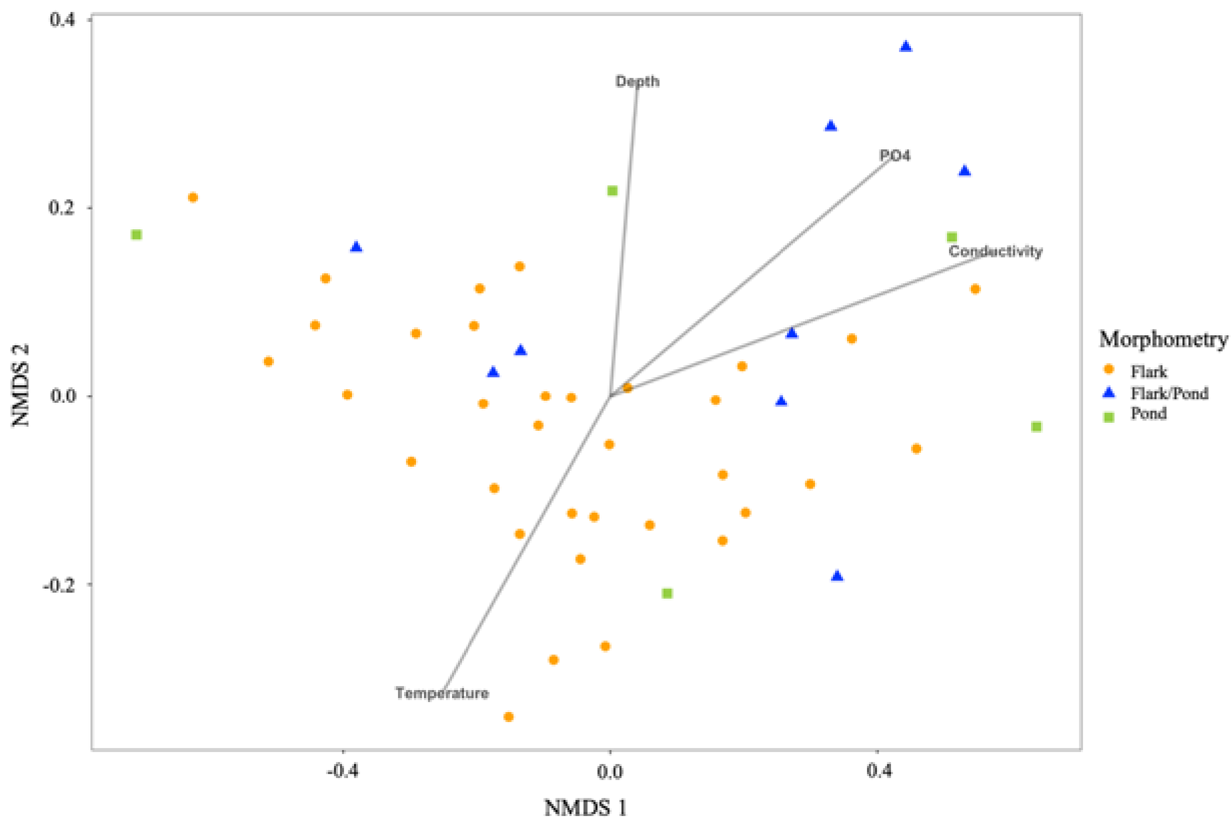

Figure A1.2: Non metric multi-dimensional scaling (NMDS) analysis scatterplot plot with points representing sites (Table A1.17). Point colour represents the morphometry classification of each site. Points are coloured accordingly: Flark (orange), flark/pond (blue), pond (green). Vectors were fitted to the unconstrained ordination plot via regression of environmental variables onto the ordination components (Table A1.16). Only significant variables were plotted as vectors.

Table A1.16: Vector fitting table showing regression of environmental variables onto unconstrained ordination (Figure A1.2).

Variable (Unit)	NMDS1	NMDS2	R2	p-value
Specific Conductance (µS/cm)	0.966	0.259	0.531	**0.001**
PO4 (µg/L)	0.857	0.515	0.368	**0.001**
Mn (mg/L)	0.742	0.671	0.096	0.113
Dissolved Oxygen (mg/L)	-0.257	0.967	0.100	0.103
Water Temperature (˚C)	-0.624	-0.782	0.242	**0.002**
NH4 (µg/L)	0.877	0.480	0.005	0.902
Maximum Depth (cm)	0.122	0.993	0.170	**0.021**
Al (mg/L)	-0.162	0.987	0.035	0.443

Table A1.17: Site scores for NMDS Analysis (Figure A1.2)

Site Code	NMDS1	NMDS2	Morphometry
SFC-A-003	-0.394	0.002	Flark
SFC-A-004	-0.298	-0.070	Flark
SFC-A-007	-0.190	-0.008	Flark
SFC-A-009	-0.135	-0.147	Flark
SFC-A-010	-0.057	-0.125	Flark
SFC-A-012	0.026	0.009	Flark
SFC-A-015	-0.001	-0.052	Flark
SFC-A-019	0.202	-0.124	Flark
SFC-A-020	-0.007	-0.266	Flark
SFC-A-026	0.168	-0.154	Flark
SFC-A-027	-0.058	-0.002	Flark
SFC-A-033	0.059	-0.137	Flark
SFC-A-036	-0.291	0.067	Flark
SFC-A-039	-0.024	-0.128	Flark
SFC-A-041	-0.381	0.158	Flark/Pond
SFC-A-042	-0.625	0.211	Flark
SFC-A-043	-0.512	0.037	Flark
SFC-A-051	0.158	-0.004	Flark
SFC-A-056	0.300	-0.094	Flark
SFC-A-068	0.443	0.371	Flark/Pond
SFC-A-074	0.272	0.066	Flark/Pond
SFC-A-076	0.003	0.218	Pond
SFC-A-077	-0.195	0.114	Flark
SFC-A-078	0.340	-0.192	Flark/Pond
SFC-A-079	0.638	-0.033	Pond
SFC-A-080	-0.085	-0.280	Flark
SFC-A-081	-0.108	-0.031	Flark
SFC-A-082	-0.173	-0.098	Flark
SFC-B-003	-0.426	0.125	Flark
SFC-B-004	-0.442	0.075	Flark
SFC-B-005	-0.097	0.000	Flark
SFC-B-006	-0.136	0.138	Flark
SFC-B-010	-0.204	0.075	Flark
SFC-B-035	-0.175	0.025	Flark/Pond
SFC-B-038	-0.134	0.048	Flark/Pond
SFC-B-039	-0.710	0.172	Pond
SFC-B-051	0.085	-0.210	Pond
SFC-B-052	-0.045	-0.173	Flark

SFC-B-055	-0.152	-0.341	Flark
SFC-B-058	0.197	0.032	Flark
SFC-B-059	0.256	-0.006	Flark/Pond
SFC-B-060	0.168	-0.084	Flark
SFC-B-062	0.512	0.169	Pond
SFC-B-063	0.531	0.238	Flark/Pond
SFC-B-064	0.331	0.286	Flark/Pond
SFC-B-065	0.459	-0.056	Flark
SFC-B-068	0.362	0.061	Flark
SFC-B-069	0.547	0.114	Flark

Table A1.18: Species scores for NMDS Analysis (Figure A1.2)

Taxa	NMDS1	NMDS2
Hydracarina	-0.107	-0.301
Acari	-0.241	-0.178
Collembola	-0.150	-0.157
Oligochaeta	0.098	-0.145
Lymnaeidae.Other	-0.438	0.015
Stagnicola	-0.535	0.155
Lymnaea stagnalis	-0.229	0.036
Fossaria	-0.426	0.229
Physa	-0.193	-0.274
Planorbidae	-0.357	-0.053
Hydrobiidae	-0.245	0.153
Coenagrionidae<0.5mm	-0.429	0.087
Nehalennia	-0.430	0.120
Aeshna	-0.456	-0.027
Sympetrum	-0.604	0.097
Somatochlora	-0.472	-0.010
Pachidyplax longipennis	-0.400	-0.036
Libellulidae	-0.314	-0.039
Corixidae.Other	0.321	0.369
Dasycorixa	0.505	0.413
Trichocorixa	0.331	0.295
Mesovelia	0.086	0.322
Notonectidae	-0.156	0.188
Gerridae	-0.105	0.201
Saldidae	-0.120	0.192
Phryganeidae	-0.465	0.047
Dytiscidae.Other	0.174	-0.072
Dytiscus	0.167	0.018
Hydaticus	0.229	-0.029
Agabus	-0.199	-0.088
Ilybius	-0.284	0.026
Liodessus	0.015	-0.081
Laccophilus	-0.246	0.072
Hydrophilidae.Other	0.071	-0.126
Cymbiodyta	0.154	0.036
Berosus	-0.076	-0.035
Hydraenidae	-0.011	0.007

Chironomidae	-0.054	-0.022
Ceratopogonidae.Other	0.098	-0.001
Dasyhelea	0.071	-0.198
Bezzia	0.167	-0.049
Atrichopogon	-0.184	-0.440
Forcipomyia	-0.041	0.042
Culicidae.Other	0.544	0.049
Aedes	0.415	0.049
Culiseta	0.536	0.188
Culex	0.395	-0.064
Ephydridae	0.112	-0.061
Psychodidae.Other	0.152	0.069
Psychoda	-0.122	-0.056
Pericoma	0.150	-0.103
Sciomyzidae	-0.010	0.010
Dixidae.Pup	-0.089	0.183
Dixella	-0.356	0.075
Dolichopodidae	0.223	-0.164
Muscidae	0.155	-0.040
Tipulidae	0.181	0.020
Tabanidae	-0.088	-0.050
Stratiomyidae	0.571	0.227
Empididae	-0.093	-0.147

Discussion

While the greatest values of both family richness and total abundance occurred in sites classified as flarks, the ranges of family richness and abundance overlapped greatly between the various wetland types (Table A1.10). Of the 38 flarks sampled, 32 had total abundance values less than 5,000 individuals, which is very similar to the abundances found in other wetland types (Table A1.10). A one-way analysis of variance expressed insignificant results, suggesting there are no differences in total abundance, or family richness among wetland types (Table A1.13; Table A1.14). The scatterplot of the NMDS analysis ordination in two dimensions suggests that the morphometry types present in the fen all contain similar macroinvertebrate community compositions, as sites of the same morphometry do not cluster together (Figure A1.1). This is corroborated by results from the IndVal analysis, as none of the taxa analyzed obtained a statistically significant association with any of the wetland types present in the saline fen complex (Table A1.15). There were no statistically significant differences in the macroinvertebrate community associated with variations in morphometry within the saline fen complex.

Conclusion

Upon analysis, there seems to be no major differences in macroinvertebrate community composition or water chemistry among wetland types in the saline fen complex. Neither family richness, nor total abundance were influenced by morphometry. There were no visual distinctions observed when viewing the NMDS analysis ordination scatterplot, and none of the taxa analyzed in the IndVal analysis were identified as indicators of wetland type. Furthermore, the only environmental variable correlated with morphometry classification through analysis with Pearson's correlation coefficient was depth ($r=0.512$; Holm's $p=0.116$), and the principal component analysis had similar results to those observed in chapter 2 (Figure 2.4; Table 2.2), containing only flark sites. There was no visual distinction between morphometries observed when viewing the scatterplot of the first two varimax rotated principal components (Figure A1.1).

Appendix A2: Summary Tables and Figures of Chapter 2 Analyses

Table A2.1: Site name, location, collection date and environmental parameters measured at 38 flarks and incorporated into analysis for Chapter 2. Sites and entries that are italicized were identified as outliers using Dixon's Q-test (Table A2.5) and were excluded from the principal component analysis (Figure 2.4), the Pearson's correlation coefficient calculations (Table 2.2) and the redundancy analysis (chapter 3, Fig 3.5).

Site Code	Collection Date (2020)	Easting	Northing	Water Temp (˚C)	Dissolved Oxygen (mg/L)	Specific Conductance (µS/cm)	pH	Redox (mV)	Maximum Depth (cm)
SFC-A-003	09-08	-111.27444	56.57316	13.5	5.11	6866	6.73	129.6	15
SFC-A-004	09-07	-111.27422	56.57318	14.4	6.55	6271	7.12	197.4	9
SFC-A-007	09-06	-111.27393	56.57314	13.8	8.79	4972	7.41	171.2	13
SFC-A-009	09-08	-111.27375	56.57275	13.4	5.76	7021	7.2	181.2	10
SFC-A-010	09-08	-111.27384	56.57265	14.1	5.07	6804	6.66	144.6	6
SFC-A-012	09-06	-111.27394	56.57183	15.2	9.03	10283	7.24	217.2	16.5
SFC-A-015	09-07	-111.27396	56.57182	15.5	5.58	12564	6.95	202.8	17
SFC-A-019	09-07	-111.27364	56.57159	13.9	6.71	8515	7.18	193.8	17.5
SFC-A-020	09-08	-111.27283	56.57164	17	3.5	7400	6.27	122.2	8
SFC-A-026	09-06	-111.27268	56.57115	13.2	9.34	6401	7.64	207.8	10.33
SFC-A-027	09-08	-111.27268	56.571	14	8.31	9125	7.27	206.9	24
SFC-A-033	09-08	-111.27288	56.57089	13.2	8.03	10692	7.11	173.6	7.5
SFC-A-036	09-08	-111.2727	56.57064	15.6	9.02	6314	6.8	106.9	20
SFC-A-039	09-08	-111.2727	56.57049	16	7.97	9369	6.8	135.3	24
SFC-A-042	09-07	-111.27209	56.57028	13.7	10.03	5812	6.85	102.4	22
SFC-A-043	09-07	-111.27197	56.57003	13	9.71	7783	6.89	102.9	14
SFC-A-051	09-07	-111.27072	56.56809	12.1	7.45	16529	7.06	91.3	6.5
SFC-A-056	09-06	-111.26942	56.56739	12.9	6.22	11478	7.33	107.6	12.5
SFC-A-077	09-07	-111.27426	56.57154	13.2	4.74	8814	7.37	179.8	24
SFC-A-080	09-08	-111.27325	56.56941	13.3	5.84	9116	7.15	182.2	9

SFC-A-081	09-08	-111.27412	56.57037	14.4	7.28	10627	7.15	216.9	9
SFC-A-082	09-08	-111.27438	56.57059	15.3	7.7	10163	7.15	209.7	12
SFC-B-003	09-07	-111.27753	56.57433	14.1	7.3	4816	7.16	205.3	20
SFC-B-004	09-08	-111.27704	56.5743	10	6.6	5125	6.88	116.6	16
SFC-B-005	09-08	-111.27631	56.57436	10.1	6.32	5151	7.01	98.9	9.5
SFC-B-006	09-08	-111.27622	56.57412	11	6.15	5474	6.96	110.2	12
SFC-B-010	09-08	-111.27655	56.57359	11.6	5.48	5123	6.8	109.7	11.5
SFC-B-011	09-06	-111.27621	56.57352	13.9	5.44	4845	*3.9*	125.8	6
SFC-B-026	09-05	-111.27743	56.57455	14.8	8.55	4160	*4.2*	91.3	17.5
SFC-B-049	09-07	-111.27278	56.56965	11.5	4.05	10892	7.18	80.5	14
SFC-B-052	09-07	-111.2732	56.5693	13.4	7.66	9402	6.65	54.4	6.5
SFC-B-055	09-06	-111.27265	56.5689	13.9	8.11	3757	6.78	185.4	12.5
SFC-B-058	09-06	-111.27065	56.56798	13.6	5.91	15918	6.99	199.5	11
SFC-B-060	09-07	-111.27037	56.56786	10.7	6.76	18628	7.36	187.6	27.5
SFC-B-065	09-07	-111.26936	56.56812	10.7	3.65	9392	6.46	47.4	18.5
SFC-B-068	09-07	-111.26873	56.56795	8.5	3.33	17106	7.26	126.2	14.5
SFC-B-069	09-07	-111.26923	56.56759	9.4	7.59	9498	6.92	158.8	22.5
SFC-B-070	09-06	-111.27283	56.56906	13.7	3.59	9572	7.32	189.9	13

Table A2.2: Concentrations of major anions and nutrients in water samples collected from 52 waterbodies described in Table A1.1. Sites and entries that are italicized were identified as outliers and were excluded from the principal component analysis (Figure 2.4), the Pearson's correlation coefficient calculations (Table 2.2) and the redundancy analysis (chapter 3, Fig 3.5). Values shown in red were below the limit of detection, and adjusted using the R2D method (Antweiler 2015).

Site Code	Cl (mg/L)	SO4-S (mg/L)	NH4-N (µg/L)	PO4-P (µg/L)	TON-N (µg/L)	NO3-N (µg/L)	S (mg/L)
SFC-A-003	1683	7.120	89.91	2.828	39.21	39.21	8.085
SFC-A-004	1542	0.283	254.7	4.802	17.56	17.56	4.265
SFC-A-007	1320	0.283	19.84	5.963	12.02	12.02	4.019
SFC-A-009	1631	0.283	222.7	5.470	18.64	18.64	3.048
SFC-A-010	1710	0.283	76.92	4.832	29.53	29.53	2.397
SFC-A-012	2712	0.283	208.8	4.961	20.27	20.27	1.884
SFC-A-015	3009	0.283	180.3	4.513	22.82	19.22	4.523
SFC-A-019	2109	1.210	35.43	7.954	21.43	21.43	8.346
SFC-A-020	1713	1.184	293.3	8.806	26.99	26.99	2.401
SFC-A-026	1835	0.283	50.81	5.510	16.61	16.61	2.047
SFC-A-027	2173	0.283	180.5	4.478	16.61	16.61	2.497
SFC-A-033	2403	17.96	171.08	2.828	55.01	55.01	19.683
SFC-A-036	1432	0.283	25.06	5.574	15.58	15.58	2.267
SFC-A-039	2126	0.283	372.3	2.828	16.03	16.03	2.854
SFC-A-042	1496	0.283	89.92	4.599	36.02	36.02	2.411
SFC-A-043	2052	0.283	22.85	4.705	21.38	21.38	7.044
SFC-A-051	4508	36.84	302.7	10.42	26.63	26.63	33.618
SFC-A-056	3332	3.759	53.75	21.41	49.11	49.11	7.585
SFC-A-077	2275	15.33	205.0	4.147	24.30	21.19	12.874
SFC-A-080	2301	0.283	112.5	2.828	11.09	11.09	6.356
SFC-A-081	2626	17.38	210.6	4.195	18.60	15.95	17.364
SFC-A-082	2464	16.90	24.61	4.193	10.29	10.29	13.040
SFC-B-003	1206	0.283	289.0	2.828	19.44	15.94	2.073
SFC-B-004	1431	0.283	24.17	5.131	22.41	22.41	2.491
SFC-B-005	1593	0.283	23.01	2.828	11.50	11.50	4.343
SFC-B-006	1533	4.448	287.2	2.828	16.99	15.95	5.294
SFC-B-010	1355	0.283	85.30	4.012	37.64	37.64	2.836
SFC-B-011	1634	2.596	121.9	2.828	17.92	17.92	5.456
SFC-B-026	787	0.283	76.57	2.828	18.39	15.83	1.962
SFC-B-049	3043	27.36	*1591*	*133.1*	*590.0*	*590.0*	23.897
SFC-B-052	2363	8.072	34.89	4.287	8.830	8.830	9.128

SFC-B-055	985	0.283	24.83	4.842	10.16	10.16	4.408
SFC-B-058	5170	54.44	34.64	5.087	10.32	10.32	45.806
SFC-B-060	5395	51.35	29.80	5.652	10.43	10.43	46.613
SFC-B-065	3568	9.973	66.73	12.38	31.37	31.37	19.321
SFC-B-068	4581	1.726	37.78	16.47	23.43	23.43	16.957
SFC-B-069	2517	28.34	44.74	15.80	37.38	37.38	31.162
SFC-B-070	2942	25.71	*1558*	*140.2*	*422.3*	*309.8*	24.352

Table A2.3: Concentrations of major cations in water samples collected from 38 flarks described in Table A1.1. Sites and entries that are italicized were identified as outliers and were excluded from the principal component analysis (Figure 2.4), the Pearson's correlation coefficient calculations (Table 2.2) and the redundancy analysis (chapter 3, Fig 3.5). Values shown in red were below the limit of detection, and adjusted using the R2D method (Antweiler 2015).

Site Code	Al (mg/L)	B (mg/L)	Ba (mg/L)	Ca (mg/L)	Fe (mg/L)	K (mg/L)	Li (mg/L)	Mg (mg/L)	Mn (mg/L)	Na (mg/L)	Si (mg/L)	Sr (mg/L)
SFC-A-003	2.994	2.204	0.041	53.516	0.313	6.484	0.508	29.307	0.061	977.290	2.327	2.974
SFC-A-004	3.455	2.517	0.042	46.539	0.543	5.225	0.449	26.132	0.093	911.090	2.830	2.555
SFC-A-007	3.516	2.337	0.089	95.860	0.239	7.517	0.557	48.745	0.150	1663.930	1.732	5.245
SFC-A-009	2.942	2.080	0.042	45.882	1.083	5.836	0.438	25.134	0.114	1763.587	2.147	2.469
SFC-A-010	3.457	1.991	0.043	50.055	0.453	3.046	0.329	27.141	0.045	976.393	1.943	2.773
SFC-A-012	4.071	2.530	0.042	66.751	0.434	4.929	0.363	28.497	0.090	1043.162	2.054	2.896
SFC-A-015	3.472	2.874	0.096	103.130	0.262	6.233	0.515	53.850	0.251	1810.690	2.482	5.837
SFC-A-019	2.633	2.173	0.041	49.433	0.197	4.119	0.318	26.356	0.044	1180.340	2.595	2.879
SFC-A-020	4.575	2.435	0.040	49.638	1.478	2.504	0.258	25.159	0.093	1036.734	3.379	2.701
SFC-A-026	3.206	1.867	0.042	45.125	0.786	3.918	0.249	19.623	0.129	728.357	2.118	1.895
SFC-A-027	2.964	2.089	0.042	64.372	0.242	4.139	0.358	35.195	0.036	1269.549	2.189	3.632
SFC-A-033	3.715	2.254	0.047	76.712	0.276	6.016	0.381	42.332	0.048	1562.504	3.745	4.505
SFC-A-036	2.837	1.980	0.042	42.909	0.435	3.689	0.346	21.624	0.033	901.282	2.847	2.149
SFC-A-039	2.815	1.945	0.066	73.196	0.421	4.090	0.438	39.540	0.156	1390.034	3.033	4.039
SFC-A-042	3.852	2.090	0.042	34.959	0.389	2.651	0.235	21.020	0.024	847.351	3.892	2.209

SFC-A-043	3.572	2.292	0.051	62.484	0.416	3.945	0.355	35.905	0.033	1320.825	3.323	3.709
SFC-A-051	2.777	2.997	0.042	99.202	0.589	11.143	0.533	62.194	0.072	2708.529	2.209	6.768
SFC-A-056	3.017	2.433	0.042	63.634	2.643	5.133	0.368	38.855	0.049	1772.226	3.300	4.677
SFC-A-077	3.550	2.358	0.051	65.538	0.255	4.448	0.229	36.442	0.100	1271.341	2.531	3.655
SFC-A-080	3.259	2.209	0.059	71.958	0.208	5.077	0.317	39.769	0.055	1374.806	1.653	4.006
SFC-A-081	5.264	2.140	0.064	84.009	0.263	6.801	0.365	46.605	0.053	1627.990	3.264	4.624
SFC-A-082	2.879	2.224	0.051	81.096	0.261	5.780	0.353	43.786	0.058	1449.039	3.386	4.051
SFC-B-003	2.975	2.484	0.043	40.605	0.425	3.403	0.211	21.284	0.088	709.679	2.622	1.902
SFC-B-004	5.193	2.074	0.070	49.059	0.726	2.408	0.209	24.352	0.167	835.613	3.628	2.329
SFC-B-005	2.771	1.940	0.044	52.215	0.423	1.174	0.193	23.771	0.027	823.755	2.310	2.207
SFC-B-006	4.066	1.935	0.042	43.251	0.404	1.174	0.232	25.617	0.025	850.373	2.253	2.232
SFC-B-010	3.493	2.011	0.042	40.861	0.538	1.174	0.231	23.301	0.053	795.363	2.481	1.993
SFC-B-011	3.776	2.179	0.047	44.869	0.462	1.841	0.229	26.055	0.075	837.151	2.768	2.284
SFC-B-026	1.898	2.410	0.048	38.230	0.378	2.151	0.157	18.607	0.045	623.262	2.867	1.781
SFC-B-049	3.940	2.550	0.046	78.978	0.826	7.219	0.398	45.669	0.105	1701.535	6.527	4.511
SFC-B-052	2.943	2.239	0.064	75.772	0.317	4.244	0.290	41.896	0.066	1431.588	1.700	3.976
SFC-B-055	3.176	1.980	0.042	39.057	0.380	1.863	0.151	19.624	0.040	633.723	2.723	1.413
SFC-B-058	3.578	2.989	0.042	121.682	0.384	12.429	0.562	77.949	0.052	3157.420	2.173	7.987
SFC-B-060	2.996	3.139	0.049	120.195	0.306	12.985	0.471	72.886	0.043	3131.340	2.290	8.019
SFC-B-065	2.756	2.392	0.078	147.692	5.194	5.999	0.562	85.440	0.175	3195.040	4.730	8.931

SFC-B-068	2.596	2.516	0.070	115.414	3.273	13.302	0.443	67.172	0.119	2799.060	3.810	7.155
SFC-B-069	3.093	2.430	0.070	94.639	1.985	2.965	0.312	49.891	0.129	1706.057	3.445	4.791
SFC-B-070	7.186	2.099	0.052	84.730	0.970	6.769	0.309	48.612	0.140	1787.623	6.602	4.731

Table A2.4a: Pearson's correlation coefficient for environmental variables. Above the matrix midline is Pearson's correlation coefficient values. Those with a Holm's adjusted p value less than 0.05 are bold-faced (Aickin & Gensler 1996; Holm 1979). Below the matrix midline are the adjusted p-values that are statistically significant ((*p* <0.05). Sites containing outliers were removed using Dixon's test. n=34 sites (Table A2.5). (Split into 3 tables). Specific conductance values, and concentrations of nutrients, cations and anions were log transformed before the analysis.

	Easting	Northing	Water Temp (˚C)	Dissolved Oxygen (mg/L)	Specific Conductance (µS/cm)	pH	Redox (mV)	Maximum Depth (cm)	Cl (mg/L)
Easting		**-0.913**	-0.211	-0.06	**0.65**	0.017	-0.178	0.165	**0.683**
Northing	**<0.001**		0.166	-0.022	**-0.68**	-0.019	0.123	-0.138	**-0.707**
Water Temperature (˚C)				0.255	-0.109	-0.138	0.367	-0.084	-0.254
Dissolved Oxygen (mg/L)					-0.211	0.303	0.186	0.163	-0.257
Specific Conductance (µS/cm)	**0.021**	**0.006**				0.214	0.099	0.1	**0.967**
pH							0.595	0.147	0.203
Redox (mV)						0.126		0.122	0.01
Maximum Depth (cm)									0.099
Cl (mg/L)	**0.006**	**0.002**			**<0.001**				
SO4-S (mg/L)		0.726			**0.036**				**0.011**
NH4-N (µg/L)									
PO4-P (µg/L)	**0.001**	0.119							
TON-N (µg/L)									
NO3-N (µg/L)									
Al (mg/L)									

B (mg/L)			**0.002**	**0.001**
Ba (mg/L)				
Ca (mg/L)	0.127	0.092	**<0.001**	**<0.001**
Fe (mg/L)	0.993	1		
K (mg/L)	0.325	0.758	**<0.001**	**<0.001**
Li (mg/L)			**0.02**	**0.048**
Mg (mg/L)	**0.045**	**0.024**	**<0.001**	**<0.001**
Mn (mg/L)				
Na (mg/L)	**0.003**	**0.009**	**<0.001**	**<0.001**
S (mg/L)	0.306	**0.018**	**0.002**	**<0.001**
Si (mg/L)				
Sr (mg/L)	**0.018**	**0.033**	**<0.001**	**<0.001**

Table A2.4b: Pearson's correlation coefficient for environmental variables. Above the matrix midline is Pearson's correlation coefficient values. Those with a Holm's adjusted p value less than 0.05 are bold-faced (Aickin & Gensler 1996; Holm 1979). Below the matrix midline are the adjusted p-values of the above correlations. Sites containing outliers were removed using Dixon's test. n=34 sites (Table A2.5). (Split into 3 tables). Specific conductance values, and concentrations of nutrients, cations and anions were log transformed before the analysis.

	SO4-S (mg/L)	**NH4-N (µg/L)**	**PO4-P (µg/L)**	**TON-N (µg/L)**	**NO3-N (µg/L)**	**Al (mg/L)**	**B (mg/L)**	**Ba (mg/L)**	**Ca (mg/L)**
Easting	0.429	-0.197	**0.731**	0.16	0.203	-0.358	0.434	0.159	0.595
Northing	-0.532	0.23	-0.597	0.009	-0.02	0.312	-0.441	-0.166	-0.605
Water Temp (˚C)	-0.271	0.351	-0.322	-0.144	-0.164	0.162	-0.068	-0.209	-0.255
D O (mg/L)	-0.231	-0.186	-0.244	-0.212	-0.197	0.054	-0.222	-0.124	-0.244
Spec Cond (µS/cm)	**0.634**	0.089	0.389	0.041	0.042	-0.202	**0.703**	0.208	**0.789**
pH	0.024	-0.039	0.019	-0.182	-0.199	-0.133	0.133	-0.034	0.107
Redox (mV)	-0.057	0.187	-0.244	-0.264	-0.301	0.147	0.155	-0.087	0.008
Maximum Depth (cm)	0.005	-0.025	0.057	0.034	0.014	-0.199	0.122	0.166	0.109
Cl (mg/L)	**0.667**	-0.01	0.451	0.023	0.028	-0.212	**0.718**	0.226	**0.836**
SO4-S (mg/L)		-0.023	0.258	0.09	0.084	-0.049	0.505	0.059	0.608
NH4-N (µg/L)			-0.233	0.312	0.262	0.222	0.085	-0.173	-0.123
PO4-P (µg/L)				0.33	0.359	-0.22	0.366	0.163	0.369
TON-N (µg/L)					**0.993**	0.142	0.01	-0.089	-0.099
NO3-N (µg/L)				**<0.001**		0.113	-0.009	-0.115	-0.099
Al (mg/L)							-0.067	0.059	-0.186
B (mg/L)								0.182	**0.658**
Ba (mg/L)									0.615
Ca (mg/L)	0.087						**0.015**	0.068	
Fe (mg/L)			**<0.001**						
K (mg/L)							**0.004**		**0.001**

Li (mg/L)		0.311		**0.002**
Mg (mg/L)	**0.012**	**0.005**	0.419	**<0.001**
Mn (mg/L)			**0.027**	
Na (mg/L)	**0.04**	**0.004**		**<0.001**
S (mg/L)	**<0.001**	0.117		**<0.001**
Si (mg/L)				
Sr (mg/L)	**0.035**	**0.002**	0.811	**<0.001**

Table A2.4c: Pearson’s correlation coefficient for environmental variables. Above the matrix midline is Pearson’s correlation coefficient values. Those with a Holm’s adjusted p value less than 0.05 are bold-faced (Aickin & Gensler 1996; Holm 1979). Below the matrix midline are the adjusted p-values of the above correlations. Sites containing outliers were removed using Dixon’s test. n=34 sites (Table A2.5). (Split into 3 tables). Specific conductance values, and concentrations of nutrients, cations and anions were log transformed before the analysis.

	Fe (mg/L)	K (mg/L)	Li (mg/L)	Mg (mg/L)	Mn (mg/L)	Na (mg/L)	S (mg/L)	Si (mg/L)	Sr (mg/L)
Easting	0.519	0.562	0.491	**0.628**	0.083	**0.7**	0.565	0.298	**0.654**
Northing	-0.341	-0.53	-0.343	**-0.646**	0.013	**-0.671**	**-0.654**	-0.244	**-0.637**
Water Temperature (˚C)	-0.433	0.044	0.087	-0.277	0.003	-0.262	-0.422	-0.175	-0.232
Dissolved Oxygen (mg/L)	-0.426	-0.09	-0.144	-0.279	-0.288	-0.301	-0.231	-0.108	-0.272
Specific Cond. (μS/cm)	0.13	**0.775**	**0.65**	**0.814**	0.151	**0.85**	**0.708**	0.073	**0.848**
pH	-0.226	0.36	0.102	0.075	0.044	0.121	0.105	-0.287	0.101
Redox (mV)	-0.446	0.269	0.057	-0.051	0.129	-0.062	-0.033	-0.251	-0.06
Maximum Depth (cm)	-0.024	0.063	0.018	0.106	0.097	0.085	0.014	0.245	0.119
Cl (mg/L)	0.236	**0.737**	**0.626**	**0.859**	0.151	**0.882**	**0.757**	0.095	**0.881**
SO4-S (mg/L)	0.092	0.467	0.337	**0.665**	-0.046	**0.631**	**0.898**	0.17	**0.635**
NH4-N (μg/L)	-0.037	-0.002	0.094	-0.087	0.185	-0.058	-0.181	-0.042	-0.06
PO4-P (μg/L)	**0.755**	0.311	0.271	0.38	0.275	0.487	0.326	0.373	0.42
TON-N (μg/L)	0.419	-0.078	0.07	-0.049	0.097	-0.004	0.004	0.502	0.024
NO3-N (μg/L)	0.444	-0.078	0.085	-0.05	0.073	0.005	0.007	0.499	0.025
Al (mg/L)	-0.153	-0.227	-0.244	-0.195	0.018	-0.258	-0.19	0.122	-0.187
B (mg/L)	0.103	**0.692**	0.564	**0.686**	0.272	**0.689**	0.598	0	**0.704**
Ba (mg/L)	0.126	0.268	0.325	0.553	**0.642**	0.421	0.217	0.158	0.527
Ca (mg/L)	0.191	**0.722**	**0.704**	**0.979**	0.389	**0.909**	**0.748**	0.086	**0.963**
Fe (mg/L)		0.039	0.11	0.194	0.367	0.288	0.105	0.522	0.204
K (mg/L)			**0.812**	**0.735**	0.32	**0.79**	0.582	-0.026	**0.773**
Li (mg/L)		**<0.001**		**0.722**	0.338	**0.769**	0.445	-0.033	**0.771**
Mg (mg/L)		**0.001**	**0.001**		0.3	**0.946**	**0.806**	0.117	**0.986**

Mn (mg/L)						0.275	-0.015	0.101	0.301
Na (mg/L)		**<0.001**	**<0.001**	**<0.001**			**0.774**	0.116	**0.957**
S (mg/L)		0.189		**<0.001**		**<0.001**		0.177	**0.768**
Si (mg/L)	0.927								0.125
Sr (mg/L)		**<0.001**	**<0.001**	**<0.001**		**<0.001**	**<0.001**		

Table A2.5: Results of Dixon's Q-test to identify outliers within the dataset (Table A2.1; Table A2.2; Table A2.3)

Site Code	Variable (units)	Value	Q	n	Critical value	p-value
SFC-B-026	pH	4.2	0.602	37	0.3498	>0.05
SFC-B-070	NH4-N (µg/L)	1558	0.771	37	0.3498	>0.05
SFC-B-049	PO4-P (µg/L)	133.1	0.857	37	0.3498	>0.05
SFC-B-070	TON-N (µg/L)	422.3	0.888	37	0.3498	>0.05
SFC-B-070	NO3-N (µg/L)	309.8	0.847	37	0.3498	>0.05

Table A2.6: Eigenvalues and proportion of variance of principal component analysis used to determine the number of rotated components to use in Factor Analysis (Figure 2.4). The first 10 principal components are shown here.

	PC1	PC2	PC3	PC4	PC5	PC6	PC7	PC8	PC9	PC10
Eigenvalue	10.324	3.240	2.129	1.728	1.601	1.273	1.184	0.951	0.704	0.536
Proportion of Variance	0.39707	0.12461	0.0819	0.06647	0.06157	0.04895	0.04555	0.03657	0.02707	0.0206
Cumulative Proportion	0.39707	0.52169	0.60359	0.67006	0.73163	0.78059	0.82613	0.8627	0.88978	0.91038

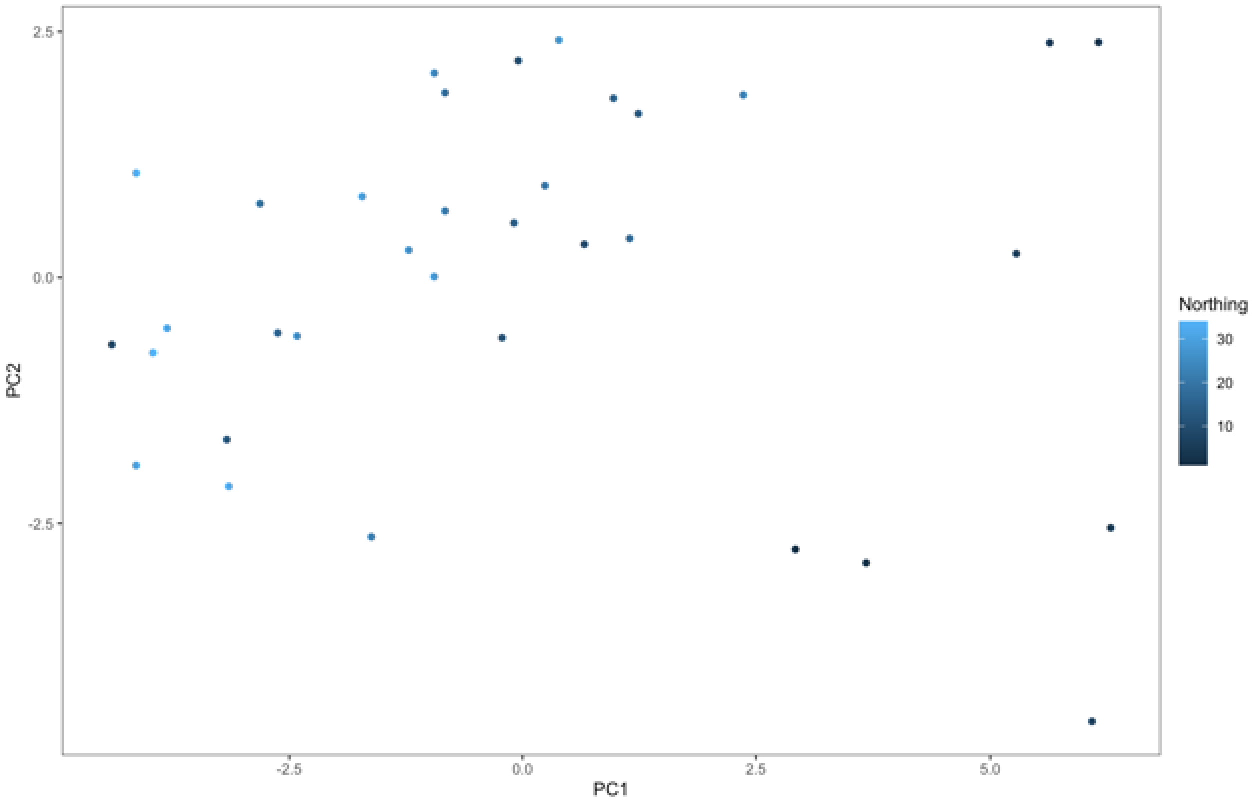

Figure A2.1: Principal component analysis of environmental condition loadings plotted on 2 axes (n=34). The colour gradient depicts the location of the site within the saline fen complex, where the northernmost site was given a northing score of 1, therefore increased colour saturation implies a site further north within the complex

Table A2.7: Site scores for principal component analys before varimax rotation.

Site Code	PC1	PC2	PC3	PC4	PC5	PC6	PC7	PC8
SFC-A-003	-0.947	0.009	-0.637	1.459	-0.654	-0.530	-0.024	1.575
SFC-A-004	-1.719	0.823	-1.520	0.626	0.933	-0.803	-0.643	-0.494
SFC-A-007	0.388	2.414	-1.150	-3.505	-0.938	-0.509	0.235	-1.240
SFC-A-009	-1.220	0.279	-1.200	-0.085	0.939	-1.932	-1.498	0.076
SFC-A-010	-2.416	-0.595	-0.529	1.050	-0.799	-1.704	-0.040	-0.301
SFC-A-012	-0.946	2.078	-1.077	0.332	1.863	0.020	-0.060	-0.717
SFC-A-015	2.364	1.856	-3.709	-1.231	-0.076	0.058	0.783	0.386
SFC-A-019	-0.830	0.677	1.439	-0.001	0.927	-0.198	-0.580	0.608
SFC-A-020	-1.620	-2.637	-2.533	2.477	0.156	-1.049	1.125	-1.042
SFC-A-026	-2.813	0.751	0.806	-1.486	1.920	-0.602	-1.573	-1.625
SFC-A-027	-0.831	1.878	0.787	-0.279	1.675	0.035	0.211	1.321
SFC-A-033	1.147	0.397	-0.262	2.320	0.023	1.651	0.304	-0.502
SFC-A-036	-2.624	-0.564	1.843	-0.725	1.076	-0.956	1.976	0.515
SFC-A-039	-0.092	0.555	-1.675	-1.230	0.898	-0.283	2.293	1.954
SFC-A-042	-3.170	-1.648	1.425	0.617	1.752	1.459	1.905	0.209
SFC-A-043	-0.220	-0.612	1.526	-0.391	-0.047	0.442	1.729	-0.682
SFC-A-051	5.280	0.243	0.497	2.147	0.023	-1.370	-0.415	-0.055
SFC-A-056	2.913	-2.764	1.193	0.801	2.265	-0.764	-0.845	-0.998
SFC-A-077	0.239	0.934	-0.709	0.523	0.145	1.903	-1.314	1.274
SFC-A-080	-0.047	2.205	0.130	-0.295	-1.216	-1.030	-0.240	-0.157
SFC-A-081	1.240	1.666	-1.117	1.443	-0.701	2.143	0.609	-1.909
SFC-A-082	0.973	1.822	1.077	-0.206	-0.467	0.471	0.630	-0.423
SFC-B-003	-4.130	1.062	-1.168	-0.175	1.055	0.554	-1.045	1.375
SFC-B-004	-3.148	-2.123	-1.714	-1.911	-1.457	2.301	-0.594	-1.215
SFC-B-005	-3.951	-0.765	1.998	-0.745	-2.562	-0.359	-1.325	0.817
SFC-B-006	-3.809	-0.516	0.369	1.626	-2.009	0.943	-1.011	0.681
SFC-B-010	-4.131	-1.911	-0.369	0.635	-1.058	0.063	-0.971	0.602
SFC-B-052	0.661	0.338	1.256	-0.479	-2.849	-1.598	1.299	-0.267
SFC-B-055	-4.391	-0.682	2.416	-0.807	0.094	-0.149	0.751	-1.017
SFC-B-058	5.637	2.387	1.039	1.481	-1.131	-0.350	0.237	-0.809
SFC-B-060	6.160	2.392	2.237	-0.145	-0.079	1.276	-0.563	1.199
SFC-B-065	6.091	-4.503	-1.429	-1.083	-0.881	-0.336	0.923	1.059
SFC-B-068	6.291	-2.545	0.042	-1.512	0.412	-0.598	-1.874	-0.058
SFC-B-069	3.671	-2.902	0.717	-1.244	0.767	1.802	-0.396	-0.140

Table A2.8: Principal component loadings of environmental data before varimax rotation. Bold-faced values indicate the strongest association of each variable with a varimax rotated component. Specific conductance values, and concentrations of nutrients, cations and anions were log transformed before the analysis.

Variable (Units)	PC1	PC2	PC3	PC4	PC5	PC6	PC7	PC8
Na (mg/L)	**0.300**	0.032	-0.026	-0.001	-0.056	-0.057	0.010	0.031
Sr (mg/L)	**0.299**	0.052	-0.068	-0.023	-0.100	0.028	0.079	0.041
Mg (mg/L)	**0.296**	0.054	-0.049	-0.043	-0.163	0.052	0.072	0.044
Ca (mg/L)	**0.288**	0.073	-0.078	-0.121	-0.158	0.050	0.064	-0.002
Cl (mg/L)	**0.287**	0.057	0.050	0.122	0.020	0.008	-0.066	0.021
Specific Conductance (µS/cm)	**0.276**	0.109	0.012	0.164	0.082	-0.004	-0.006	0.036
S (mg/L)	**0.256**	0.020	0.180	0.161	-0.201	0.210	-0.084	0.001
K (mg/L)	**0.250**	0.211	-0.064	-0.003	0.151	-0.116	0.002	-0.083
B (mg/L)	**0.230**	0.121	-0.101	0.125	0.055	0.017	-0.066	-0.002
Fe (mg/L)	0.106	**-0.444**	-0.094	-0.074	0.159	-0.159	-0.189	-0.116
Redox	-0.015	**0.396**	-0.095	-0.018	0.293	0.186	-0.217	-0.180
PO4-P (µg/L)	0.176	**-0.302**	0.053	-0.098	0.272	-0.142	-0.138	-0.275
TON-N (µg/L)	0.019	**-0.314**	-0.202	0.280	0.269	0.177	-0.078	0.066
Mn (mg/L)	0.095	-0.033	**-0.500**	-0.344	0.078	-0.046	-0.109	-0.075
NH4-N (µg/L)	-0.029	0.078	**-0.406**	0.395	0.203	-0.011	-0.048	0.262
Northing	-0.235	0.082	**-0.274**	-0.013	-0.160	0.042	-0.219	0.145
Ba (mg/L)	0.131	-0.020	-0.288	**-0.478**	-0.237	0.184	0.173	-0.068
SO4-S (mg/L)	0.215	0.008	0.133	**0.312**	-0.182	0.255	-0.058	0.017
Easting	0.241	-0.153	0.194	-0.021	**0.260**	-0.137	0.155	-0.106
Si (mg/L)	0.060	-0.353	-0.064	0.035	0.195	**0.407**	0.219	-0.036
Li (mg/L)	0.227	0.134	-0.185	0.002	0.068	**-0.251**	0.140	0.074
Water Temp (˚C)	-0.091	0.246	-0.193	0.174	0.247	-0.236	**0.502**	-0.095
pH	0.040	0.299	0.129	-0.179	0.293	0.154	**-0.517**	-0.135
DO (mg/L)	-0.089	0.195	0.282	-0.167	0.258	0.181	**0.352**	-0.220
Depth	0.040	0.009	0.050	-0.267	0.322	0.410	0.132	**0.609**
Al (mg/L)	-0.084	0.018	-0.271	0.205	-0.121	0.438	0.112	**-0.544**

Table A2.9: Site scores for varimax rotated principal component analysis (Figure 2.3).

Site Code	PC1	PC2	PC3	PC4	PC5	PC6	PC7	PC8
SFC-A-003	-0.012	-0.853	-0.515	-0.178	1.486	-0.931	-0.701	0.129
SFC-A-004	-0.494	0.190	0.247	0.723	1.065	0.835	-0.016	-0.877
SFC-A-007	-0.074	-0.853	2.572	0.494	-1.742	0.894	-0.127	-0.721
SFC-A-009	-0.612	0.489	0.474	0.203	1.122	0.889	-1.395	-1.166
SFC-A-010	-0.632	-0.079	-0.245	0.343	0.556	-0.809	-0.411	-1.583
SFC-A-012	-0.143	0.099	0.103	1.367	0.570	1.520	0.429	-0.091
SFC-A-015	0.747	-0.823	2.491	1.023	0.963	0.082	0.204	0.396
SFC-A-019	-0.242	-0.026	-0.882	-0.104	-0.095	0.733	-0.905	0.456
SFC-A-020	-0.452	1.193	-0.041	1.341	1.593	-1.616	1.203	-1.425
SFC-A-026	-1.260	1.084	0.128	0.229	-0.920	2.339	-0.342	-0.845
SFC-A-027	-0.115	-0.514	-0.572	0.756	0.231	0.853	-1.090	1.405
SFC-A-033	0.790	-0.150	-1.037	0.054	0.741	0.066	1.868	0.200
SFC-A-036	-0.837	0.254	-0.739	1.517	-1.177	-0.913	-1.038	0.878
SFC-A-039	-0.020	-0.661	1.220	1.721	0.541	-1.119	-0.973	1.983
SFC-A-042	-0.940	0.772	-1.376	1.046	-0.479	-0.675	0.960	1.901
SFC-A-043	-0.015	0.237	-0.471	0.734	-1.565	-0.766	0.646	0.446
SFC-A-051	1.838	0.471	-1.064	0.136	0.754	-0.139	-0.655	-1.166
SFC-A-056	0.369	2.783	-1.003	0.038	0.015	0.556	-0.323	-0.478
SFC-A-077	0.200	-0.758	-0.098	-1.271	1.324	0.905	0.419	1.306
SFC-A-080	0.265	-1.231	0.246	0.094	-0.380	0.252	-0.612	-1.075
SFC-A-081	0.898	-0.589	-0.012	0.366	-0.067	0.537	3.011	-0.457
SFC-A-082	0.604	-0.806	-0.299	0.313	-1.038	0.296	0.385	0.081
SFC-B-003	-1.260	-0.687	0.195	-0.216	1.435	0.997	-0.488	1.033
SFC-B-004	-1.417	0.222	1.861	-1.585	-0.603	-0.077	2.180	0.168
SFC-B-005	-1.244	-1.146	-0.508	-2.169	-0.804	-0.671	-1.017	-0.563
SFC-B-006	-0.832	-1.197	-1.044	-1.694	0.811	-0.646	0.646	-0.277
SFC-B-010	-1.360	-0.138	-0.264	-1.265	0.876	-0.742	0.007	-0.313
SFC-B-052	0.471	-1.180	0.087	0.108	-1.579	-1.768	-0.658	-1.358
SFC-B-055	-1.408	0.281	-0.869	0.384	-1.916	-0.152	0.154	-0.191
SFC-B-058	2.284	-0.754	-0.813	0.218	-0.505	0.184	0.332	-1.163
SFC-B-060	2.149	-0.896	-0.825	-1.031	-0.604	0.981	-0.614	1.414
SFC-B-065	1.178	1.514	1.630	-0.774	0.265	-2.455	-0.580	0.770
SFC-B-068	1.087	2.004	1.045	-1.621	-0.145	0.462	-1.139	-0.245
SFC-B-069	0.492	1.746	0.377	-1.299	-0.729	0.099	0.640	1.429

Appendix A3: Summary Tables and Figures of Chapter 3 Analyses

Table A3.1: Summary table of sites' total abundance, family richness and their respective specific conductance values.

Site Code	**Specific Conductance (µS/cm)**	**Total Abundance**	**Family Richness**
SFC-A-003	6866	860.40	22
SFC-A-004	6271	2509.68	21
SFC-A-007	4972	4153.17	23
SFC-A-009	7021	6370.54	24
SFC-A-010	6804	2799.14	22
SFC-A-012	10283	1020.95	23
SFC-A-015	12564	1005.25	21
SFC-A-019	8515	2052.88	15
SFC-A-020	7400	4093.56	17
SFC-A-026	6401	3315.27	17
SFC-A-027	9125	1882.97	23
SFC-A-033	10692	21556.47	13
SFC-A-036	6314	644.00	14
SFC-A-039	9369	4534.69	22
SFC-A-042	5812	27611.00	22
SFC-A-043	7783	1203.56	18
SFC-A-051	16529	956.71	17
SFC-A-056	11478	2599.48	15
SFC-A-077	8814	2581.78	23
SFC-A-080	9116	10206.06	21
SFC-A-081	10627	3471.55	25
SFC-A-082	10163	3039.04	24
SFC-B-003	4816	9118.84	20
SFC-B-004	5125	3246.70	14
SFC-B-005	5151	1033.00	18
SFC-B-006	5474	1389.80	21
SFC-B-010	5123	1826.00	23
SFC-B-011	4845	2397.45	20
SFC-B-026	4160	4058.93	23
SFC-B-049	10892	5313.16	18
SFC-B-052	9402	10332.35	15
SFC-B-055	3757	3607.14	28
SFC-B-058	15918	892.26	19
SFC-B-060	18628	2773.52	17
SFC-B-065	9392	294.00	9

SFC-B-068	17106	1134.55	12
SFC-B-069	9498	815.63	14
SFC-B-070	9572	5770.18	25

Table A3.2: Linear regression of relationship between specific conductance and aquatic invertebrate abundance in 38 flarks (R^2 =0.01, $p>0.05$)

	Estimate (SE)	**t-Value**	**p-Value**
Intercept	16832 (20385)	0.826	0.414
Log(Specific conductance (μS/cm))	-3215 (5213)	-0.617	0.541

Table A3.3: Linear regression of relationship between specific conductance and aquatic invertebrate family richness in 32 flarks (R^2 =0.11, $p<0.05$).

	Estimate (SE)	**t-Value**	**p-Value**
Intercept	51.44 (14.97)	3.443	0.001
Log(Specific conductance (μS/cm))	-8.186 (3.829)	-2.138	0.039

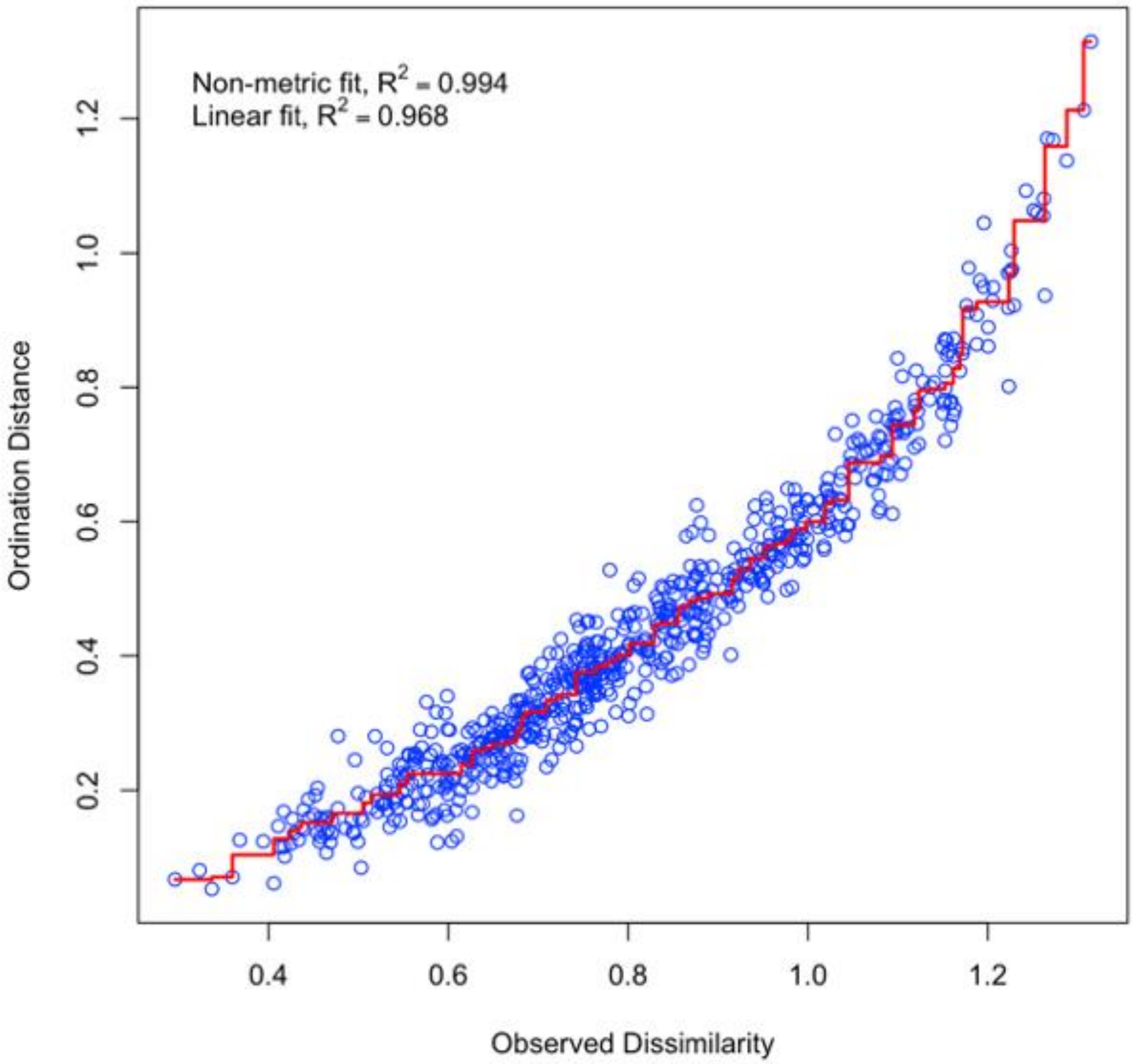

Figure A3.1: Goodness of fit plot for NMDS (Figure 3.4) with 3 axes. Stress value is 0.08

Table A3.4: Site scores for NMDS analysis (Figure 3.4)

Site Code	MDS1	MDS2	MDS3
SFC-A-003	-0.380	-0.044	0.103
SFC-A-004	-0.281	0.085	0.028
SFC-A-007	-0.170	-0.015	-0.019
SFC-A-009	-0.085	0.146	-0.074
SFC-A-010	0.008	0.128	0.004
SFC-A-012	0.078	-0.076	-0.222
SFC-A-015	0.070	-0.029	-0.163
SFC-A-019	0.294	-0.022	-0.174
SFC-A-020	0.050	0.244	-0.181
SFC-A-026	0.265	0.053	-0.176
SFC-A-027	-0.017	-0.084	-0.044
SFC-A-033	0.153	0.117	0.003
SFC-A-036	-0.265	-0.102	0.029
SFC-A-039	0.059	0.108	-0.079
SFC-A-042	-0.661	-0.150	-0.165
SFC-A-043	-0.499	-0.030	-0.090
SFC-A-051	0.247	-0.054	0.019
SFC-A-056	0.411	0.053	0.017
SFC-A-077	-0.142	-0.187	0.058
SFC-A-080	0.035	0.221	0.206
SFC-A-081	-0.050	0.009	0.010
SFC-A-082	-0.124	0.084	-0.079
SFC-B-003	-0.427	-0.135	-0.022
SFC-B-004	-0.429	-0.130	0.121
SFC-B-005	-0.032	-0.012	0.076
SFC-B-006	-0.077	-0.036	0.259
SFC-B-010	-0.152	-0.094	0.163
SFC-B-052	0.033	0.191	-0.003
SFC-B-055	-0.057	0.336	0.198
SFC-B-058	0.268	-0.132	-0.122
SFC-B-060	0.262	0.100	0.054
SFC-B-065	0.570	-0.097	-0.033
SFC-B-068	0.428	-0.137	0.185
SFC-B-069	0.615	-0.309	0.113

Table A3.5: Species scores for NMDS analysis (Figure 3.4). Bold-faced values indicate the strongest association of each taxa with a component. Variables are sorted in decreasing order of their strength of association with their most highly-associated component.

	MDS1	**MDS2**	**MDS3**
Stratiomyidae	**0.630**	-0.297	0.111
Culicidae<0.5mm	**0.604**	-0.176	0.017
Culiseta	**0.585**	-0.234	0.140
Sympetrum	**-0.530**	-0.138	-0.050
Culex	**0.516**	-0.103	-0.095
Stagnicola	**-0.485**	-0.121	-0.068
Aedes	**0.476**	-0.091	-0.043
Lymnaeidae.Other	**-0.454**	0.017	0.318
Aeshna	**-0.446**	0.031	-0.073
Phryganeidae	**-0.437**	-0.081	0.066
Nehalennia	**-0.433**	-0.158	0.058
Coenagrionidae <0.5mm	**-0.392**	-0.120	0.097
Planorbidae	**-0.356**	0.037	0.095
Dixella	**-0.324**	-0.059	0.085
Pachydiplax longipennis	**-0.321**	0.010	-0.028
Somatochlora	**-0.299**	0.093	-0.067
Dixidae.Pup	**-0.289**	-0.159	0.094
Ilybius	**-0.283**	-0.115	0.187
Corixidae.Other	**0.272**	-0.237	-0.062
Pericoma	**0.243**	0.023	-0.184
Muscidae	**0.237**	-0.105	-0.087
Trichocorixa	**0.227**	-0.216	-0.225
Dytiscidae.Other	**0.196**	-0.033	-0.177
Bezzia	**0.182**	0.068	0.028
Acari	**-0.182**	0.178	-0.083
Hydaticus	**0.170**	-0.056	-0.163
Ephydridae	**0.161**	-0.004	-0.039
Sciomyzidae	**0.039**	-0.076	0.004
Gerridae	0.074	**-0.428**	0.366
Atrichopogon	-0.116	**0.413**	0.131
Dasycorixa	0.365	**-0.395**	-0.069
Empididae	-0.079	**0.341**	-0.003
Notonectidae	-0.216	**-0.322**	0.016
Hydrobiidae	-0.113	**-0.290**	-0.197
Fossaria	-0.183	**-0.259**	0.002

Physa	-0.130	**0.235**	0.077
Dasyhelea	0.109	**0.170**	-0.056
Saldidae	0.090	**-0.164**	-0.043
Collembola	-0.044	**0.138**	0.007
Dolichopodidae	-0.050	**0.096**	0.035
Tabanidae	-0.035	**0.084**	0.081
Forcipomyia	-0.045	**0.081**	-0.008
Psychoda	-0.005	**-0.047**	0.034
Hydracarina	-0.036	0.318	**0.548**
Dytiscus	0.271	-0.243	**-0.508**
Libellulidae	0.249	0.148	**-0.344**
Hydrophilidae.Other	0.204	0.012	**-0.303**
Laccophilus	-0.047	-0.147	**-0.267**
Agabus	-0.093	0.115	**0.211**
Mesovelia	-0.191	-0.181	**0.206**
Tipulidae	0.179	0.115	**0.188**
Liodessus	0.060	0.001	**-0.186**
Psychodidae.Other	0.163	-0.039	**-0.184**
Oligochaeta	0.112	0.106	**-0.182**
Hydraenidae	-0.013	0.043	**-0.173**
Lymnaea stagnalis	-0.159	-0.116	**0.160**
Ceratopogonidae.Other	0.087	-0.074	**0.156**
Berosus	0.042	0.098	**-0.104**
Cymbiodyta	0.061	-0.007	**-0.075**
Chironomidae	-0.024	0.016	**0.035**

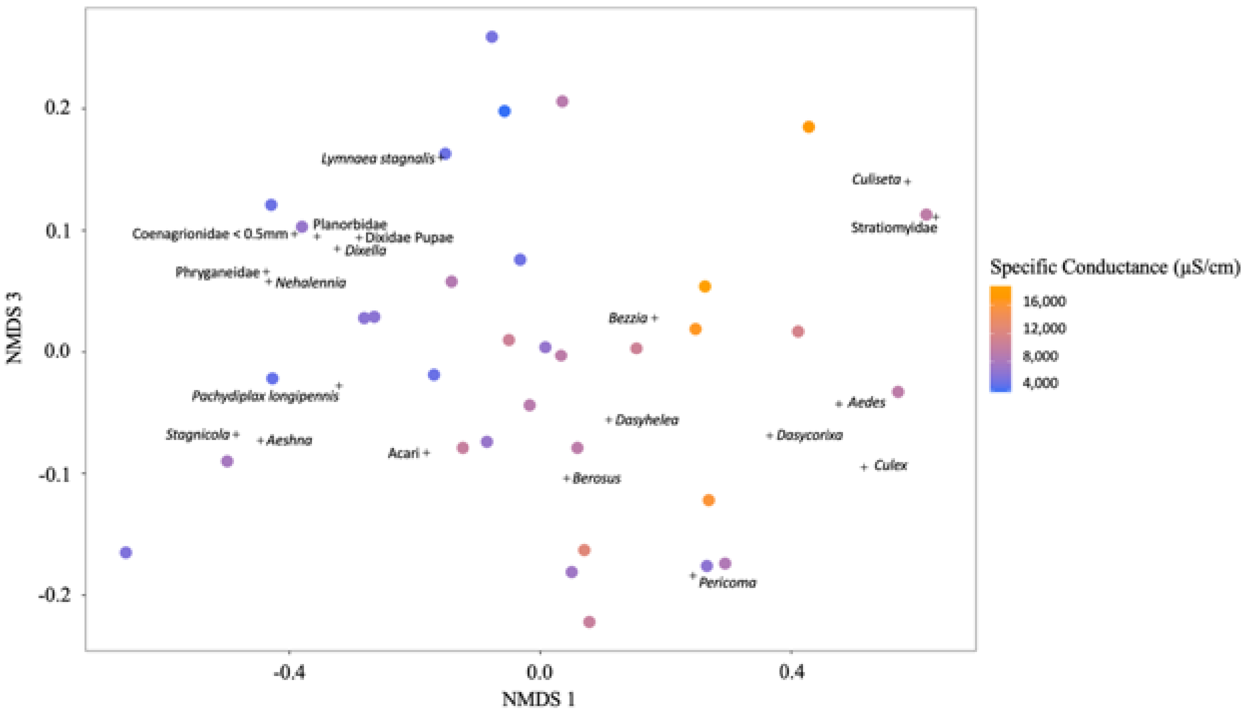

Figure A3.2: Nonmetric multi-dimensional scaling (NMDS) ordination of relative community composition of aquatic invertebrates in 34 flarks of the saline fen complex on NMDS axes 1 and 3. Coloured points represent sites. Points are coloured to correspond with the specific conductance of the sample site. Taxa listed are those identified as indicators of sensitivity or tolerance to specific conductance as determined by TITAN (Fig 3.6).

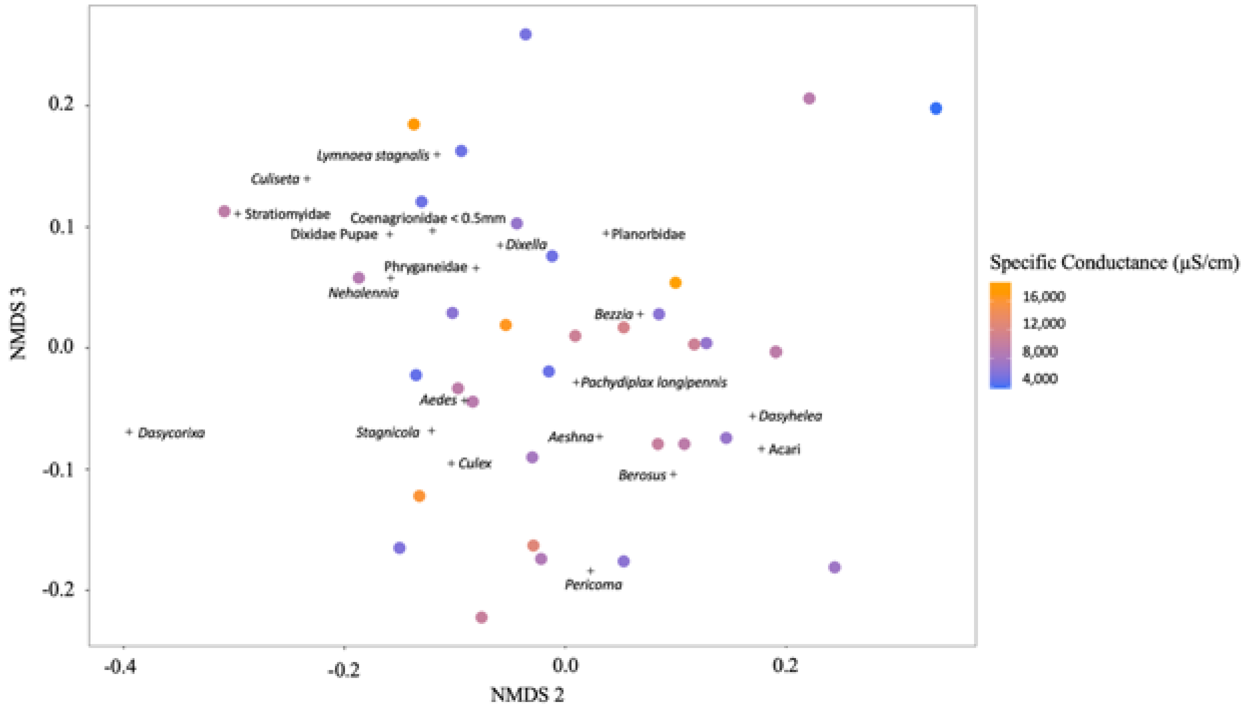

Figure A3.3: Nonmetric multi-dimensional scaling (NMDS) ordination of relative community composition of aquatic invertebrates in 34 flarks of the saline fen complex on NMDS axes 2 and 3. Coloured points represent sites. Points are coloured to correspond with the specific conductance of the sample site. Taxa listed are those identified as indicators of sensitivity or tolerance to specific conductance as determined by TITAN (Fig 3.6).

Table A3.6: Site scores for the first six constrained components for the redundancy analysis (Fig 3.5)

Site Code	RDA1	RDA2	RDA3	RDA4	RDA5	RDA6
SFC-A-003	-0.458	-0.462	0.001	0.422	0.267	-0.288
SFC-A-004	-0.368	-0.066	0.287	0.798	0.036	-0.109
SFC-A-007	-0.271	-0.101	-0.161	0.039	-0.102	0.754
SFC-A-009	-0.133	0.428	0.042	0.517	-0.231	0.233
SFC-A-010	-0.023	0.455	0.438	0.153	-0.163	0.006
SFC-A-012	0.105	0.282	-0.581	-0.288	0.926	-0.289
SFC-A-015	0.074	0.343	-0.625	-0.392	0.674	0.290
SFC-A-019	0.409	0.209	-0.410	-0.150	-0.104	0.273
SFC-A-020	0.078	0.557	0.051	1.090	0.457	-0.901
SFC-A-026	0.376	0.192	-0.767	0.026	-0.120	0.588
SFC-A-027	-0.047	0.124	-0.195	-0.652	-0.334	-0.620
SFC-A-033	0.196	0.464	0.310	-0.700	0.002	0.039
SFC-A-036	-0.450	-0.321	-0.105	-0.098	-0.085	-0.562
SFC-A-039	0.017	0.508	-0.170	-0.428	0.018	-0.259
SFC-A-042	-0.480	-0.712	-1.207	0.173	-0.977	-0.434
SFC-A-043	-0.505	-0.478	-0.759	0.433	-0.455	0.152
SFC-A-051	0.426	0.212	0.183	-0.469	-0.118	-0.358
SFC-A-056	0.616	0.020	0.030	-0.105	-0.726	0.506
SFC-A-077	-0.252	-0.205	-0.157	-0.725	0.459	-0.488
SFC-A-080	-0.050	0.259	0.586	-0.346	-0.617	0.419
SFC-A-081	-0.122	0.219	0.162	0.069	0.279	-0.109
SFC-A-082	-0.217	0.339	-0.233	0.552	-0.382	0.315
SFC-B-003	-0.542	-0.631	-0.420	-0.171	-0.299	0.099
SFC-B-004	-0.515	-0.662	0.021	0.215	0.823	0.812
SFC-B-005	-0.122	0.055	0.558	-0.256	0.013	0.194
SFC-B-006	-0.210	-0.216	1.008	-0.505	0.523	0.005
SFC-B-010	-0.296	-0.190	0.681	-0.247	0.474	-0.538
SFC-B-052	0.005	0.538	0.369	-0.059	-0.002	0.031
SFC-B-055	-0.129	0.281	0.830	0.433	-0.889	0.180
SFC-B-058	0.401	0.224	-0.165	0.267	0.407	0.271
SFC-B-060	0.422	0.180	0.297	-0.527	0.062	0.344
SFC-B-065	0.703	-0.467	-0.165	0.419	0.488	-0.233
SFC-B-068	0.644	-0.525	0.412	0.082	0.070	-0.155
SFC-B-069	0.718	-0.852	-0.151	0.431	-0.374	-0.169

Table A3.7: Species scores for the first six constrained components of the redundancy analysis plot (Fig 3.5)

	RDA1	RDA2	RDA3	RDA4	RDA5	RDA6
Aedes	**0.418**	-0.063	-0.007	0.034	0.056	-0.002
Stagnicola	**-0.415**	-0.142	-0.174	-0.003	-0.057	0.039
Culiseta	**0.326**	-0.150	0.011	-0.036	-0.047	0.014
Culicidae<0.5mm	**0.298**	-0.164	-0.015	0.060	-0.039	0.059
Pericoma	**0.197**	0.223	-0.190	-0.012	0.013	0.033
Chironomidae	**-0.181**	0.128	0.131	-0.124	0.048	0.024
Nehalennia	**-0.168**	-0.092	-0.066	-0.030	-0.019	-0.020
Bezzia	**0.163**	0.067	0.062	0.026	-0.088	0.004
Planorbidae	**-0.126**	-0.005	0.058	0.073	0.043	0.104
Dixella	**-0.125**	-0.048	0.001	0.020	0.016	0.044
Lymnaeidae.Other	**-0.094**	-0.082	0.054	0.030	0.071	0.044
Stratiomyidae	**0.075**	-0.045	-0.006	0.006	0.008	-0.014
Coenagrionidae<0.5mm	**-0.070**	-0.017	0.008	-0.046	0.006	-0.042
Pachydiplax longipennis	**-0.067**	-0.010	-0.024	-0.001	-0.006	-0.028
Collembola	**-0.065**	0.064	0.030	0.052	-0.051	-0.012
Dasycorixa	**0.062**	-0.045	-0.029	-0.015	0.019	-0.030
Culex	**0.062**	-0.033	-0.003	0.024	0.036	-0.041
Corixidae.Other	**0.040**	0.016	0.003	-0.004	-0.010	-0.006
Muscidae	**0.040**	0.009	-0.011	-0.007	-0.001	-0.008
Sciomyzidae	**0.034**	-0.031	-0.012	0.026	0.015	0.017
Somatochlora	**-0.034**	0.020	-0.011	-0.008	-0.016	-0.020
Phryganeidae	**-0.031**	-0.016	0.002	-0.011	0.005	0.007
Dixidae.Pup	**-0.030**	-0.009	0.004	-0.009	0.009	0.006
Ilybius	**-0.024**	-0.009	0.005	-0.020	0.005	0.013
Tipulidae	**0.018**	-0.008	0.005	-0.004	**-0.018**	0.015
Notonectidae	**-0.005**	0.001	-0.003	0.001	**-0.005**	-0.002
Mesovelia	**0.004**	-0.003	**0.004**	**-0.004**	<0.001	<0.001
Dasyhelea	0.112	**0.301**	-0.015	-0.076	-0.038	0.051
Oligochaeta	0.016	**0.109**	-0.010	0.017	-0.022	0.019
Cymbiodyta	0.022	**0.029**	0.004	0.010	0.004	0.006
Physa	-0.018	**0.028**	0.012	0.013	-0.006	0.023
Dytiscidae.Other	0.012	**0.025**	-0.002	<0.001	0.014	-0.007
Berosus	0.010	**0.022**	0.003	0.002	-0.007	0.003
Hydraenidae	-0.004	**0.022**	-0.009	-0.003	0.004	0.007
Gerridae	-0.003	**-0.022**	0.008	-0.004	0.006	-0.007
Sympetrum	-0.019	**-0.022**	-0.011	0.002	0.016	0.012

Hydrophilidae.Other	0.004	**0.020**	-0.016	-0.006	<0.001	0.002
Tabanidae	-0.007	**0.015**	0.011	<0.001	-0.015	0.010
Trichocorixa	0.008	**0.012**	-0.011	0.004	-0.002	0.002
Dytiscus	0.003	**0.011**	-0.008	-0.002	**0.011**	0.002
Hydracarina	-0.081	-0.019	**0.086**	-0.015	-0.064	<0.001
Fossaria	-0.014	-0.005	**-0.050**	-0.031	0.008	-0.001
Lymnaea stagnalis	-0.039	-0.021	**0.044**	-0.020	-0.035	-0.011
Psychodidae.Other	0.029	0.034	**-0.038**	-0.032	0.037	-0.028
Ceratopogonidae.Other	0.030	-0.009	**0.034**	0.012	0.020	-0.004
Agabus	-0.009	0.012	**0.031**	-0.005	-0.004	-0.002
Hydrobiidae	-0.007	-0.005	**-0.027**	-0.021	0.008	-0.007
Saldidae	0.002	0.001	**-0.007**	-0.003	-0.005	<0.001
Acari	-0.125	0.172	0.001	**0.213**	0.009	-0.070
Psychoda	0.010	0.016	0.020	**-0.063**	-0.035	-0.046
Atrichopogon	-0.061	0.077	0.028	**0.080**	-0.051	0.040
Hydaticus	0.001	0.010	-0.013	**-0.016**	-0.001	-0.002
Empididae	-0.008	0.005	-0.005	**0.013**	0.001	0.005
Dolichopodidae	-0.004	<0.001	-0.007	**-0.010**	-0.009	-0.003
Liodessus	0.010	0.051	-0.048	<0.001	**0.068**	0.008
Ephydridae	0.040	-0.006	-0.013	-0.010	**-0.044**	0.008
Forcipomyia	-0.013	0.020	-0.020	-0.012	**0.035**	0.016
Aeshna	-0.017	-0.005	-0.012	0.006	**-0.025**	-0.004
Laccophilus	0.002	0.015	-0.011	-0.001	**0.013**	-0.002
Libellulidae	-0.002	0.003	-0.004	-0.002	0.002	**0.006**

Table A3.8: Summary table for TITAN community level change point analysis with confidence limits (Fig 3.8). Values are log transformed specific conductance values.

	Change Point	5%	10%	50%	90%	95%
sumz-	3.911	3.738	3.802	3.911	3.972	3.972
sumz+	4.048	3.816	3.895	3.966	4.068	4.119
fsumz-	3.911	3.803	3.842	3.949	3.972	3.972
fsumz+	3.911	3.802	3.803	3.9	3.96	3.966

Table A3.9: Summary table for TITAN individual taxon change point analysis and their respective confidence intervals (Fig 3.7). “zenv.cp” is the change point associated with the zscore for the taxon, and “filter” determines whether the taxa are indicated as sensitive (filter = 1), tolerant (filter = 2), or did not pass the filter test (reliability & Purity < 0.95, filter = 0). Values are log transformed specific conductance values.

	zenv.cp	5%	10%	50%	90%	95%	filter
Hydracarina	3.960	3.684	3.690	3.803	3.966	3.992	0
Acari	4.028	3.880	3.891	3.998	4.032	4.036	1
Collembola	4.028	3.751	3.880	4.010	4.032	4.033	0
Oligochaeta	3.842	3.820	3.826	3.866	4.037	4.131	0
Lymnaeidae.Other	3.960	3.684	3.685	3.768	3.960	3.997	0
Stagnicola	3.911	3.837	3.846	3.911	3.972	3.973	1
Lymnaea stagnalis	3.725	3.697	3.710	3.738	3.972	3.972	1
Fossaria	4.048	3.691	3.697	3.900	3.994	4.019	0
Physa	4.028	3.725	3.750	3.862	4.028	4.029	0
Planorbidae	3.911	3.764	3.799	3.911	3.930	3.960	1
Hydrobiidae	3.725	3.751	3.803	3.960	4.019	4.033	0
Coenagrionidae.Other	3.972	3.711	3.712	3.966	3.975	3.977	1
Nehalennia	3.972	3.840	3.842	3.966	3.973	3.979	1
Aeshna	3.972	3.691	3.709	3.925	3.972	3.973	1
Sympetrum	4.028	3.711	3.723	3.880	3.972	3.994	0
Somatochlora	3.966	3.684	3.684	3.895	4.032	4.079	0
Pachydiplax longipennis	3.803	3.723	3.781	3.858	4.021	4.028	1
Libellulidae	3.803	3.785	3.803	3.956	4.004	4.019	0
Corixidae.Other	4.079	3.868	3.945	4.060	4.151	4.151	0
Dasycorixa	3.960	3.896	3.918	3.960	4.060	4.069	2
Trichocorixa	4.048	3.910	3.975	4.044	4.068	4.068	0
Mesovelia	3.858	3.684	3.690	3.858	4.202	4.218	0
Notonectidae	3.710	3.691	3.691	3.711	3.823	4.100	0
Gerridae	3.710	3.691	3.691	3.711	3.781	3.849	0

Saldidae	4.079	3.803	3.817	4.044	4.151	4.151	0
Phryganeidae	3.966	3.703	3.736	3.914	3.966	3.972	1
Dytiscidae.Other	4.010	3.685	3.835	4.010	4.151	4.151	0
Dytiscus	4.079	3.725	3.979	4.010	4.079	4.079	0
Hydaticus	3.938	3.803	3.900	3.938	4.010	4.048	0
Agabus	3.858	3.710	3.751	3.858	4.010	4.010	0
Ilybius	3.960	3.710	3.751	3.934	3.960	4.028	0
Liodessus	4.079	3.840	3.960	4.060	4.079	4.131	0
Laccophilus	4.079	3.781	3.797	3.997	4.079	4.131	0
Hydrophilidae.Other	3.911	3.815	3.817	3.963	3.993	4.099	0
Cymbiodyta	4.048	3.817	3.880	4.044	4.068	4.079	0
Berosus	3.880	3.849	3.862	3.880	3.994	4.019	2
Hydraenidae	3.979	3.725	3.797	3.979	4.048	4.119	0
Chironomidae	3.751	3.684	3.711	3.806	4.048	4.048	0
Ceratopogonidae.Other	3.703	3.691	3.697	3.975	4.151	4.151	0
Dasyhelea	3.781	3.759	3.781	3.803	3.842	3.952	2
Bezzia	4.033	3.737	3.820	3.991	4.037	4.048	2
Atrichopogon	4.048	3.691	3.703	3.781	3.952	4.021	0
Forcipomyia	3.979	3.703	3.769	3.977	4.019	4.019	0
Culicidae.Other	3.803	3.781	3.802	3.966	4.048	4.151	0
Aedes	3.966	3.802	3.803	3.918	3.972	3.975	2
Culiseta	3.952	3.900	3.900	3.966	4.032	4.151	2
Culex	3.960	3.799	3.803	3.938	3.966	3.972	2
Ephydridae	3.725	3.691	3.697	3.803	4.099	4.151	0
Psychodidae.Other	3.979	3.951	3.960	3.979	4.028	4.115	0
Psychoda	3.711	3.798	3.802	3.972	4.081	4.202	0
Pericoma	3.799	3.764	3.785	3.803	3.858	3.900	2
Sciomyzidae	3.975	3.685	3.781	3.975	4.033	4.151	0
Dixidae.Pup	3.858	3.738	3.751	3.853	3.958	3.966	1

Dixella	3.911	3.806	3.826	3.911	3.966	3.997	1
Dolichopodidae	3.960	3.710	3.903	3.960	3.992	4.025	0
Muscidae	3.975	3.781	3.820	3.966	4.029	4.033	0
Tipulidae	4.033	3.696	3.710	4.033	4.151	4.151	0
Tabanidae	3.979	3.697	3.710	3.953	4.027	4.033	0
Stratiomyidae	3.952	3.915	3.918	3.966	4.033	4.044	2
Empididae	3.703	3.703	3.703	3.806	4.028	4.028	0

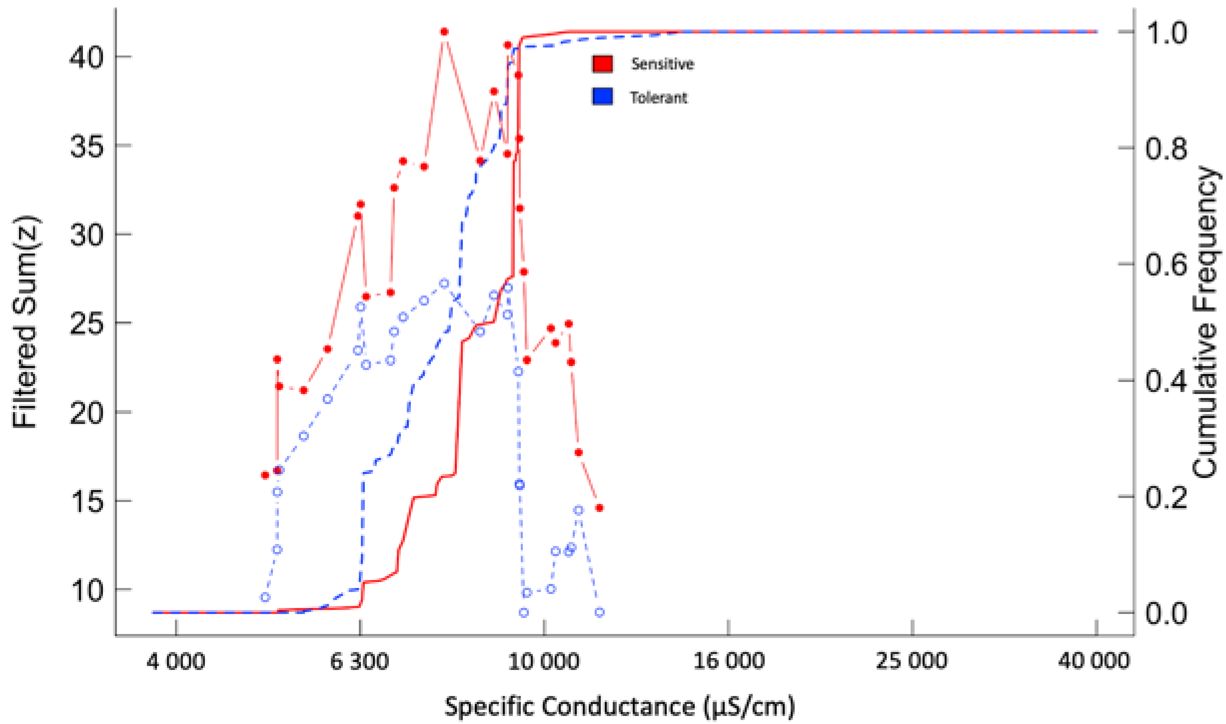

Figure A3.4: The sum of z-scores for filtered sensitive (red) and tolerant (blue) taxa (y-axis) are plotted along a specific conductance gradient (x-axis) as points. Greater sum z scores are associated with greater rates of change within the community. Lines represent cumulative distribution frequency of change points from bootstrap replicates.

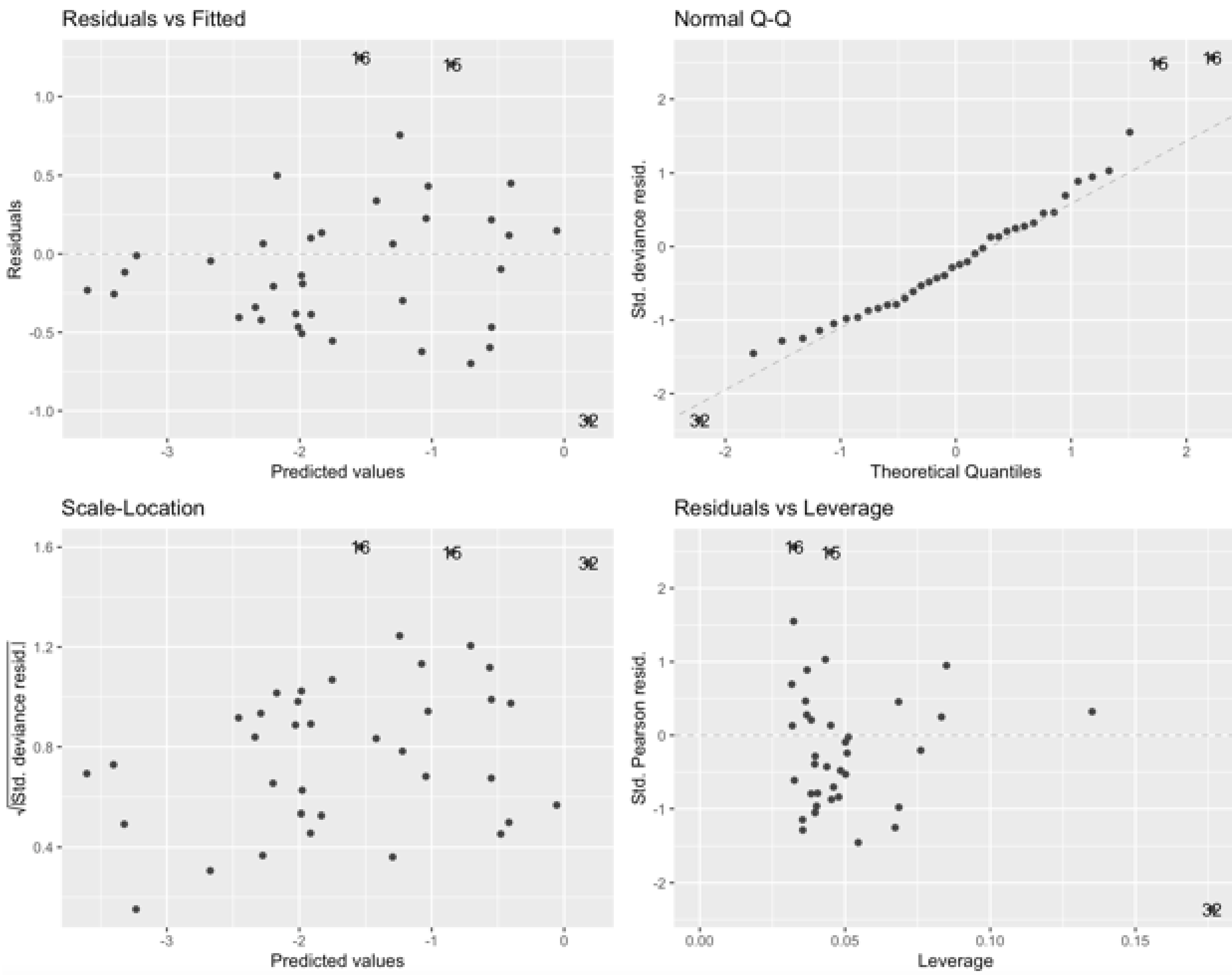

Figure A3.5: Standard plots showing the fit of data to the quasi-binomial logistic regression model for relationship between the saline-sensitive index and log transformed specific conductance values in flarks of the saline fen complex (Fig 3.9)

Table A3.10: Quasi-binomial logistic regression of relationship between specific conductance, and Saline-Sensitive Index values in flarks.

	Estimate (SD)	**t-Value**	**p-value**
Intercept	19.67 (5.521)	3.563	0.001057
Log(Specific conductance (μS/cm))	-5.45 (1.443)	-3.777	0.000574

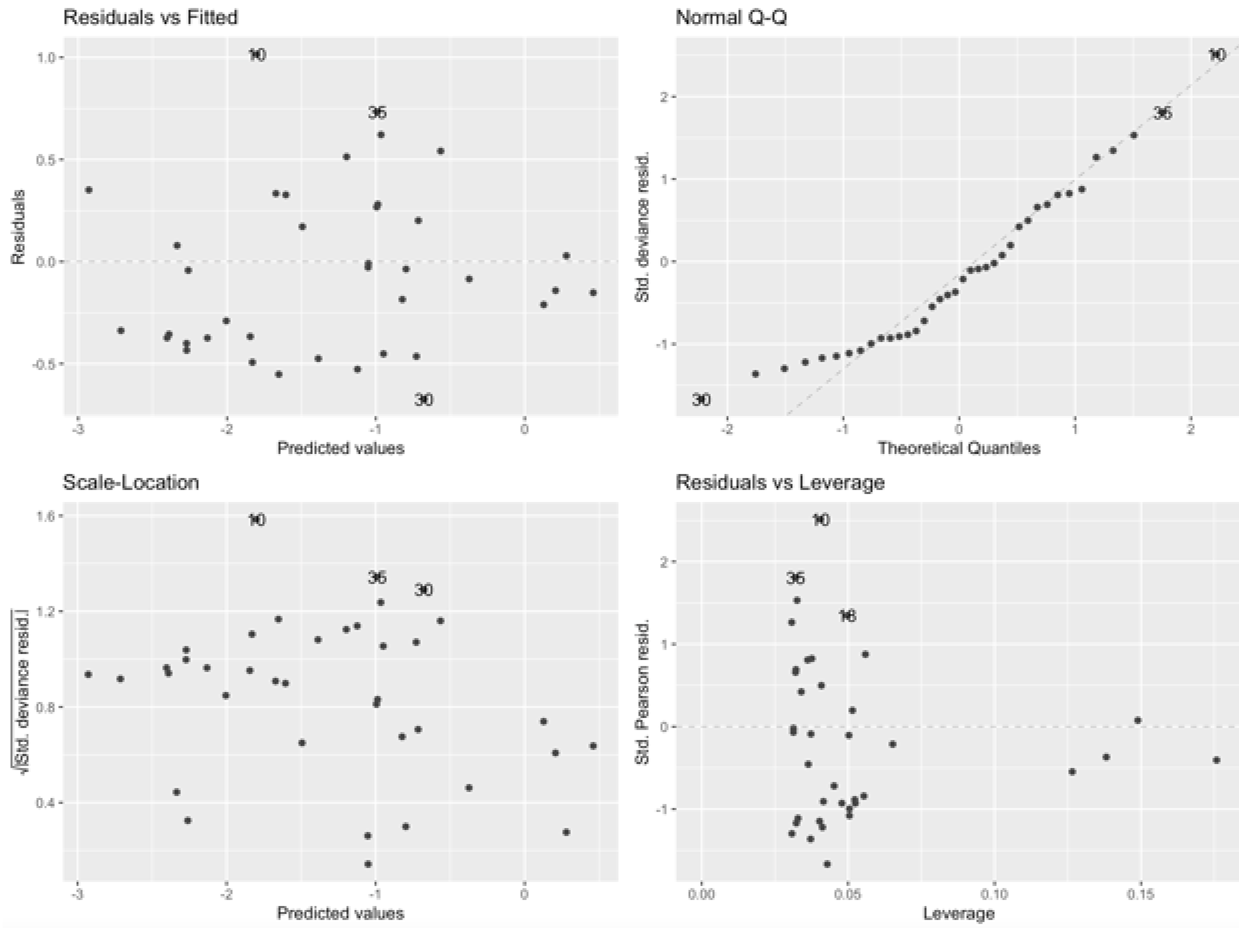

Figure A3.6: Standard plots showing the fit of data to the quasi-binomial logistic regression model for relationship between the saline-tolerant index and log transformed specific conductance values in flarks of the saline fen complex (Fig 3.10)

Table A3.11: Quasi-binomial logistic regression of relationship between specific conductance, and Saline-Tolerant Index values in flarks.

	Estimate (SD)	t-Value	p-value
Intercept	-20.35 (4.149)	-4.905	0.0000201
Log(Specific Conductance (μS/cm))	4.873 (1.044)	4.667	0.0000414

Appendix A4: Taxonomic Affiliations of Invertebrates Identified for Included Analyses

Table A4.1: Taxonomic affiliations of invertebrates identified for included analyses

Phylum	Subphylum	Class	Order	Suborder	Family	Genus	Species
Annelida		Clitellata	Oligochaeta				
			Rhynchobdellida		Glossiphonidae		
Mollusca		Gastropoda	Basommatophora		Lymnaeidae	*Lymnaea*	*stagnalis*
						Stagnicola	
						Fossaria	
						Radix	*auricularia*
					Physidae	*Physa*	
					Planorbidae	*Gyralus*	
						Planorbila	*campestris*
						Promenetus	*umbilicatelus*
			Littorinimorpha		Hydrobiidae		
			Heterostropha		Valvatidae	*Valvata*	*sincera hellicoidea*
Arthropoda	Chelicerata	Arachnida	Trombidiformes	Acari			
			Trombidiformes	Hydracarina			
	Hexapoda	Collembola					
		Insecta	Odonata	Anisoptera	Aeshnidae	*Aeshna*	
					Corduliidae	*Somatochlora*	
					Libellulidae	*Libellula*	
						Pachydiplax	*longipennis*
						Sympetrum	
				Zygoptera	Coenagrionidae	*Coenagrion*	
						Enallagma	
						Ishnura	

			Nehalennia	
Hemiptera	Heteroptera	Corixidae	*Calicorixa*	
			Corisella	
			Cymatia	*americanus*
			Dasycorixa	
			Palmocorixa	
			Sigata	
			Trichocorixa	
		Gerridae	*Limnopourus*	
		Mesoveliidae	*mesovelia*	
		Noronectidae	*Buenoa*	
			Notonecta	
		Saldidae		
		Veliidae	*microvelia*	
Trichoptera	Annulipalpia	Polycentropidae	*polycerntropus*	
	Integripalpia	Brachycentridae	*Amiacentrus*	
		Phryganeidae	*Agrypnia*	
			Banksiola	
			Phryganea	
Coleoptera	Adephaga	Curculionidae		
		Dytiscidae	*Agabus*	
			Dytiscus	
			Hydaticus	
			Hydropourus	
			Hygrotus	
			Ilybius	
			Laccornis	
			Laccophilus	
			Liodessus	

			Potamonectes
			Rhantus
		Gyrinidae	*Gyrinus*
		Haliplidae	*Brychius*
			Haliplus
	Polyphaga	Chrysomelidae	*Pyrrhalta*
		Emidae	*Narpus*
		Hydraenidae	*Hydraena*
			Octhebius
		Hydrophillidae	*Anacaena*
			Berossus
			Cymbiodyta
			Enochrus
			Helophorus
			Hydrobius
			Hydrochus
			Laccobius
			Limnebius
			Paracymus
Lepidoptera		Noctuidae	
		Pyraliidae	
Diptera	Brachycera	Dolichopodidae	
		Ephydridae	*Octhera*
			Setacera
		Empididae	*Hemerodromia*
		Muscidae	
		Sciomyzidae	*Tetanocera*
		Stratiomyidae	*Allagnosta*
			Euparyohus

		Syrphidae	*Eristalis*
		Tabanidae	*Chrysops*
			Tabanus
	Nematocera	Ceratopogindae	*Atrichopogon*
			Bezzia
			Dasyhelea
			Forcipomyia
		Chaoboridae	*Chaoborus*
		Chironomidae	
		Culicidae	*Aedes*
			Culex
			Culiseta
		Dixidae	*Dixella*
		Psychodidae	*Pericoma*
			Psychoda
		Thaumaleidae	
		Tipulidae	*Prionoccra*
			Tipula